Title

Redefining the Role of Netrin1 as an Axon Guidance Cue in the Developing Spinal Cord

Permalink

https://escholarship.org/uc/item/0vb9s6p9

Author

Varadarajan, Supraja

Publication Date

2017

Peer reviewed|Thesis/dissertation

UNIVERSITY OF CALIFORNIA

Los Angeles

Redefining the Role of Netrin1 as an Axon Guidance Cue

in the Developing Spinal Cord

A dissertation submitted in partial satisfaction of the

requirements for the degree Doctor of Philosophy

in Neuroscience

by

Supraja Varadarajan

2017

ABSTRACT OF THE DISSERTATION

Redefining the Role of Netrin1 as an Axon Guidance Cue

in the Developing Spinal Cord

by

Supraja Varadarajan

Doctor of Philosophy in Neuroscience

University of California, Los Angeles, 2017

Professor Bennett G. Novitch, Chair

Localized diffusible chemotropic signals are canonical sources of guidance information for axons extending towards their synaptic targets. Equally important, but less well understood, are the contact-dependent regional boundaries that provide either permissive or non-permissive substrates for axon growth. Classic work has demonstrated the importance of netrin1 as a floor plate chemoattractant for commissural axons in the developing spinal cord; subsequent studies in different systems have suggested that netrin1 also has short-range guidance activities. Here, I have further analyzed the role of netrin1 in the spinal cord and find that netrin1 mediates short-range growth boundaries that guide many additional classes of spinal axons. All spinal axons grow precisely around the ventricular zone (VZ), without innervating it, suggesting that the edge of the VZ represents a growth boundary. Multiple lines of evidence suggest that this boundary is

mediated by netrin1: first, netrin1 is expressed by neural progenitors in the VZ and transported to the progenitor end feet at the pial surface; second, neurofilament (NF)$^+$ axons initiate oriented growth coincident with the dorsal boundary of VZ-netrin1; third, several axons project aberrantly into the VZ in the absence of netrin1. This phenotype is observed only when netrin1 is ablated from the VZ, not the FP. Moreover, the selective ablation of netrin1 from the VZ is sufficient to locally reshape the trajectories of NF$^+$ axons. Our studies have shown that netrin1 mediates the growth boundary acting primarily through the Dcc receptor and that netrin1 accumulates in axons in a Dcc dependent manner. Taken together, our data suggest that netrin1 establishes local "hederal" boundaries that provide an adhesive substrate while also preventing local innervation.

The dissertation of Supraja Varadarajan is approved.

Samantha J. Butler

S. Lawrence Zipursky

Kelsey C. Martin

Alvaro Sagasti

Bennett G. Novitch, Committee Chair

University of California, Los Angeles

2017

DEDICATION

For my parents, Sujatha and Varadarajan, for all their sacrifices

My Grandad, Sampathkumar, to whom this would mean a lot

My husband, Gautam, for his unconditional love.

And

My son Vikram - Dreams do come true.

TABLE OF CONTENTS

LIST OF FIGURES

ACKNOWLEDGMENTS

This work would not have been possible without the love and support of many people. First and foremost, I would like to thank my mentor Samantha Butler for her constant guidance, patience, and advice. She has had a unique strategy of being sympathetic to my fears while also helping me overcome them every step of the way. Not only has she taught me to be a better scientist but has also shown me how to balance my personal and professional life. I can't thank her enough for her unending encouragement and for always being available, whether it was about a scientific question or random discussions. Every knock on her office door has always been met with a smile.

I would also like to thank Bennett Novitch for his endless support and many wonderful insights about my project. I really appreciate him whole-heartedly sharing all of the enthusiasm, anxiety and lengthy email exchanges that we have had to deal with this past year. I am particularly thankful to him for constantly pushing me to challenge myself and do better. I would also like to thank all my thesis committee members: Larry Zipursky, Alvaro Sagasti and Kelsey Martin for so readily getting on board and agreeing to serve on my committee even before meeting me, and for their strong support throughout.

I have had the pleasure of working with so many wonderful and talented lab members over the years: First, I would like to thank Keith Phan, who has practically taught me every technique I learnt in the lab. I want to thank him for giving me the challenge of getting him to open up and for participating so sportingly in our sibling-like quarrels. I would like to thank Ginger Hazen, Michele Frendo, Stephen Tymanskyj and Ken Yamauchi for encouraging me to join the Butler Lab, and taking care of me the first few years. I can't thank Madeline Andrews

enough for being the best Ph.D. sibling one can ask for: I don't know what I would have done without her by my side, always ready to listen, help and exchange stories with. Graduate school has been a blast, thanks to her.

Moving mid-way to UCLA was one of the best possible blessings in disguise: NSDIP members, especially Felix Schweizer, and the Neurobiology office have been instrumental in helping me transition smoothly and become a part of this incredible institution.

I am also grateful to members of the Novitch lab for all the discussion-rich joint lab meetings. I would especially like to thank Jennifer Kong and Caroline Pearson for practice talks, readily understanding the joys and sorrow of working with mice, and reminders to stay positive. I would also like to thank Alexandra da Silva, Destaye Moore and the rest of the Butler-Novitch members for making this such an enjoyable lab environment that feels just like family.

Next, I am so thankful to my parents Sujatha and Varadarajan, my in-laws Chandra and Muralidhar, my aunt Hema, my brother Srivathsan and my cousin Lavan for their constant love and support and for being such a wonderful source of inspiration. I am extremely lucky to have parents who have always supported me and had faith in all my decisions; they have given me the best skillset to get through life in showing me how to be grateful for the positive things that come my way and how to stay strong and fight through the tough times.

Finally, I would like to thank Gautam Muralidhar for all his love and kindness and for being there every time I needed him and for giving me exactly what I needed even if I didn't know what that was. I can't thank him enough for being such a cheerful, happy person and for constantly supporting me throughout; I know it couldn't have been easy dealing with me, so thank you for never complaining. And last but not least, I would like to thank my son Vikram, for giving me the strongest motivation to be an efficient and persevering scientist.

<div align="center">**VITA**</div>

EDUCATION

New Jersey Institute of Technology (NJIT)   2006-2008

Master of Science in Biomedical Engineering

Visvesvaraya Technological University (Bangalore, India)   2002-2006

Bachelor of Engineering in Biotechnology Engineering

First-class with Distinction

EMPLOYMENT

University of California, Irvine   2008 - 2010

Staff Research Associate II with Dr. Aileen Anderson

Teaching Assistant, New Jersey Institute of Technology   2007 - 2008

Elementary Science Outreach Program at the Center for Pre-College Programs

AWARDS

Samuel Eiduson Student Lecturer   2017

Dissertation Year Fellowship, University of California Los Angeles   2016-2017

Phi-Beta Kappa Alumni in Southern California International Scholarship Award   2016

Brain Research Institute/Semel Institute Neuroscience Travel Award   2016

Qualcomm Innovation Fellowship Finalist, Qualcomm, San Diego   2013

PUBLICATIONS

Varadarajan, SG, Kong, JH, Phan, KD, Cardin, J, Panaitof, SC, Kania, A, Novitch, BG and Butler, SJ (2017). Netrin1 produced by neural progenitors, not floor plate cells, is required for axon guidance in the spinal cord. *Neuron 94: 1-10*

Varadarajan, S.G. and Butler, SJ (2017). Netrin1 establishes multiple short-range axon guidance boundaries in the developing spinal cord. ***In preparation.***

Yamauchi, K., **Varadarajan, S.G.**, Li, J.E., and Butler, S.J., 2013. Type Ib BMP receptors mediate the rate of commissural axon extension through inhibition of cofilin activity. *Development 140: 333-342*

PRESENTATIONS

Varadarajan, SG (2016). Netrin1 establishes multiple boundaries to locally guide axons in the developing spinal cord. Axon and dendrite development Nanosymposium, Society for Neuroscience, San Diego. *Platform Presentation.*

Varadarajan, SG (2016). Netrin1 establishes multiple boundaries to locally guide axons in the developing spinal cord. Axon guidance, Synapse Formation & Regeneration Meeting, Cold Spring Harbor Laboratory, NY. *Platform Presentation.*

CHAPTER 1 – INTRODUCTION

The functional ability of humans to perform complex tasks depends on precisely wired neural circuits. Billions of neurons each connect with 1000 or so target cells, creating trillions of synapses in the brain. Even in lower-order organisms as simple as *C.elegans*, which only have ~300 neurons, a precisely wired neural circuit dictates the ability of the worm to carry out basic functions such as mechanosensation and locomotion[1,2]. This precise wiring begins during embryonic development when axons interact with molecular cues in the embryonic environment and navigate a specific path in order to reach their synaptic targets. Any errors in these trajectories can lead to devastating deficits in an organisms' ability to perform daily functions such as cognition, respiration, movement and speech.

1-1: Spinal cord development

During the earliest stages of development, progenitor cells are present in abundance in a region called the ventricular zone (VZ)[3]. Signaling molecules induced from the polar ends of the spinal cord include Sonic Hedgehog (Shh) from the notochord and subsequently from the floor plate (FP), the Bone Morphogenetic Proteins (BMPs) from the roof plate (RP) and retinoic acid (RA) from the paraxial mesoderm[4]. These signaling molecules pattern the spinal cord along the dorsoventral axis such that different progenitor domains express unique combinations of transcription factors[5]. Based on the differential ability of each progenitor pool to transduce the signaling cues, as well as cross repressive interactions between each class of transcription factor, the progenitors are further divided into 11 distinct progenitor domains[6]. Despite these unique identities, all progenitors have a uniform radial architecture with apical attachments on the lumen

1

side of the neuroepithelium and basal attachments (arrows, **Figure 1-1 A**) via their endfeet that contact the basement membrane, also known as the pial surface[7]. The cell bodies of the progenitors continue dividing along this apical-basal axis in the ventricular zone until they are ready to exit the cell cycle and differentiate into mature neuronal subtypes[3] (**Figure 1-1 B**). The newly formed neurons lose their apical-basal attachment and migrate out of the ventricular zone into the mantle zone.

1-2: Axon guidance

Newly formed neurons in the mantle zone send axons into the marginal zone that typically follow the path of the growth cone, known as the leading edge of the axon (**Figure 1-1 C**). Growth cones participate in a dynamic interaction with several molecular cues in the embryonic environment until they find the correct cue that enables them to grow forward and reach the correct target. Axons on the other hand follow suit in the path paved by the growth cone, and have a more passive growth in comparison. These mechanisms are evolutionarily conserved in worms, flies and vertebrates. The long distances that axons need to navigate towards their synaptic partners in all species, for example between ~300-1000um in a mouse embryo, is made achievable by the presence of several intermediate targets, usually comprised of a cluster of cells, positioned to strategically divide the trajectory of axons into smaller segments. The molecular cues that specify an axon's trajectory, both at the intermediate or final target, are called guidance cues, and are critical in specifying axon trajectories with minimum error.

Long range vs short range

Guidance cues can be broadly classified as attractive or repulsive cues. And each of these classes can be further subdivided into two categories: 1) long-range cues that are secreted and diffusible, thus enabling their effect over 100s of microns from their originl; these are also known as chemoattractive or chemorepulsive cues and 2) short-range or contact-dependent cues that are membrane-bound or tethered to an extracellular matrix (ECM) component, limiting the range of effect to their immediate vicinity[8].

Long-range cues have historically been studied in great detail, perhaps because of the greater distances these cues can influence. However, axons navigate short segments at a time interacting with several intermediate targets that serve as specific spatial and temporal choice points during development. Short-range cues play a remarkably important role in determining the precision with which axons encounter these transitional gateways, which cumulatively determine the accuracy with which axons find their synaptic partners. Short-range cues, usually exert their effect within a one to two cell diameter range and can act in several different ways to carry out these functions: 1) providing permissive substrates that may or may not be adhesive, 2) non-permissive substrates that can range from causing growth-cone collapse to a simple deflection and 3) combinatorial substrates that comprise of permissive substrates surrounded by repulsive cues so as to hem axons through a corridor[8]. The most well-studied guidance cues include, but are not limited to, Netrins, Slits, Ephrins, Semaphorins and Cell Adhesion Molecules (CAMs) (**Table 1-1**[8-12]).

Plasticity of guidance cues

Many studies over the last 15 years have shown that cues once identified as an attractive signal may also act as a repulsive signal in other systems or species. Intracellular second messenger states have shown to be key determinants in switching the response of axons to a given cue: by altering the levels of cyclic AMP in an in vitro assay, Ming et al. showed that Netrin1, an attractive cue, could elicit a repulsive response from a growth cone. Additionally, this response could be blocked by adding a cAMP competitive analog[13]. Ephs and Ephrins were originally identified as ligand and receptor pair respectively; however studies have shown that these molecules can reverse signal such that Ephrins can act as the ligand, signaling to the Ephs[11]. Bashaw and Goodman have demonstrated that the extracellular and intracellular components of a receptor each play a specific role in the response towards a guidance cue. By using chimeric constructs, they have shown the ecto domain to be responsible for recognizing the correct ligand, while the cytoplasmic domain is responsible for deciding the response; further, by replacing either one of these domains, the binding partner and response can be altered[14]. Together, these studies indicate that the response of a growth cone is not predetermined and that the context in which a cue is presented is as important as the cue itself in eliciting a response.

Spinal cord as a model system for studying axon guidance

The developing spinal cord of mouse embryos serves as an excellent system to study axon guidance for two main reasons: first, the embryonic spinal cord has well-defined polarized ends and second, there is an abundance of cues acting from the dorsal and ventral poles. There are 11 different populations of neurons along the dorsoventral axis that are born from embryonic day E10.5 through E14.5[15,16] (**Figure 1-1 B**), and can be broadly classified as dorsal

4

interneurons, association neurons, ventral interneurons and motor neurons[16]. Most dorsal interneurons and some ventral interneurons are commissural neurons as their axons project to the contralateral side of the spinal cord through the ventral commissure, connecting the right and left sides of the spinal cord. Ipsilaterally projecting axons also follow a circumferential trajectory but turn away from the FP and project longitudinally without crossing the midline. On the toher hand, motor neurons project axons outside the spinal cord into the periphery, while sensory neurons that have their cell bodies in the dorsal root ganglia (DRG), project their central branches into the spinal cord after E12.5 (**Figure 1-1 C**)[15,17]. Each of these classes of axons have unique trajectories and respond to different combination of cues; however they share one common feature: all these axons that can be identified with an antibody against neurofilament (NF), project around the edges of the ventricular zone without entering this region. My main hypothesis revolves around this unique feature and identifying the cue(s) that prevents axons from entering the VZ and the mechanism by which this cue helps axons maintain their trajectories.

Commissural axon trajectory

The early born dorsal commissural axons, i.e. the pioneering axons, are born adjacent to the RP. Shortly thereafter, they receive chemorepulsive cues from the BMPS in the RP and project away from the dorsal spinal cord[18], taking a circumferential trajectory around the VZ, without innervating it. The most well-known canonical guidance model suggests that these axons also sense chemoattractive cues from the FP, namely Netrin1 and Shh and grow towards the FP[19,20], where they cross the ventral midline and project longitudinally. Later-born commissural axons follow selective fasciculation and chase the trajectories established by the pioneers.

Opposing forces present at the polar ends work in combination to exert a push and pull force to direct commissural axon growth, making it an excellent setup to assess axon guidance defects and further understand the role of guidance cues.

1-3: Bone Morphogenetic Proteins

BMPs, like Shh, have diverse functions in neural development[18,21,22]. The BMPs produced by the RP first play a key role in determining cell fate of dorsal spinal progenitors and differentiation of these progenitors into distinct classes of spinal interneurons[23]. At later stages of development, the BMPs also specify chemorepulsive cues from the RP acting as a guidance cue, and repel the dorsal most interneurons to project axons away from the RP[18,24]. The BMPs determine cell fate through the canonical signaling pathway that involves BMP receptors, BmprIa and BmprIb, and receptor-activated Smads[25,26]. However the axon guidance roles are regulated through a non-canonical signaling pathway involving Lim kinase (Limk) and cofilin[27]. The BMP ligand binds to BmprI and BmprII, releasing Limk1, which phosphorylates and inactivates cofilin. This signaling cascade subsequently inhibits depoylmerization of actin thus arresting the cyto-skeletal reorganization of actin filaments, and preventing growth of the axon[28].

1-4: Netrins

Netrins are a family of laminin-like proteins that were first identified in the early 90s, as the prototypical axon guidance cue. The most seminal observations by Santiago Ramón y Cajal in 1890 hypothesized that chemoattractive cues at the midline guide commissural axons[29]; however it wasn't until many years later that such a cue was identified. Studies in *C. elegans* identified the genes that encoded Unc6 and demonstrated its role in regulating axon growth in the nematode[30,31]. In parallel, in vitro experiments using rat dorsal spinal explants and FP

explants[32] demonstrated that the FP was indeed a source of chemoattractive cues in the vertebrate spinal cord. One of the major developments that significantly influenced the field of axon guidance was the identification of this cue as netrin1 (originating from the Sanskrit word, *netr*, meaning "one who guides") by Tessier-Lavigne and colleagues, using biochemical assays from chicken brains[33]. These studies led to a series of experiments that established netrin1 as long-range chemoattractant acting from the FP to guide commissural axons in the spinal cord[19,33,34]. Other members of the netrin family that were subsequently identified include netrin 2 in chicken embryos[33,34], netrin A and B in flies[35,36], netrin G1 and G2 (GPI anchored membrane proteins)[37] and netrin 3 and 4 in mammals[38,39]. Mouse netrin1 is most homologous to human-netrin1 (98.8%), and to a lesser extent to netrin in other species: chicken netrin1 (87.2%), chicken netrin2(71.4%) and mouse netrin3 (55.2 %)[40].

Structure of netrins

Netrins are structurally similar to the laminin family of proteins, although they are considerably smaller in size than laminin molecules: netrins consist of 600 aminoacids and are ~70kDa in size. The N-terminus of netrin1 and netrin3 are composed of two domains that are similar to domains V and VI of the laminin γ1-chain, while netrin4 and netrin G1/G2 are most similar to the laminin β1-chain. The C-terminus is not similar to laminin, and can bind ECM molecules like heparin and some integrins, namely α3β1 and α6β4[37,40-42].

Netrin1 receptors

Netrin1 mediates its activity through two classes of receptors: Dcc and the Unc5 family[37,43-45]. In vertebrates, Dcc was found to mediate attractive properties of netrin1[46], while

the Unc5 family comprising of 4 members, Unc5 A-D, mediates the repulsive properties of netrin1[43,47-49]. In chickens neogenin, an orthologue of mouse neogenin is thought to replace the functions of Dcc[50]. However, in rodents, not only does the expression pattern differ compared to chickens, but neogenin does not act as a receptor for netrin1[50]. In *Drosophila,* Frazzled (Fra), an orthologue of *Dcc*, carries out the same functions of vertebrate *Dcc*, by promoting midline crossing in the ventral nerve cord[35,51].

1-5: Versatility of netrin1 mediated guidance

Other than its role in directing spinal commissural axons, netrin1 has been implicated in the proper development of many axonal tracts, namely the thalamocortical tract[52], corticospinal tract[52] and all commissure formations including the anterior commissure at E14.5, hippocampal commissure at E15.5, corpus callosum at E17.5[53,54]. Apart from these functions, netrin1 has been studied in great detail in many other species, and is known to have many diverse functions outside the central nervous system, as described below. Interestingly, these various roles have demonstrated that netrin1 can act at short or long range, and as a secreted or membrane-bound protein. However, it still remains unclear which of these roles netrin1 assumes in the vertebrate spinal cord.

Short-range interactions of netrin1

In *Drosophila*, netrin is present as NetA and NetB, and studies in the *Drosophila* nerve cord have shown that either one are sufficient for commissure formation[35,36]. Remarkably, tethering NetB to the membrane in NetA$^\Delta$ mutants was sufficient to establish commissure formation as well as Unc5-mediated repulsion[55], indicating that netrin1 can specify guidance

information at short-range. Similarly, outside the nerve cord, a subtype of motoneurons in *Drosophila* have been shown to require short-range interactions with netrin[56]. In these experiments, while the RP3 motoneurons were able to reach their target muscle even in the absence of Net or Fra, these growth cones were unable to attach onto the target muscles 6 and 7 and were found to wander aberrantly[56], indicating that netrin was mediating guidance locally at the nerve-muscle junction.

Recent studies have also shown that Net-Fra are required for sustained attachment of growth cones to the medulla[57]. Despite the absence of Net or Fra, growth cones were able to reach the targets, but were unable to attach, indicating that the long-range activity of netrin was not necessary in this context. Rather suggesting, that instead of acting as a ligand-receptor pair to mediate chemoattraction, Net-Fra interactions are more consistent with providing an adhesive substrate acting locally[57]. Together, these studies demonstrate the sufficiency of short-range activities of netrin at the midline, indicating that the ability of a molecule to act over a distance *in vitro* does not in itself necessitate a long-range activity *in vivo* as well.

Chemotaxis vs Haptotaxis

MacLennan et al., have shown that netrin1 protein is present along the lateral edges of the spinal cord at stages when axons are growing ventrally[58], thus arguing against the necessity for chemotaxis described before[19,33,34,59]. Instead, the authors proposed a model in which netrin1 mediates axon guidance by haptotaxis[58], i.e. movement along an adhesive substrate or a membrane-bound attractant. Supporting this model, analysis of ventral spinal cords from rat embryos have shown that most of the netrin1 protein *in vivo* is present in bound form[59]. Subsequent studies *in vitro* have also shown that substrate binding is necessary for netrin1-

mediated attraction as immobilizing netrin1 was an important step in the activation of mechanosensory proteins such as focal adhesion kinase (FAK) and Crk-associated substrate (CAS)[60]. Similarly, recent live imaging studies have also shown that in *Drosophila*, Net-Fra interactions are required for the traction of R8 growth cones onto their targets, rather than for chemoattraction[57]. Taken together, these studies provide further evidence for netrin1 providing adhesive substrates and promoting short-range, membrane-bound guidance.

Netrin1 dependent precursor cell migration

Netrin1 has been known to play a role in the migration of many cells including granule cell progenitors, precerebellar progenitors and precerebellar neurons[40,41,61]. Oligodendrocyte precursor cells (OPCs) have also been shown to migrate away from the FP near the 3rd ventricle and migrate along the optic nerve in response netrin1 secreted by cells at the optic chiasm[62]. Subsequent studies *in vitro* also showed that OPCs in the spinal cord migrate away from ventral explants or a source of netrin1[63,64], mimicking the migratory pattern of OPCs *in vivo*. Similarly, pontine cerebellar nuclei that express Dcc receptors have also been shown to migrate towards a source of netrin1 expressed at the midline of the hindbrain to form the pons[40].

Tissue morphogenesis

Netrin1 has also been implicated in a variety of functions outside the CNS. For example, in the developing mammary gland, netrin1 and the Dcc homologue, neogenin, play a key role in promoting adhesion between two different types of cells in order to form the terminal end buds of the mammary ducts[41]. Another function for netrin1 is in embryonic lung development, where together with Dcc and Unc5B, netrin1 regulates branching morphogenesis by preventing

excessive branch formation[41]. In pancreatic development, netrin1 interacts with ECM molecules like collagen, fibronectin and the integrins to promote cell-matrix adhesion, perhaps through its C-terminal domain[41,42,65]. Netrin is also known to have additional roles in leukocyte migration[41], and in vascular formation and angiogenesis where it regulates endothelial cell migration[66,67]. Apart from its well-known function in axon guidance, these studies also demonstrate the ability of netrin1 in promoting cell-cell and cell-substrate adhesion, cell migration and survival.

1-6: Netrin1 in the spinal cord

The initial studies that identified netrin1 also further characterized the activity using E13 rat floor plates[33]: homogenates of the floor plates were fractionated and surprisingly, all detectable activity was found associated with the membrane bound fraction. Interestingly, due to its more economical nature, embryonic chicken brains were used to purify netrin1 and netrin2; these genes were subsequently cloned into vectors to test their activity in *in vitro* explant assays[33] as well as used to characterize the expression of the transcript[19,34] and protein *in vivo*[59]. COS7 cells transfected with either netrin1 or netrin2 and were found to mimic the activity seen with the floor plates: the cos cells secreting netrin1, and to a lesser extent netrin2, were able to promote outgrowth as well as reorient commissural axons *in vitro*[33]. *In vivo*, chicken netrin1 mRNA expression is restricted to the floor plate cells in Hamburger-Hamilton stage HH 15-16 embryos, while chicken netrin2 is present in the ventricular zone above the floor plate, well into the intermediate and dorsal VZ. Subsequent studies in mouse embryos showed that mice mutant for netrin1 exhibited severe defects in commissural axon guidance and growth[19]. Antibodies made specifically against chicken netrin1 demonstrated that the protein was present in the FP and the VZ[59], suggesting that the protein diffused from the FP into the VZ to form a gradient. Taken

11

together, these studies laid the basis for the classic canonical model that netrin1 produced in the FP acted as a long-range chemoattractant to guide commissural axons to the ventral midline. Netrin 3 is only expressed in the spinal cord after commissural axons have crossed the FP[52] and is also expressed in the DRGs, mesenchyme and muscle cells[38,52]. Netrin G1 is expressed in the dorsal thalamus and olfactory bulb, while netrin G2 is expressed in the cerebral cortex, primarily by neurons[52,68,69]. Interestingly, netrin 4 is expressed in the dorsal FP starting at E11.5, but its contribution to axon guidance, if any, remains largely unknown[39,52].

Netrin1 mouse models

The first netrin1 mutant mouse was made using a *lacZ* gene trap vector inserted into an intron of the netrin1 gene[19,70]. This resulted in a fusion protein comprising of extracellular and transmembrane netrin1 domains and a cytoplasmic b-geo domain (b-galactosidase + neomycin cassette), that gave rise to a severely hypomorphic allele in homozygous mutants. These mutants express ~1-5% of wildtype netrin1 protein[71], and are therefore not considered complete nulls[19]. Remarkably, it wasn't until twenty years after the initial studies, that a complete knockout for netrin1 was generated. Three groups, independently, each made a netrin1-floxed allele to create either conditional knockouts of netrin1 or complete knockout models: 1) Brunet et al. 2014 inserted loxP sites around exon 3 of the netrin1 gene[72] 2) Bin et al. inserted loxP sites flanking exon 1 and crossed the resulting netrin1$^{flox/+}$ with a CMV::cre to generate netrin1$^{+/-}$ heterozygous colonies[71] and ultimately homozygous mutants 3) Yung et al. inserted loxP sites flanking exon 2 and crossed the resulting netrin1$^{flox/+}$ with an EIIa::cre to generate netrin1$^{+/-}$ heterozygous colonies[73]. All these models are extremely important in order to address the role of netrin1 in

different systems using stronger and more specific genetic manipulations without any residual netrin1 expression.

1-7: Summary

Redundancy of signaling cues allows the use of only a handful of cues to generate complex neural circuits. Conversely, the interpretation of a single guidance cue in many ways, allows for a small number of cues to function in multiple ways and affect larger populations of axons. Therefore, it is extremely important to not only understand the mechanisms and signaling pathways involved in axon guidance, but it is equally important to understand the context in which each signaling cue can be interpreted.

Numerous studies have identified the different mechanisms that are involved in netrin1 signaling pathway. However, the following caveats mentioned by some of the initial studies necessitates a re-evaluation of the role of netrin1 in the spinal cord and perhaps in other systems as well: 1) the COS7 cells transfected to express netrin1 or netrin2 were assessed for the percentage of netrin present in salt extracts versus conditioned medium: only 20% of the salt-extractable, i.e. membrane-bound netrin1, was found to be soluble and only 10% of the salt-extractable netrin2 was found to be soluble[34]. This suggests that most of the netrin1 present is likely to be membrane-bound[33]. 2) In the explant studies using these transfected cos7 cells, the entire setup is encased in collagen, i.e. an ECM molecule. Since netrin1 is known to interact with ECM molecules, netrin1 produced by the COS7 cells may in fact be tethered to the membrane and providing a substrate for growth rather than acting from a distance. 3) In mouse embryonic spinal cords, netrin1 mRNA is expressed through most of the VZ, well into the dorsal spinal

13

cord; thus making it difficult to assess the diffusivity of netrin1 from the FP to the VZ in mouse embryos.

In Chapter 2, I have distinguished between the roles of FP-derived netrin1 and VZ-derived netrin1 in providing axon guidance cues. I find that, VZ-derived netrin1 acts locally to specify a growth boundary, that both restricts growth into the VZ as well as promotes fasciculation. I also found that in the absence of FP-derived netrin1, axons continue grow normally towards the FP and cross the ventral midline with only minor defasciculation defects, indicating that it is VZ-derived netrin1 that is required to specify this boundary and not FP-derived netrin1.

In Chapter 3, I have further examined the activity of VZ-derived netrin1 in both earlier and later stages of development. I find that in earlier stages, VZ-derived netrin1 is required to promote ventrally oriented growth of the pioneering axons, and that two days later in development, VZ-derived netrin1 is still required to specify the growth boundary, in addition to other transiently expressed netrin1 boundaries that regulate sensory axon invasion into the spinal cord.

In Chapter 4, we have addressed the mechanistic details by which BMPs regulate commissural axon growth. We find that BmprIb controls the rate of commissural axon growth by modulating cofilin activity. We show that constitutive activation of BmprIb slows commissural axon growth and conversely, neurons from BmprIb$^{-/-}$ mutant embryos extend longer axons in vitro. This activity plays a crucial role in maintaining the balance between Limk1-cofilin thereby controlling the speed of axon extension as the growth cones sense cues in their environment.

Figure 1-1: Stages of neural development
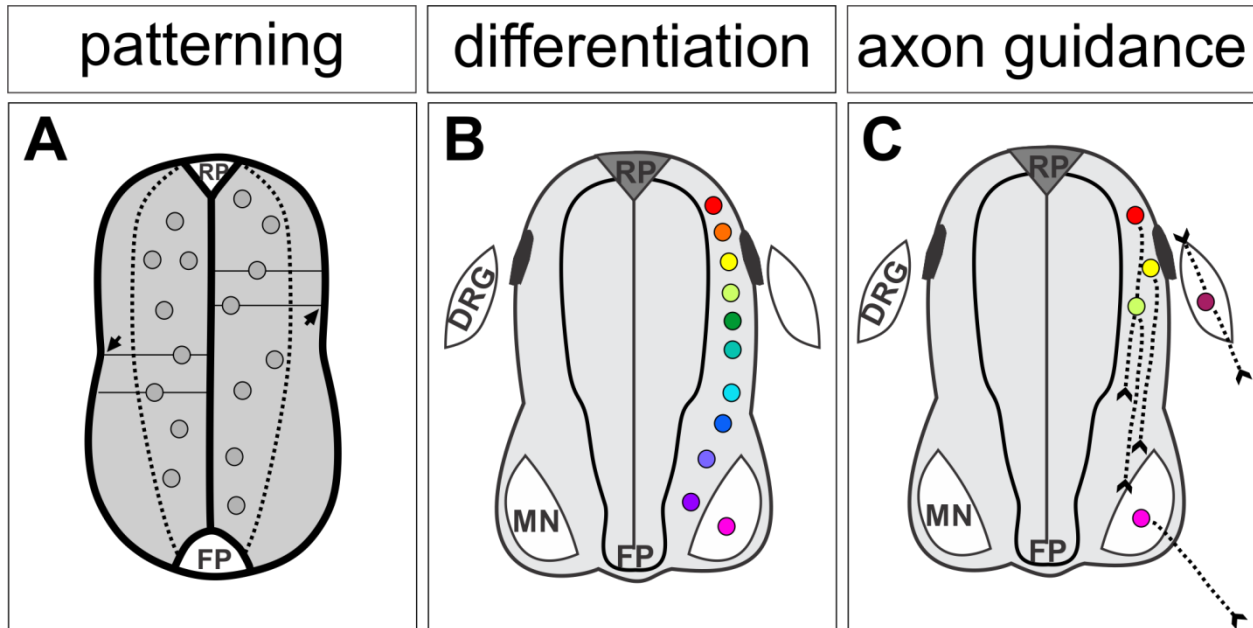
(A) Shortly after neural tube closure, proliferating cells are present in abundance in the VZ (inside the dotted lines). These cells are also referred to as neural progenitors. Progenitors have radial processes that have an apical attachment at the luminal surface of the VZ, and a basal attachment at the pial surface of the spinal cord (arrows). Inductive signals from the RP and FP pattern these progenitors into different classes.

(B) Patterned progenitors, continue dividing, and soon give rise to differentiated neurons of a specific identity, indicated by different colors. These differentiated neurons lose their apical and basal attachments and migrate into the mantle zone, adjacent to the VZ.

(C) Differentiated neurons give rise to axons that broadly travel in one of three directions: commissural axons that grow towards the ventral midline (red, green and yellow), motor axons

that grow outside the spinal cord (pink) and central branches of sensory axons that grow inside

the spinal cord (burgundy).

TABLE 1-1: Summary of guidance cues and their receptors

Ligand	Receptor	Response	Range
Netrins/Unc6	Unc5	Repulsion	Long-range
	Dcc/Fra/Unc40	Attraction	Short/Long
Slits	Robo	Repulsion	Short/Long
Ephrins	Ephs	Repulsion & adhesion	Short-range
Semaphorins	Plexins, Neuropilin	Repulsion	Short/Long

BIBLIOGRAPHY

1. Hilliard MA, Bargmann CI, Bazzicalupo P. C. elegans responds to chemical repellents by integrating sensory inputs from the head and the tail. Curr Biol 2002;12(9):730-4.

2. Hart AC, Sims S, Kaplan JM. Synaptic code for sensory modalities revealed by C. elegans GLR-1 glutamate receptor. Nature 1995;378(6552):82-5.

3. Butler SJ, Bronner ME. From classical to current: analyzing peripheral nervous system and spinal cord lineage and fate. Dev Biol 2015;398(2):135-46.

4. Le Dréau G, Martí E. Dorsal-ventral patterning of the neural tube: a tale of three signals. Dev Neurobiol 2012;72(12):1471-81.

5. Jessell TM. Neuronal specification in the spinal cord: inductive signals and transcriptional codes. Nat Rev Genet 2000;1(1):20-9.

6. Briscoe J, Novitch BG. Regulatory pathways linking progenitor patterning, cell fates and neurogenesis in the ventral neural tube. Philos Trans R Soc Lond B Biol Sci 2008;363(1489):57-70.

7. Rousso DL, Pearson CA, Gaber ZB, Miquelajauregui A, Li S, Portera-Cailliau C, Morrisey EE, Novitch BG. Foxp-mediated suppression of N-cadherin regulates neuroepithelial character and progenitor maintenance in the CNS. Neuron 2012;74(2):314-30.

8. Tessier-Lavigne M, Goodman CS. The molecular biology of axon guidance. Science 1996;274(5290):1123-33.

9. Yu TW, Bargmann CI. Dynamic regulation of axon guidance. Nat Neurosci 2001;4 Suppl:1169-76.

17

10.   Bashaw GJ, Klein R. Signaling from axon guidance receptors. Cold Spring Harb Perspect Biol 2010;2(5):a001941.

11.   Dickson BJ. Molecular mechanisms of axon guidance. Science 2002;298(5600):1959-64.

12.   Simpson JH, Bland KS, Fetter RD, Goodman CS. Short-range and long-range guidance by Slit and its Robo receptors: a combinatorial code of Robo receptors controls lateral position. Cell 2000;103(7):1019-32.

13.   Ming GL, Song HJ, Berninger B, Holt CE, Tessier-Lavigne M, Poo MM. cAMP-dependent growth cone guidance by netrin-1. Neuron 1997;19(6):1225-35.

14.   Bashaw GJ, Goodman CS. Chimeric axon guidance receptors: the cytoplasmic domains of slit and netrin receptors specify attraction versus repulsion. Cell 1999;97(7):917-26.

15.   Alaynick WA, Jessell TM, Pfaff SL. SnapShot: spinal cord development. Cell 2011;146(1):178-178.e1.

16.   Lai HC, Seal RP, Johnson JE. Making sense out of spinal cord somatosensory development. Development 2016;143(19):3434-3448.

17.   Watanabe K, Tamamaki N, Furuta T, Ackerman SL, Ikenaka K, Ono K. Dorsally derived netrin 1 provides an inhibitory cue and elaborates the 'waiting period' for primary sensory axons in the developing spinal cord. Development 2006;133(7):1379-87.

18.   Augsburger A, Schuchardt A, Hoskins S, Dodd J, Butler S. BMPs as mediators of roof plate repulsion of commissural neurons. Neuron 1999;24(1):127-41.

19.   Serafini T, Colamarino SA, Leonardo ED, Wang H, Beddington R, Skarnes WC, Tessier-Lavigne M. Netrin-1 is required for commissural axon guidance in the developing vertebrate nervous system. Cell 1996;87(6):1001-14.

20. Charron F, Stein E, Jeong J, McMahon AP, Tessier-Lavigne M. The morphogen sonic hedgehog is an axonal chemoattractant that collaborates with netrin-1 in midline axon guidance. Cell 2003;113(1):11-23.

21. Timmer JR, Wang C, Niswander L. BMP signaling patterns the dorsal and intermediate neural tube via regulation of homeobox and helix-loop-helix transcription factors. Development 2002;129(10):2459-72.

22. Le Dréau G, Martí E. The multiple activities of BMPs during spinal cord development. Cell Mol Life Sci 2013;70(22):4293-305.

23. Wine-Lee L, Ahn KJ, Richardson RD, Mishina Y, Lyons KM, Crenshaw EB. Signaling through BMP type 1 receptors is required for development of interneuron cell types in the dorsal spinal cord. Development 2004;131(21):5393-403.

24. Butler SJ, Dodd J. A role for BMP heterodimers in roof plate-mediated repulsion of commissural axons. Neuron 2003;38(3):389-401.

25. Heldin CH, Miyazono K, ten Dijke P. TGF-beta signalling from cell membrane to nucleus through SMAD proteins. Nature 1997;390(6659):465-71.

26. Hazen VM, Andrews MG, Umans L, Crenshaw EB, Zwijsen A, Butler SJ. BMP receptor-activated Smads confer diverse functions during the development of the dorsal spinal cord. Dev Biol 2012;367(2):216-27.

27. Phan KD, Hazen VM, Frendo M, Jia Z, Butler SJ. The bone morphogenetic protein roof plate chemorepellent regulates the rate of commissural axonal growth. J Neurosci 2010;30(46):15430-40.

28. Meberg PJ, Bamburg JR. Increase in neurite outgrowth mediated by overexpression of actin depolymerizing factor. J Neurosci 2000;20(7):2459-69.

29.   de Castro F, López-Mascaraque L, De Carlos JA. Cajal: lessons on brain development. Brain Res Rev 2007;55(2):481-9.

30.   Hedgecock EM, Culotti JG, Hall DH. The unc-5, unc-6, and unc-40 genes guide circumferential migrations of pioneer axons and mesodermal cells on the epidermis in C. elegans. Neuron 1990;4(1):61-85.

31.   Ishii N, Wadsworth WG, Stern BD, Culotti JG, Hedgecock EM. UNC-6, a laminin-related protein, guides cell and pioneer axon migrations in C. elegans. Neuron 1992;9(5):873-81.

32.   Placzek M, Tessier-Lavigne M, Jessell T, Dodd J. Orientation of commissural axons in vitro in response to a floor plate-derived chemoattractant. Development 1990;110(1):19-30.

33.   Serafini T, Kennedy TE, Galko MJ, Mirzayan C, Jessell TM, Tessier-Lavigne M. The netrins define a family of axon outgrowth-promoting proteins homologous to C. elegans UNC-6. Cell 1994;78(3):409-24.

34.   Kennedy TE, Serafini T, de la Torre JR, Tessier-Lavigne M. Netrins are diffusible chemotropic factors for commissural axons in the embryonic spinal cord. Cell 1994;78(3):425-35.

35.   Harris R, Sabatelli LM, Seeger MA. Guidance cues at the Drosophila CNS midline: identification and characterization of two Drosophila Netrin/UNC-6 homologs. Neuron 1996;17(2):217-28.

36.   Mitchell KJ, Doyle JL, Serafini T, Kennedy TE, Tessier-Lavigne M, Goodman CS, Dickson BJ. Genetic analysis of Netrin genes in Drosophila: Netrins guide CNS commissural axons and peripheral motor axons. Neuron 1996;17(2):203-15.

37. Moore SW, Tessier-Lavigne M, Kennedy TE. Netrins and their receptors. Adv Exp Med Biol 2007;621:17-31.

38. Wang H, Copeland NG, Gilbert DJ, Jenkins NA, Tessier-Lavigne M. Netrin-3, a mouse homolog of human NTN2L, is highly expressed in sensory ganglia and shows differential binding to netrin receptors. J Neurosci 1999;19(12):4938-47.

39. Yin Y, Sanes JR, Miner JH. Identification and expression of mouse netrin-4. Mech Dev 2000;96(1):115-9.

40. Bradford D, Cole SJ, Cooper HM. Netrin-1: diversity in development. Int J Biochem Cell Biol 2009;41(3):487-93.

41. Lai Wing Sun K, Correia JP, Kennedy TE. Netrins: versatile extracellular cues with diverse functions. Development 2011;138(11):2153-69.

42. Cirulli V, Yebra M. Netrins: beyond the brain. Nat Rev Mol Cell Biol 2007;8(4):296-306.

43. Engelkamp D. Cloning of three mouse Unc5 genes and their expression patterns at mid-gestation. Mech Dev 2002;118(1-2):191-7.

44. Keino-Masu K, Masu M, Hinck L, Leonardo ED, Chan SS, Culotti JG, Tessier-Lavigne M. Deleted in Colorectal Cancer (DCC) encodes a netrin receptor. Cell 1996;87(2):175-85.

45. Leonardo ED, Hinck L, Masu M, Keino-Masu K, Ackerman SL, Tessier-Lavigne M. Vertebrate homologues of C. elegans UNC-5 are candidate netrin receptors. Nature 1997;386(6627):833-8.

46. Fazeli A, Dickinson SL, Hermiston ML, Tighe RV, Steen RG, Small CG, Stoeckli ET, Keino-Masu K, Masu M, Rayburn H and others. Phenotype of mice lacking functional Deleted in colorectal cancer (Dcc) gene. Nature 1997;386(6627):796-804.

47. Dillon AK, Jevince AR, Hinck L, Ackerman SL, Lu X, Tessier-Lavigne M, Kaprielian Z. UNC5C is required for spinal accessory motor neuron development. Mol Cell Neurosci 2007;35(3):482-9.

48. Williams ME, Lu X, McKenna WL, Washington R, Boyette A, Strickland P, Dillon A, Kaprielian Z, Tessier-Lavigne M, Hinck L. UNC5A promotes neuronal apoptosis during spinal cord development independent of netrin-1. Nat Neurosci 2006;9(8):996-8.

49. Leonardo ED, Hinck L, Masu M, Keino-Masu K, Fazeli A, Stoeckli ET, Ackerman SL, Weinberg RA, Tessier-Lavigne M. Guidance of developing axons by netrin-1 and its receptors. Cold Spring Harb Symp Quant Biol 1997;62:467-78.

50. Phan KD, Croteau LP, Kam JW, Kania A, Cloutier JF, Butler SJ. Neogenin may functionally substitute for Dcc in chicken. PLoS One 2011;6(7):e22072.

51. Kolodziej PA, Timpe LC, Mitchell KJ, Fried SR, Goodman CS, Jan LY, Jan YN. frazzled encodes a Drosophila member of the DCC immunoglobulin subfamily and is required for CNS and motor axon guidance. Cell 1996;87(2):197-204.

52. Barallobre MJ, Pascual M, Del Río JA, Soriano E. The Netrin family of guidance factors: emphasis on Netrin-1 signalling. Brain Res Brain Res Rev 2005;49(1):22-47.

53. Wahlsten D. Prenatal schedule of appearance of mouse brain commissures. Brain Res 1981;227(4):461-73.

54. Ashwell KW, Waite PM, Marotte L. Ontogeny of the projection tracts and commissural fibres in the forebrain of the tammar wallaby (Macropus eugenii): timing in comparison with other mammals. Brain Behav Evol 1996;47(1):8-22.

55. Brankatschk M, Dickson BJ. Netrins guide Drosophila commissural axons at short range. Nat Neurosci 2006;9(2):188-94.

56. Winberg ML, Mitchell KJ, Goodman CS. Genetic analysis of the mechanisms controlling target selection: complementary and combinatorial functions of netrins, semaphorins, and IgCAMs. Cell 1998;93(4):581-91.

57. Akin O, Zipursky SL. Frazzled promotes growth cone attachment at the source of a Netrin gradient in the Drosophila visual system. Elife 2016;5.

58. MacLennan AJ, McLaurin DL, Marks L, Vinson EN, Pfeifer M, Szulc SV, Heaton MB, Lee N. Immunohistochemical localization of netrin-1 in the embryonic chick nervous system. J Neurosci 1997;17(14):5466-79.

59. Kennedy TE, Wang H, Marshall W, Tessier-Lavigne M. Axon guidance by diffusible chemoattractants: a gradient of netrin protein in the developing spinal cord. J Neurosci 2006;26(34):8866-74.

60. Moore SW, Zhang X, Lynch CD, Sheetz MP. Netrin-1 attracts axons through FAK-dependent mechanotransduction. J Neurosci 2012;32(34):11574-85.

61. Alcántara S, Ruiz M, De Castro F, Soriano E, Sotelo C. Netrin 1 acts as an attractive or as a repulsive cue for distinct migrating neurons during the development of the cerebellar system. Development 2000;127(7):1359-72.

62. Ono K, Yasui Y, Rutishauser U, Miller RH. Focal ventricular origin and migration of oligodendrocyte precursors into the chick optic nerve. Neuron 1997;19(2):283-92.

63. Tsai HH, Tessier-Lavigne M, Miller RH. Netrin 1 mediates spinal cord oligodendrocyte precursor dispersal. Development 2003;130(10):2095-105.

64. Jarjour AA, Manitt C, Moore SW, Thompson KM, Yuh SJ, Kennedy TE. Netrin-1 is a chemorepellent for oligodendrocyte precursor cells in the embryonic spinal cord. J Neurosci 2003;23(9):3735-44.

65. Yebra M, Montgomery AM, Diaferia GR, Kaido T, Silletti S, Perez B, Just ML, Hildbrand S, Hurford R, Florkiewicz E and others. Recognition of the neural chemoattractant Netrin-1 by integrins alpha6beta4 and alpha3beta1 regulates epithelial cell adhesion and migration. Dev Cell 2003;5(5):695-707.

66. Wilson BD, Ii M, Park KW, Suli A, Sorensen LK, Larrieu-Lahargue F, Urness LD, Suh W, Asai J, Kock GA and others. Netrins promote developmental and therapeutic angiogenesis. Science 2006;313(5787):640-4.

67. Lu X, Le Noble F, Yuan L, Jiang Q, De Lafarge B, Sugiyama D, Bréant C, Claes F, De Smet F, Thomas JL and others. The netrin receptor UNC5B mediates guidance events controlling morphogenesis of the vascular system. Nature 2004;432(7014):179-86.

68. Nakashiba T, Ikeda T, Nishimura S, Tashiro K, Honjo T, Culotti JG, Itohara S. Netrin-G1: a novel glycosyl phosphatidylinositol-linked mammalian netrin that is functionally divergent from classical netrins. J Neurosci 2000;20(17):6540-50.

69. Nakashiba T, Nishimura S, Ikeda T, Itohara S. Complementary expression and neurite outgrowth activity of netrin-G subfamily members. Mech Dev 2002;111(1-2):47-60.

70. Skarnes WC, Moss JE, Hurtley SM, Beddington RS. Capturing genes encoding membrane and secreted proteins important for mouse development. Proc Natl Acad Sci U S A 1995;92(14):6592-6.

71. Bin JM, Han D, Lai Wing Sun K, Croteau LP, Dumontier E, Cloutier JF, Kania A, Kennedy TE. Complete Loss of Netrin-1 Results in Embryonic Lethality and Severe Axon Guidance Defects without Increased Neural Cell Death. Cell Rep 2015;12(7):1099-106.

72. Brunet I, Gordon E, Han J, Cristofaro B, Broqueres-You D, Liu C, Bouvree K, Zhang J, del Toro R, Mathivet T and others. Netrin-1 controls sympathetic arterial innervation. J Clin Invest 2014;124(7):3230-40.

73. Yung AR, Nishitani AM, Goodrich LV. Phenotypic analysis of mice completely lacking netrin 1. Development 2015;142(21):3686-91.

CHAPTER 2 - Netrin1 produced by neural progenitors, not floor plate cells, is required for axon guidance in the spinal cord

ABSTRACT

Netrin1 has been proposed to act from the floor plate (FP) as a long-range diffusible chemoattractant for commissural axons in the embryonic spinal cord. However, *netrin1* mRNA and protein are also present in neural progenitors within the ventricular zone (VZ), raising the question of which source of netrin1 promotes ventrally-directed axon growth. Here, we use genetic approaches in mice to selectively remove netrin from different regions of the spinal cord. Our analyses show that 1) the FP is not the source of netrin1 directing growth cones to the ventral midline and 2) by contrast, local VZ-supplied netrin1 is required for this step in axon guidance. Furthermore, netrin1 protein is not present as a gradient, it rather accumulates on the pial surface adjacent to the path of commissural axon extension. Thus, netrin1 does not act as a long-range secreted chemoattractant, but instead promotes ventrally-directed axon outgrowth by haptotaxis, i.e. directed growth along an adhesive surface.

SGV performed all experiments. JK, KDP, T-JK, BGN, JC and AK provided tissue reagents. HE provided a mouse line. SJB and SGV conceived and designed the experiments with input from BGN. SJB and SGV wrote the manuscript.

INTRODUCTION

The establishment of neural circuits during development requires neurons to extend axons along precise pathways towards their synaptic targets. Axons can navigate over considerable distances, using molecular cues in the embryonic environment to both spatially and temporally orient their growth cones[1,2]. These guidance cues have been proposed to fall into four major categories: attractive or repulsive signals that act as either long-range diffusible molecules or short-range contact-dependent signals, i.e. tethered to a cellular membrane or the extracellular matrix (ECM)[3]. Particular attention has been placed on identifying diffusible cues from "guidepost" source cells, which could direct axonal growth cones over long distances.

The textbook example of a chemotropic guidance factor is netrin1, a member of the laminin superfamily first characterized in the vertebrate spinal cord[4,5]. Studies in chicken and mouse led to the proposal that netrin1 emanates from the floor plate (FP) and acts as a diffusible chemoattractant to direct the ventral growth of spinal commissural axons[4]. Considerable work using soluble netrin1 in *in vitro* assays supported the hypothesis that it can act at a distance to orient axon growth[6-8]. However, subsequent investigation in other systems, including angiogenesis and retinal, pancreatic and mammary gland development, have indicated that netrin1 acts between cells, and between cells and the ECM, to regulate cell adhesion and tissue morphogenesis[9]. Notably, studies in the Drosophila nerve cord and visual system have shown that membrane-tethered netrin was sufficient to rescue axon guidance defects in *netrinA/B* mutants[10,11]. Recently, studies using live imaging in the visual system have demonstrated that target-derived netrin1 is required to attach growth cones to source cells[12]. However, despite

significant progress understanding netrin-mediated axon guidance, it has not been resolved whether netrin1 acts from the FP as a diffusible chemoattractant *in vivo*.

In the mouse spinal cord, *netrin1* is expressed by neural progenitors in ventricular zone (VZ), in addition to the FP[13]. Moreover, netrin1 protein has a complex distribution that does not fit the model of a simple continuous gradient emanating from the FP[14]. In this study, we set out to determine which source of netrin1 in the spinal cord directs axonal growth to the FP. To resolve this question, we used conditional genetic approaches in mouse to remove netrin1 expression from either the VZ or the FP. In the absence of either netrin1 or Dcc, spinal axons aberrantly innervate the VZ and commissural axons either stall or are dramatically defasciculated. However, these phenotypes are only observed when netrin1 is ablated from the VZ, but not the FP. We thus unambiguously demonstrate that the key source of netrin1 supplying guidance activities comes from neural progenitors in the VZ, rather than the FP as previously suggested. Our studies further demonstrate that the cellular geometry of spinal neural progenitors permits the establishment of a netrin1$^+$ growth substrate along the pial surface of the spinal cord, which acts to position and promote fasciculated spinal axon outgrowth, in a Dcc-dependent manner. Thus, rather than acting as a soluble diffusible molecule produced by the FP, netrin1 promotes ventrally-directed outgrowth by haptotaxis, the directed growth of cells along an adhesive surface[15].

MATERIALS AND METHODS

Generation and analysis of mutant mice: Netrin1[13], *Dcc*[16], *Gli2*[17] mice were bred into 129/Sv backgrounds; *Unc5a*[18], *Unc5c*[19], Dbx1::*cre*[20], Olig2::*cre*[21], Rosa26R::*gfp*[22], *Rbpf*$^{flox/flox}$ mice[23], *Netrin1*$^{flox/flox}$ mice, Shh::*cre*[24] and Pax3::*cre*[25] were maintained in C57BL/6 backgrounds. The *netrin1* mutant strain stems from *lacZ* having been inserted into the *netrin1* genomic locus and is considered to be a hypomorphic allele[13]. While there are trace amounts of residual *netrin1* expression in *netrin1*$^{lacZ/lacZ}$ FPs, there is no detectable *netrin1* transcript in the *netrin1*$^{lacZ/lacZ}$ VZ at any stage (Figures S1C) or any detectable netrin1 protein at either the pial surface or on spinal axons (Figure 4E). Note that as previously described[13,26], netrin1 antibodies detect both the endogenous protein associated with cell membranes and the netrin1::β-gal fusion protein, which accumulates in the cytoplasm of mutant cells.

Mice were handled and housed in accordance with the University of California Los Angeles IACUC guidelines. Embryos were derived from timed matings with heterozygous mice. The day of the plug was counted as E0.5, and embryos were harvested at E11.5. Notch OFF mice were generated by crossing Dbx1::*cre* mice with *Rbpf*$^{flox/flox}$ mice, as previously described[21]. Netrin1 conditional knockout embryos were generated by crossing Shh::*cre* or Pax3::*cre* drivers with *netrin1*$^{flox/flox}$ mice. *Netrin1*$^{lacZ/lacZ}$, *Unc5c* and *Dcc* analyses used littermate wild-type controls, except in the case of *Unc5a* mice, which were bred as homozygous mutants and compared to *Unc5c* wild-type controls. All the conditional knockout analyses used heterozygous floxed littermates as controls. Genotypes were identified by PCR reactions using cDNA for *netrin1*$^{lacZ/lacZ}$ embryos and genomic DNA for all other lines.

Immunohistochemistry: Mouse embryonic spinal cords (E10.5-E12.5) were fixed in 4% paraformaldehyde for 2 hours at 4°C, cryoprotected in 30% sucrose in PBS overnight and thin-sectioned to yield 30μm transverse sections. Antibody staining was performed by incubating the sections with primary antibodies at 4°C overnight, followed by fluorescently-labeled secondary antibodies at room temperature for 2 hours. Antibodies against the following proteins were used for immunostaining: *Rabbit:* neurofilament (NF), 1:200 (Cell Signaling Technology C28E10); Shh, 1:200 (H4[27]); Laminin, 1:1000 (Abcam #ab11575); *Goat:* human Robo3, 1:200 (R&D Systems AF3076); mouse Dcc, 1:500 (R&D Systems AF844); mouse netrin1, 1:500 (R&D Systems AF1109); β-galactosidase, 1:2000 (Biogenesis 4600-1409); Sox2, 1:2000 (Santa Cruz Biotechnology #17320); *Mouse:* cre, 1:1000 (Covance MMS-106P); Sox2, 1:1000 (Santa Cruz Biotechnology #365823); mAb Tag1 1:100 (4D7, Developmental Studies Hybridoma Bank (DSHB)); NF, 1:100 (3A10 DSHB); Nestin, 1:50 (Rat-401 DSHB); *Chicken:* GFP, 1:1000 (Aves Lab #1020); neurofilament, 1:2000 (Millipore #AB5539). Secondary antibodies (all from Jackson Immunoresearch Laboratories) were used as follows: FITC, 1:500; Alexa488, 1:1000; Cyanine3, 1:1000; Cyanine5 1:700.

Antigen retrieval: The netrin1 antibody signal was augmented using standard antigen retrieval techniques. Slides were post-fixed with 4% paraformaldehyde for 10 minutes, rinsed with PBS, and boiled in a 10mM sodium citrate buffer (pH 6.0) for 3 minutes in a microwave. Slides were allowed to cool in the buffer solution for 20 minutes at room temperature, before processing for immunohistochemistry. All netrin1 immunostaining was performed with antigen retrieval except when used with antibodies that were affected by the retrieval method; for example, Tag1 antigenicity was completely lost, while laminin antigenicity was moderately affected post-

retrieval. The netrin1 staining in Figure 3A-3C and Figure 3M were performed without retrieval to preserve the antigenicity of the sample. Netrin1 protein is most readily observed after antigen retrieval methods. See figures 3K and 3A for a respective comparison with and without antigen retrieval; the specificity of the netrin1 antibody is demonstrated in Figure 4B and 4E.

Confocal Imaging and 3D rendering: Images were acquired on Carl Zeiss LSM700, LSM800 and LSM880 with Airyscan confocal microscopes and processed using Carl Zeiss Zen 2012 and Adobe Photoshop CS6 software. Imaris x64 v8.3 and Imaris XT software from Bitplane Inc (http://bitplane.com) were used to render 3d models of images. Movies S1, S2, S3 were processed using Imaris and Imaris XT: the 'spots' function was used to render 3D models of netrin1 protein while the 'surfaces' function was used to render 3D models of nestin and NF. A threshold for intensity sum was used for each channel and spots were further classified with respect to distance from each surface using the 'spots close to surface' Matlab Imaris XTension.

In situ hybridization: Digioxigenin (DIG) labeled probes against the 3' untranslated regions of genes of interest were generated using the Roche RNA Labeling Kit and were used on 12μm transverse sections. mRNA signal was visualized using NBT/BCIP and anti-DIG antibody conjugated with an alkaline phosphatase fragment (Roche). Target sequences were amplified using cDNA from mouse embryonic spinal cord using the following primers that were designed with the Primer 3 program (http://primer3plus.com/):
Unc5A: forward 5'-TGAAGTTGTCCCTCGATGCT-3', reverse 5'-
GACATTAACCCTCACTAAAGGGAGTGATCGTGTGCCTGAATCC-3';

Unc5C: forward 5'- CCTTTGCCCATTTCTGTGTT-3', reverse 5'-

GAC<u>TAATACGACTCACTATAGGG</u>AGAAGACAGCAGGAGGGTGA-3';

The underlined text denotes either a T3 or T7 polymerase binding site. Dcc and netrin1 probes were described previously[28,13].

Quantification and statistical analysis: No statistical methods were used to predetermine sample sizes, but these were similar to those in our previous publications [1]. All quantifications were performed blind. Data were tested for normality and compared using a 2-paired 2-tail Student's *t*-test. Probability of similarity, *** $p < 0.0005$, ** $p < 0.005$, * $p < 0.05$. Variance was similar between groups being compared. n represents number of sections in all cases; for each experiment sections were analyzed and pooled together from multiple embryos from more than one litter. Data is represented as mean±SEM.

Data and software availability: All statistics and graphs were generated using Microsoft Excel and Graphpad Prism6 software. See Key Resources Table for information regarding other softwares used.

RESULTS

FP-derived netrin1 is not required for commissural axon guidance to the FP

The canonical model for netrin1 function in the spinal cord suggests that netrin1 acts as a diffusible chemoattractant emanating from the FP[13]. However, *netrin1* transcript is also expressed by many progenitors in the VZ in the mouse spinal cord[13], a region ubiquitously avoided by spinal axons (**Supplementary Figure 2-S1 A-D**)[29]. To resolve the role of FP- versus

VZ-derived netrin1, we have used multiple genetic approaches to determine the spatial requirement for netrin1 in the developing spinal cord.

First, we assessed the consequence of anatomically deleting the FP on the trajectory of neurofilament (NF)$^+$ spinal axons in E11.5 mouse embryos. Gli2 is a key transcriptional regulator that transduces sonic hedgehog (Shh) signaling[17]. The FP and V3 interneurons are ablated in *Gli2$^{-/-}$* mutants, resulting in the loss of FP-derived netrin1 (**Figures 2-1 A', B', D' and E')**[17]. Critically for our studies, the VZ expression of *netrin1* is largely unaffected in *Gli2$^{-/-}$* mutants (**Figure 2-1 B**). In contrast, *netrin1* expression is lost from the VZ in *Gli2; netrin1* double mutants (**Figure 2-1 C'**). Strikingly, the absence of the FP has no significant effect on the trajectory of NF$^+$ axons, they continue to ubiquitously avoid the VZ in similar numbers to control littermates (p>0.22, **Figures 2-1 D, E, G', H', J and K**) [30,31]. In contrast, NF$^+$ axons robustly extend into the VZ in *Gli2$^{-/-}$; netrin1$^{lacZ/lacZ}$* spinal cords (**Figures 2-1 F, I' and K**), in comparable numbers to those observed in *netrin1$^{lacZ/lacZ}$* single mutants (**Figures 2-1 BB, T**). Thus, NF$^+$ axon guidance defects are only observed in the absence of VZ-derived netrin1.

Second, we conditionally ablated netrin1 from the FP (netrin1ΔFP) using the Shh::*cre* driver line[24] in combination with a *netrin1$^{flox/flox}$* allele[32]. In these mice, the presence of cre in the FP (**Figures 2-1 N-N"**) results in the specific loss of netrin1 protein from the FP (**Figures 2-1 L-M'**). Remarkably, this manipulation resulted in no significant disruption in axonal growth (**Figures 2-1 X-AA**). In particular, both Tag1$^+$ and Robo3$^+$ commissural spinal axons project normally around the VZ and across the FP, in tightly fasciculated bundles, in a manner similar to control littermates (**Figures 2-1 P-W, BB and CC**; p>0.31). This result is in contrast to the previously characterized loss-of function allele of netrin1 (*netrin1$^{lacZ/lacZ}$*) which shows multiple perturbations in axon growth: first, many NF$^+$ axons grow medially into the VZ (arrows, **Figures**

2-1 U, BB-CC and Supplementary Figures 2-S1 C and F), second, Robo3$^+$ commissural axons are profoundly defasciculated in the ventral spinal cord (**Figures 2-1 V, and Supplementary Figures 2-S1 D and G**)[33] with many NF$^+$Robo3$^+$ axons growing medially into the VZ at all levels (**Supplementary Figures 2-S1 H-I**) and third, Tag1$^+$ commissural axons stall above the developing motor column[13] (arrows, **Figure 2-1 W**). Notably, these aberrantly projecting axons were seen to extend Robo3$^+$ growth cones at the tip of NF$^+$ axons, indicating that these axons are actively extending into the VZ and are not trailing processes (arrows, **Supplementary Figures 2-S1 E and J**). Taken together, these findings indicate that the commissural axon defects previously observed in *netrin1* mutants do not arise from the loss of netrin1 from the FP.

VZ-derived netrin1 is necessary for axon guidance to the FP

We next sought to examine whether the selective loss of netrin1 from the VZ could recapitulate the axon guidance defects seen in *netrin$^{lacZ/lacZ}$* mutants. Towards this goal, we removed netrin1 from all dorsal spinal progenitors (netrin1ΔdVZ) by recombining the *netrin1$^{flox/flox}$* allele with a Pax3::*cre* driver line[25] (**Figure 2-2 C**). Netrin1 protein decorates both the pial surface of the spinal cord, as well as commissural axons[14]. Following cre recombination, netrin1 is specifically ablated from the dorsal pial surface and axons extending within the dorsal spinal cord (**Figures 2-2 A, D**), repositioning these axons laterally such that they contact the laminin$^+$ basement membrane (**Figures 2-2 B, E**). Netrin1 levels in the netrin1ΔdVZ FP are comparable to those seen in control littermates (**Figures 2-2 F, G**).

The netrin1ΔdVZ manipulation resulted in many guidance phenotypes similar to those observed in *netrin1$^{lacZ/lacZ}$* embryos. NF$^+$ axons aberrantly grow both dorsally towards the RP and medially into the dorsal VZ (**Figures 2-2 H, L, P-S**). Robo3$^+$ commissural axons are also

significantly defasciculated compared to control littermates (**Figures 2-2 J, N, T and U**). Interestingly, the extent of defasciculation is not as profound as is observed for *netrin1^{lacZ/lacZ}* embryos (**Supplementary Figures 2-S1 F, H**), perhaps because netrin1 does belatedly accumulate on axons as they grow into the ventral netrin1$^+$ region (arrows, **Figure 2-2 D**). Nonetheless, fewer netrin1$^+$ axons appear to cross the FP (arrows, **Figures 2-2 F, G**). Tag1$^+$ axon growth is also diminished, such that fewer Tag1$^+$ fascicles extend to the FP in the netrin1ΔdVZ mutants compared to littermate controls (**Figures 2-2 K, O**).

We also examined the consequence of a smaller deletion in *netrin1* expression by focally disrupting neural progenitor maintenance. We used a Dbx1::*cre* driver line to functionally inactivate Rbpj, the key transcriptional effector of the Notch signaling pathway, specifically in the p0 progenitor domain Notch OFF; [21]. We used a ROSA26R::*gfp* reporter line to simultaneously lineage trace Dbx1$^+$ cells (**Figures 2-2 V, AA**). As previously reported[21], silencing Notch signaling in p0 progenitors results in the loss of Sox2 and other neural progenitor characteristics including *netrin1* expression (brackets, **Figures 2-2 X-Z, CC-EE**). This manipulation creates two ectopic boundaries of *netrin1* expression not seen in controls (brackets, **Figures 2-2 Y, DD**). The distribution of pial-associated netrin1 is not significantly affected by this manipulation (data not shown). Nevertheless, >2-fold more NF$^+$ axons grow into the Notch OFF GFP$^+$ region (arrows, **Figure 2-2 EE**), with many axons precisely following along the edge of the ectopic *netrin1* boundaries (brackets, **Figures 2-2 W, BB, EE and II**).

This axon growth phenotype does not result as a secondary consequence of inactivating Notch: conditionally ablating Rbpj from the pMN alters progenitor patterning[21], but does not disrupt the expression of Sox2 (**Figures 2-2 FF and HH**) or *netrin1* expression (data not shown). Consistent with these findings, NF$^+$ axon trajectories were not affected by this manipulation

(brackets, **Figures 2-2 GG and HH**). Collectively, these experiments demonstrate that the axonal growth defects observed in *netrin1* mutants are due to the loss of netrin1 derived from the VZ, not the FP.

Neural progenitors establish a netrin1$^+$ growth substrate on the pial surface of the spinal cord

We next explored the role that VZ-derived netrin1 plays guiding spinal axons. Previous studies have suggested that there is a key difference between the distribution of *netrin1* transcript, which can be detected by *in situ* hybridization or genetically encoded β-galactosidase (β-gal) from the *netrin1^{lacZ}* reporter line[13], and netrin1 protein[14]. While *netrin1* transcript is made by neural progenitors in the VZ (**Figures 2- 3 A, B**), netrin1 protein decorates the laminin$^+$ pial surface (**Figure 2-3 C**) and commissural axons (chevrons, **Figure 2-3 C'**). We observed a striking coincidence between the presence of netrin1 at the pial surface and the dorsal boundary of *netrin1* expression in the VZ (dotted lines, **Figures 2-3 A-C**). This alignment suggests that netrin1 is produced by bipolar neural progenitors and then transported via their nestin$^+$ radial processes to the basement membrane where their endfeet contact the laminin$^+$ pial surface[34]. Supporting this hypothesis, we are unable to detect netrin1 protein in the dorsal-most spinal cord (**Figures 2-3 D-F**), further suggesting that there is limited or no diffusion of netrin1. In the intermediate spinal cord, netrin1 protein can be readily detected in nestin$^+$ fibers (**Supplementary Movie 2-S1**) and endfeet as they contact the basal pial surface (arrows, **Figure 2-3 H**). Netrin1 is also co-localized with laminin on the pial surface (**Figures 2-3 G, I**).

There is also a striking correlation between the pattern of spinal axon extension and the domains of *netrin1* transcript and netrin1 protein. From early stages of axiogenesis, NF$^+$ axons

appear to preferentially extend immediately adjacent to the netrin1[+] pial substrate (**Figures 2-3 K, K'**), and do not innervate the VZ (**Figures 2-3 J, J'**). By E11.5, all axons grow alongside the laminin[+] netrin1[+] pial substrate in the dorsal-intermediate spinal cord (**Figures 2-3 M, M'**). Tag1^{+} and Robo3^{+} axons also project in a fasciculated manner precisely around the netrin1::β-gal[+] VZ (**Figures 2-3 L, M**) and then beneath the netrin1::β-gal^{+} cells in the FP (dotted lines, **Figure 2-3 L'**). Together with our genetic studies, these data supports the model that commissural axon extension is shaped by the polarized deposition of netrin1 at the pial surface.

As commissural axons grow alongside the netrin1[+] substrate, they accumulate netrin1 protein (chevrons, **Figures 2-3 K and 2-4 B**). This distribution is not an artifact of our detection methods: netrin1 is completely absent from both the pial surface and axons in *netrin1[lacZ/lacZ]* mutants (**Figures 2-4 D-F**). The remaining VZ staining (**Figure 2-4**) stems from the netrin1 antibody recognizing a cytoplasmic truncated netrin1::β-gal fusion product[13,26]. Remarkably, we find that the axonal distribution of netrin1 is dependent on Dcc, the receptor thought to mediate chemoattractive responses to netrin1[35]. In *Dcc* mutants, netrin1 is present at normal levels on the pial surface, but is greatly reduced in axons (**Figures 2-4 G-I**). Together, these results suggest that netrin1 accumulates on commissural axons in a Dcc-dependent manner to promote fasciculated axon growth around the VZ.

Dcc mediates the activity of VZ-derived netrin1

We further examined the model that Dcc is required to mediate the activities of pial-associated netrin1 by examining mice mutant for either *Dcc* or members of the *Unc5* family, the receptor complex that mediates the chemorepellent activities of netrin1[35]. *Dcc* is widely expressed in postmitotic neurons in the spinal cord (**Supplementary Figure 2-S2 A**) and Dcc

protein decorates a broad population of commissural axons (**Supplementary Figures 2-S2 D-2F**)[28]. Of the Unc5 family, only *Unc5a* and *Unc5c* have detectable expression in postmitotic neurons in the spinal cord (**Supplementary Figures 2-S2 B-2C**)[36-38]. Analysis of *Dcc*, *Unc5a* and *Unc5c* mutants, demonstrated that only the loss of *Dcc* recapitulated all of the phenotypes seen in *netrin1*[*lacZ/lacZ*] mice to quantitatively similar amounts (**Figures 2-4 P, 2-1 M and Supplementary Figure 2-S2 M**). In the absence of *Dcc*, NF$^+$ and Robo3$^+$ axons profusely project into the VZ (**Figures 2-4 M-P**) and Robo3$^+$ axons are highly defasciculated, extending throughout the motor column (**Figure 2-4 O**). In contrast, Robo3$^+$ axon extension was not perturbed in the *Unc5a* and *Unc5c* mutants (**Supplementary Figures 2-S2 G-I, and 2-S2 M**). Together, these observations support the conclusion that Dcc is the key receptor in spinal commissural axons that orients their ventrally-directed extension along the pial-netrin1 substrate and permits them to grow around the VZ.

DISCUSSION

Reassessing the role of netrin1 in the spinal cord

Netrin1 was first identified in a biochemical screen for soluble factors in chicken brain extracts that promote axon outgrowth[4,5]. Through these experiments, netrin1 became the prototypical example of a long-range diffusible chemoattractant, secreted by the FP (**Figure 2-4 Q**). Here, we propose an alternative model: VZ-derived netrin1 acts as a growth substrate that promotes ventrally-directed axonal growth by haptotaxis (**Figure 2-4 R**). Our conditional genetic analyses have distinguished between these models. Axon guidance defects are observed after netrin1 is removed from the VZ but not the FP (**Figures 2-4 T-U**). Thus, FP-derived netrin1 is not required for commissural axon guidance.

Netrin1 belongs to the laminin superfamily, most closely resembling the laminin γ chain[5], making it plausible that netrin1 functions within the context of the ECM. Our studies show that netrin1 closely associates with the laminin along the pial surface of the spinal cord, to establish a local growth substrate for axons. This result is consistent with previous studies demonstrating that netrin1 acts locally in other systems[10-12,39,40]. While our model is inconsistent with the observations that netrin1 appears to act as graded diffusible chemoattractant in *in vitro* assays, it is noteworthy that these assays usually require ECM components, such as laminin or collagen for axon extension[41]. These ECM factors might convert bath- or pipette-applied netrin1 into a tethered substrate for growth[42].

VZ-derived netrin1 mediates axon growth in a Dcc-dependent manner

Our studies suggest that netrin1 functions as a growth substrate for axons in the developing spinal cord. We propose that the netrin1 protein made by bipolar neuroepithelial progenitors is transported from the VZ to the lateral margins of the spinal cord, where the basal progenitor endfeet contact the laminin$^+$ pial surface (**Figure 2-4 S**)[43]. Pial-associated netrin1 both orients ventrally-directed axon growth and promotes fasciculation. The mechanism by which the netrin1 promotes axon fasciculation remains unclear; however, it is intriguing that netrin1 accumulates on axons after encountering pial-associated netrin in a Dcc-dependent manner. Thus, netrin1 is only observed on commissural axons as they enter the ventral spinal cord after the ablation of netrin1 from dorsal neural progenitors (**Figure 2-4 U**). Moreover, axonal netrin1 is greatly diminished in *Dcc* mutants even though netrin1 is present at the pial surface. One possibility is that Dcc and netrin interact *in cis* in commissural axons to promote their fasciculated growth around the VZ (**Figure 2-4 S**). Indeed, Netrin and Dcc (frazzled) have

previously been suggested to interact within axons in Drosophila, to permit the *en passant* presentation of netrin to subsequent axons[44].

The VZ-derived netrin1 guidance cue also appears to permit axons to grow precisely around domains of *netrin1* expression. This boundary activity was most notably observed after the focal loss of *netrin1* expression in the VZ using the Notch OFF approach. NF[+] axons deviate from their trajectories to follow the two ectopic borders of *netrin1* expression in the VZ (**Figure 2-2 EE**). The mechanistic basis of this boundary requires further study. Is the netrin1[+] pial substrate an adhesive "go" surface that that is sufficient to promote fasciculated axon growth, perhaps by "pulling" axons towards it and thereby out of the VZ? Or do the *netrin1*-expressing neural progenitors also represent a "no go" region which is actively avoided by axons?

Our studies suggest that many classes of spinal axons require netrin1 to avoid growing in the VZ. The Tag1^{+} population of dorsal commissural axons may be an exception to this general rule. Neither Tag1^{+} nor Atoh1::*taugfp*[+] (data not shown) commissural axons grow medially into the VZ as robustly as Robo3/NF[+] axons in *netrin1/Dcc* mutants, suggesting that additional factors may keep the dorsal-most dI1 axons from growing into the VZ. However, as with other populations of spinal axons, Tag1^{+} axon outgrowth is not dependent on signals from the FP. Outgrowth defects are only observed when netrin1 is ablated either entirely (**Figure 2-1 W**,[13]) or specifically from the VZ (**Figure 2-2 O**).

In summary, our studies show that FP-derived netrin1 is not required to direct axon growth within the spinal cord, suggesting that netrin1 does not act as a diffusible chemotropic guidance signal. We propose that VZ-derived netrin1 provides an adhesive axon growth substrate to orient axon extension towards the ventral midline and promote axon fasciculation.

FIGURES

Figure 2-1: FP-derived netrin1 is not required to direct the circumferential trajectory of spinal axons.
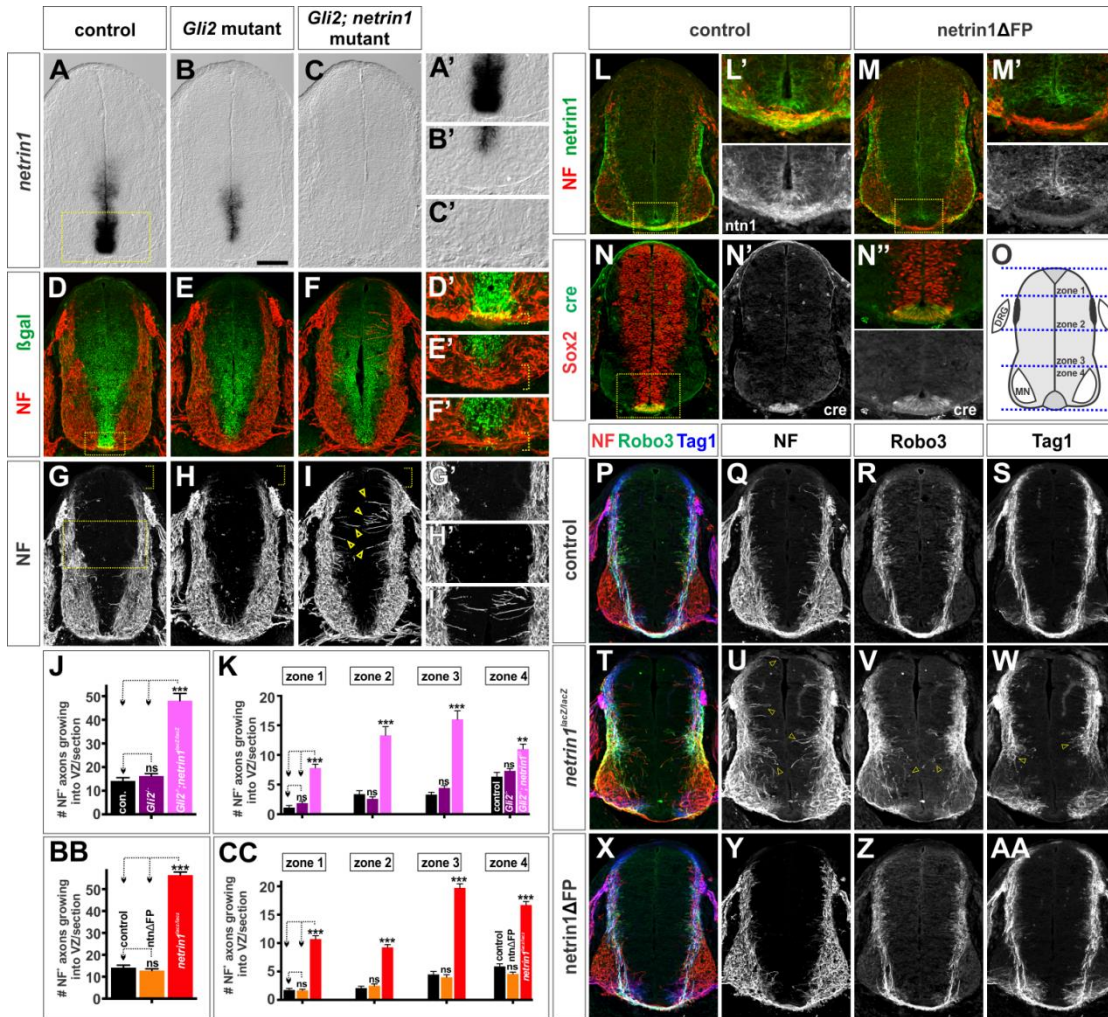
(A-I, L-AA) Thoracic level transverse sections from E11.5 *netrin1$^{+/lacZ}$; Gli2$^{+/-}$* (control, A, D, G), *netrin1$^{+/lacZ}$; Gli2$^{-/-}$* (*Gli2* mutant, B, E, H), *netrin1$^{lacZ/lacZ}$; Gli2$^{-/-}$* (*netrin1*; *Gli2* mutant, C, F,I) Shh::*cre*; *netrin1$^{flox/+}$* (control, L, N, P-S), Shh::*cre*; *netrin1$^{flox/flox}$* (netrin1ΔFP M, X-AA), *netrin1$^{lacZ/lacZ}$* (T-W) mouse spinal cords.

42

(**A-C**) *Netrin1* expression is specifically lost from the FP in *Gli2* mutants (B, FP region is shown magnified in A'-C'), and is completely absent from *Gli2; netrin1* mutants.

(**D-I**) NF$^+$ axons grow circumferentially in control and *Gli2* mutants avoiding the netrin1::β-gal$^+$ VZ (G', H'). In contrast, NF$^+$ axons extend robustly into the VZ in the *Gli2; netrin1* mutants (arrows, I').

(**J, K, O**) Quantification showed that there are 2-3 fold more NF$^+$ axons extending towards the VZ in the *Gli2; netrin1* mutants (48.1±3.1 NF$^+$ axons/section; n=26 sections from 2 embryos) compared to either control (14.2±1.4 NF$^+$ axons/section; n=26 sections from 2 embryos) or *Gli2* mutants (16.2±1.0 NF$^+$ axons/section; n=50 sections from 4 embryos). *Gli2; netrin1* mutant axons extend aberrantly into the VZ in all zones of the spinal cord (O).

(**L-M**) Netrin1 is specifically lost from the FP in the netrin1ΔFP mice compared to control (FP region magnified in L' and M').

(**N**) Cre is only present in FP cells in both control and netrin1ΔFP embryos (FP region magnified in N'').

(**O**) Quantification schematic of four zones along the dorsal-ventral axis of the spinal cord.

(**P-AA**) The NF$^+$, Tag1$^+$ and Robo3$^+$ populations of axons project apparently normally around the VZ in netrin1ΔFP spinal cords (X-AA), very similar to littermate controls (P-S) and distinct from the multiple phenotypes observed in *netrin1*$^{lacZ/lacZ}$ mutants (T-W)[13,33].

(**BB, CC**) Quantification demonstrated that there is no significant difference (p>0.31) between the number of NF$^+$ axons extending towards the VZ in control (14.2±1.1 NF$^+$ axons/section; n=53 sections from 3 embryos) and netrin1ΔFP (12.8±0.8 NF$^+$ axons/section; n=67 sections from 4 embryos) mice. In contrast, NF$^+$ axons profusely project into the VZ in *netrin1*$^{lacZ/lacZ}$ mutant

embryos (56.4±1.4 NF$^+$ axons/section; n= 68 sections from 6 embryos) at all zones of the spinal

cord (O). ** p<0.005, *** p< 0.0005, Student's *t*-test.

Figure 2-2: Selective depletion of netrin1 from the VZ results in axon guidance defects
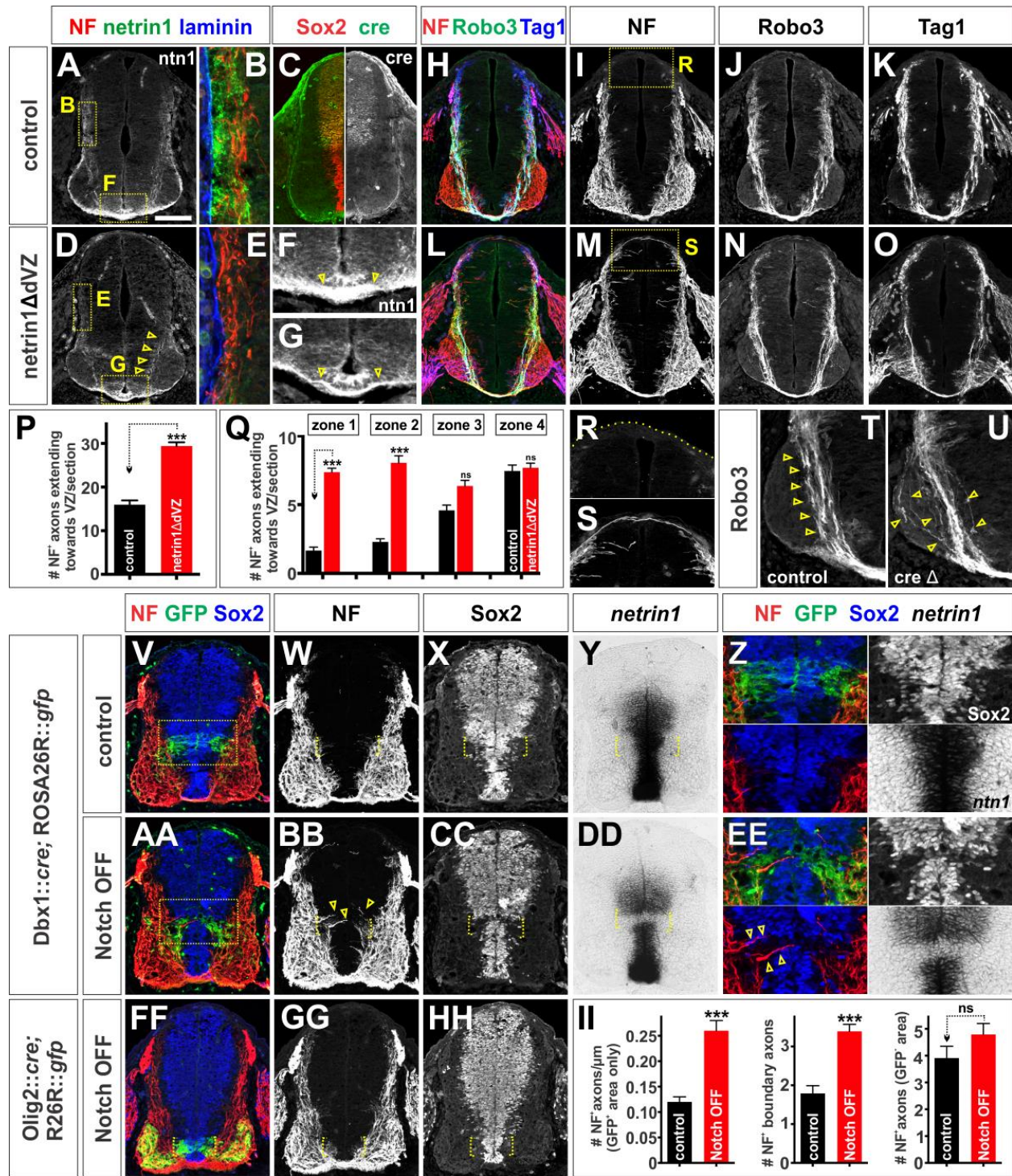
(A-U, V-HH) Thoracic level transverse sections of E11.5 Pax3::*cre*; *netrin1*$^{flox/+}$ (control, A-C, F, H-K, R, T), Pax3::*cre*; *netrin1*$^{flox/flox}$ (netrin1ΔdVZ, D-E, G, L-O, S, U), Dbx1*::cre*; ROSA26R*::gfp* (control, V-Z), Dbx1*::cre*; *Rbpj*$^{flox/flox}$; ROSA26R*::gfp* (Notch OFF, AA-EE), Olig2*::cre*; *Rbpj*$^{flox/flox}$; ROSA26R*::gfp* (Notch OFF, FF-II) mouse spinal cords.

(A-G) The Pax3::*cre* line drives expression of cre specifically in the dorsal spinal progenitors (C), resulting in the loss of netrin1 from the dorsal spinal cord of netrin1ΔdVZ embryos (D, E) and not in control littermates (A, B). The NF$^+$ axons move laterally in the netrin1ΔdVZ mice to be immediately adjacent to the laminin$^+$ pial surface (B, E).

(H-K, R, T) In control littermates, NF$^+$ axons generally avoid the VZ (I) and dorsal-most spinal cord (R), while Robo3$^+$ (J) and Tag1$^+$ (K) commissural axons project in a tightly fasciculated bundle around the VZ and towards the FP (arrows, T).

(L-O) In contrast, there are many axon guidance defects in the netrin1ΔdVZ embryos. NF$^+$ axons extend into the dorsal VZ, with some axons reaching the roof plate (magnified panel in S). Robo3$^+$ axons are defasciculated as they extend ventrally (N, arrows, U), and the number of Tag1$^+$ axons reaching the FP appears to be diminished (O).

(P, Q) Quantification demonstrated that 2-fold more NF$^+$ axons extend towards the VZ in the netrin1ΔdVZ embryos 29.4±0.9 NF$^+$ axons/section; n=102 sections from 5 embryos) compared to controls (16.0±1.0 NF$^+$ axons/section; n=64 sections from 3 embryos). These NF$^+$ axons only grew into the VZ in the dorsal zones (i.e. zones 1 and 2), where netrin1 was no longer present, while no significant difference was observed in zones 3 and 4 (p>0.11 and p>0.32 respectively).

(V-Z) The Dbx1::*cre* driver line targets GFP reporter gene expression to the p0 domain (box in V shown magnified in panel Z).

(AA-EE) The Dbx1::*cre* driver line is used to deplete Notch signaling from p0 domain, the Sox2$^+$ progenitors in this region (brackets,CC) rapidly differentiate into post-mitotic neurons [21], which do not express *netrin1* (bracket, DD). NF$^+$ axons now extend around the ectopic netrin1 boundary (arrows, BB).

(FF-HH) Loss of Notch signaling in the Olig2$^+$ pMN domain has no effect on Sox2$^+$ progenitors (bracket, HH), and does not create an ectopic netrin1 boundary or perturb NF$^+$ axon trajectories.

(II) There are >2 fold more NF$^+$ axons/μm entering the VZ in the GFP$^+$ p0 region in the Notch OFF spinal cord compared to controls. Of these, 2-fold more project precisely along the p0 GFP boundary. There was no significant difference ($p>0.15$) in the number of NF$^+$ axons projecting into the VZ outside the GFP$^+$ p0 region in the Notch OFF and control spinal cords. Control: n=47 sections from 4 mice; Notch OFF: n= 66 sections from 6 mice. ******* $p< 0.0005$ Student's *t*-test.

Figure 2-3: Spinal progenitors establish a growth substrate of netrin1 on the pial surface
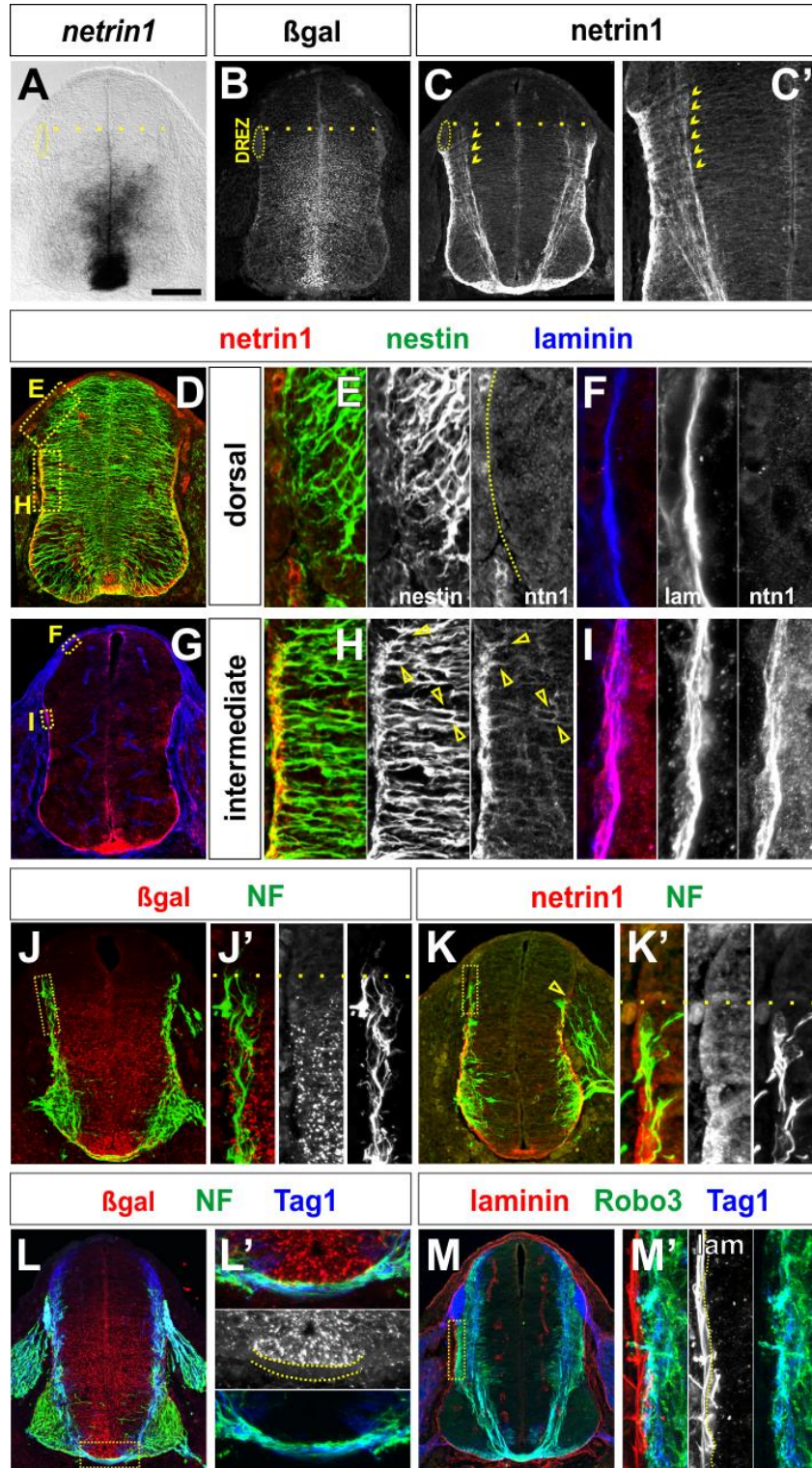
(A-M) E11.5 thoracic (A-B and L) and lumbar (J) *netrin1^{lacZ/+}* and E10.5 lumbar (K) and E11.5 thoracic (C-G and M) *netrin1^{+/+}* mouse spinal cords. Note that for netrin1 immunohistochemisty, panels G was processed without antigen retrieval.

(A, B) *Netrin1* (A) and netrin1::β-gal (B) are both present in FP cells and neural progenitors in the VZ. The domain of *netrin1* and netrin1::β-gal expression extends from the ventral midline to a dorsal boundary at the same level as the dorsal root entry zone (DREZ, dotted line).

(C) In contrast, high levels of netrin1 protein are observed around the basal pial circumference of the spinal cord starting at the same dorsal boundary observed for *netrin1* expression (dotted line), Netrin1 is also present on commissurally projecting axons (chevrons, C, C').

(D-I) Netrin1 protein co-localizes with both the nestin$^+$ progenitor processes (arrows, H) and the laminin$^+$ pial surface (I). Netrin1 is not present at the pial surface in the dorsal-most spinal cord, i.e. above the DREZ, where netrin1::β-gal is not present in the VZ (E, F). See also Movie S1.

(J, K) NF$^+$ axon extension is co-incident with the dorsal border of both netrin1::β-gal expression and netrin1 on the pial surface (dotted line, J', K').

(L) By E11.5, NF$^+$ and Tag1$^+$ axons project around a continuous border of netrin1::β-gal$^+$ cells, that spans from the dorsal VZ to the apical FP (dotted lines, L'). Commissural axons are most fasciculated as they project beneath the domain of netrin1::β-gal at the FP (L').

(L, M) Axon growth also correlates with distribution of netrin1 protein. NF$^+$ axons and Tag1$^+$ Robo3$^+$ commissural axons extend immediately adjacent to the laminin$^+$ netrin1$^+$ pial surface in the dorsal spinal cord (M').

Figure 2-4: Dcc mediates the response to VZ-derived netrin1
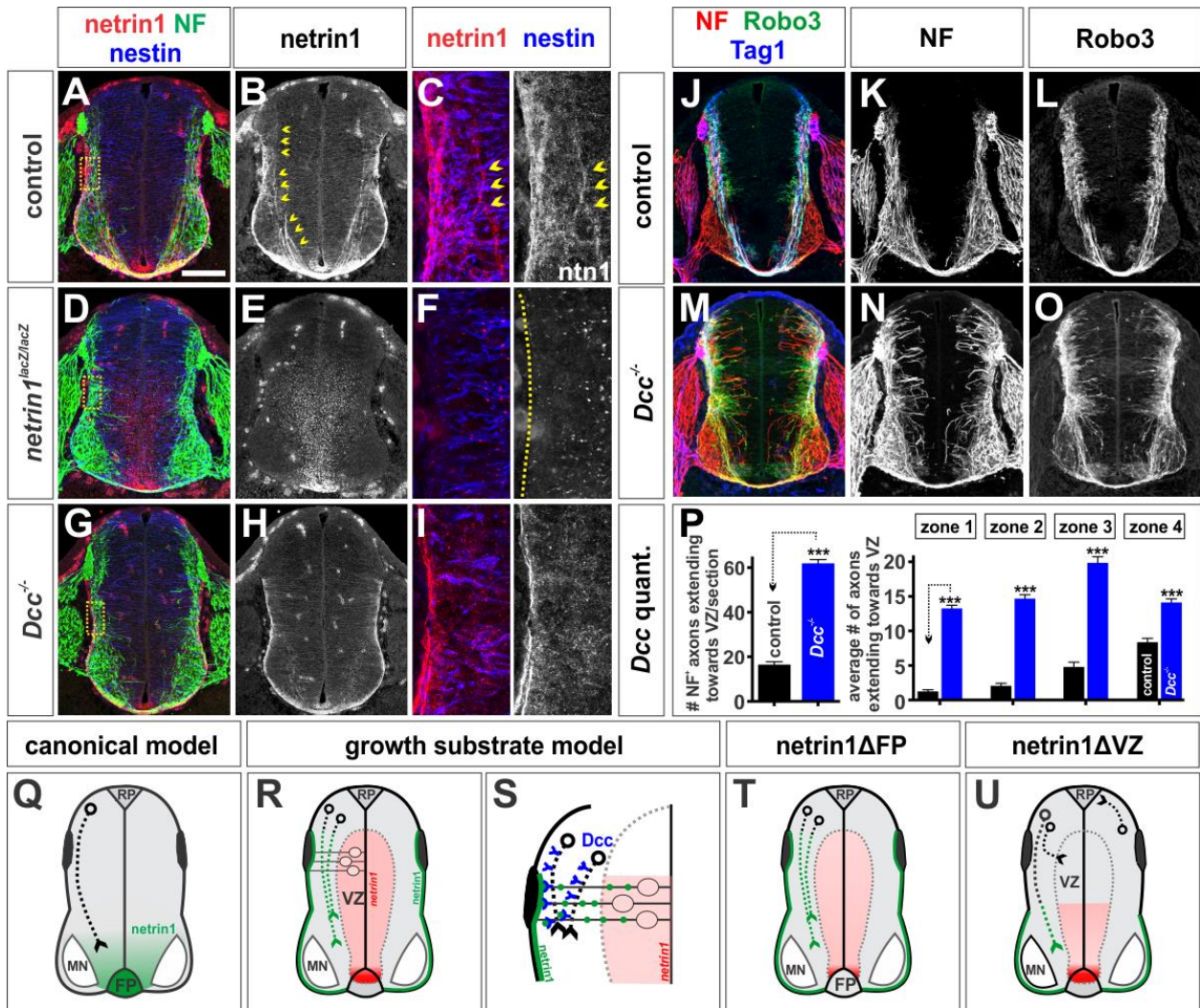
(A-O) Thoracic level transverse sections of E11.5 *netrin1*$^{+/+}$*; dcc*$^{+/+}$ (control, A-C, J-L) *netrin1*$^{lacZ/lacZ}$ (D-F), and *Dcc*$^{-/-}$ (G-I, M-O) mouse spinal cords.

(A-F) Antigen retrieval (see methods) boosts the netrin1 signal in axons (chevrons, B, C) and the pial surface (see also Movie S2). This staining is lost in *netrin1*$^{lacZ/lacZ}$ embryos (E, F). As previously described[26], netrin1 antibodies detect the netrin1::β-gal fusion protein in VZ.

50

(G-I) Netrin1 accumulation in NF$^+$ axons is greatly diminished in *Dcc* mutant spinal cords, even though pial-netrin1 remains intact (see also Movie S3).

(J-L) Control NF$^+$ (K) and Robo3$^+$ (L) axons project precisely around the VZ.

(M-O) In contrast, *Dcc* mutant NF$^+$ and Robo3$^+$ axons exuberantly project dorsally into the VZ at all levels (N, O). Robo3$^+$ axons are also profoundly defasciculated in the motor columns (O).

(P) Quantification of the average number of NF$^+$ axons extending into the VZ demonstrates that a comparable number of NF+ axons extend into the VZ in *Dcc* and *netrin1* (Figure 1M) mutant embryos. Control: n=44 sections, 3 embryos, and *Dcc*$^{-/-}$: n=105 sections, 6 embryos.

(Q) In the canonical model, netrin1 functions as a long-range chemoattractant secreted by cells in the FP.

(R, S) In the growth substrate model, netrin1 produced by neural progenitors is transported to the pial surface in their radial processes to form a growth substrate. Axons then extend adjacent to this substrate in a Dcc dependent manner.

(T, U) Our conditional analyses support the growth substrate model, by demonstrating the key requirement for VZ-derived netrin1 in guiding spinal axons. *** p< 0.0005, ** p<0.005, * p<0.05, Student's *t*-test.

Supplementary Figure 2-S1: Netrin1 is required for spinal axon orientation and fasciculation
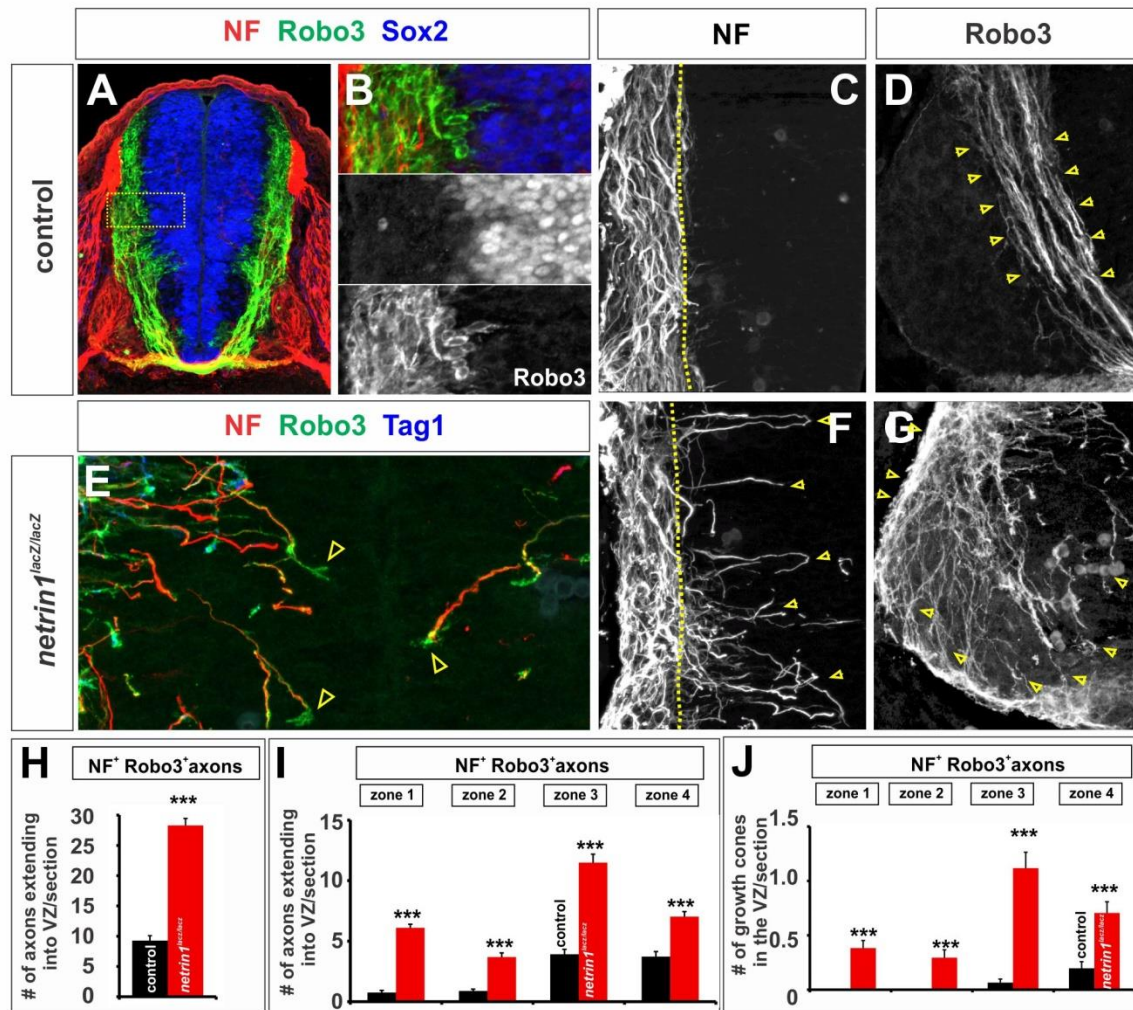
(A-B) All spinal axons, including NF$^+$ axons and the subset of Robo3$^+$ commissural axons avoid the Sox2$^+$ VZ in E11.5 spinal cords as the commissural axons complete their trajectory to the floor plate (FP) at the ventral midline. High magnification images (inset in A is shown in B) show that there is a precise, inverse relationship between all spinal axons and Sox2$^+$ neural progenitors (B).

(C-D) NF$^+$ axons grow just adjacent to the VZ without entering the VZ in control spinal cords (yellow dotted line, C). Robo3$^+$ commissural axons project in a tightly fasciculated bundle, between the motor column and the VZ (yellow arrows in D) as they extend towards the ventral midline.

(E-G) In contrast, axons extend into the VZ in *netrin1$^{lacZ/lacZ}$* mutants. Robo3$^+$ growth cones are observed at the tips of NF$^+$ axons entering the VZ (arrows, E, F). Robo3$^+$ are completely defasciculated and invade the ventral spinal cord, extending into the motor column (arrows, G).

(H) Quantification of the NF$^+$ Robo3$^+$ commissural axons projecting into the VZ in control = 9.28±0.8 NF$^+$ axons/section; n=61 sections from 5 embryos and mutant embryos = 28.31±1.1 NF$^+$ axons/section; n= 68 sections from 6 embryos. n is same as for *netrin1$^{lacZ/lacZ}$* NF$^+$ counts in Figure 1M.

(I) The NF$^+$ Robo3$^+$ mis-projecting axons in (S) were also assigned to four zones within the spinal cord (Figure 1R). Zone 1: control=0.75±0.2 NF$^+$ axons/section, mutant =6.1±0.3 NF$^+$ axons/section; zone 2: control=0.89±0.2 NF$^+$ axons/section, mutant =3.7±0.3 NF$^+$ axon/section; zone 3: control=3.9±0.4 NF$^+$ axons/section, mutant=11.5±0.7 NF$^+$ axons/section; zone 4: control=3.7±0.4 NF$^+$ axons/section, mutant=7.02±0.4 NF$^+$ axon/section. n as for (H).

(J) Quantification of the NF$^+$ Robo3$^+$ growth cones that extend into the VZ starting (represented as number of growth cones per section): control = 0, 0, 4, 12 growth cones in zones 1, 2, 3, 4 respectively, mutant = 26, 20, 76, 48 growth cones in zones 1, 2, 3, 4 respectively). n as for (H).

*** $p< 0.0005$, ** $p<0.005$, * $p<0.05$, Student's *t*-test.

Supplementary Figure 2-S2: Axons are only mildly perturbed in Unc5 mutants
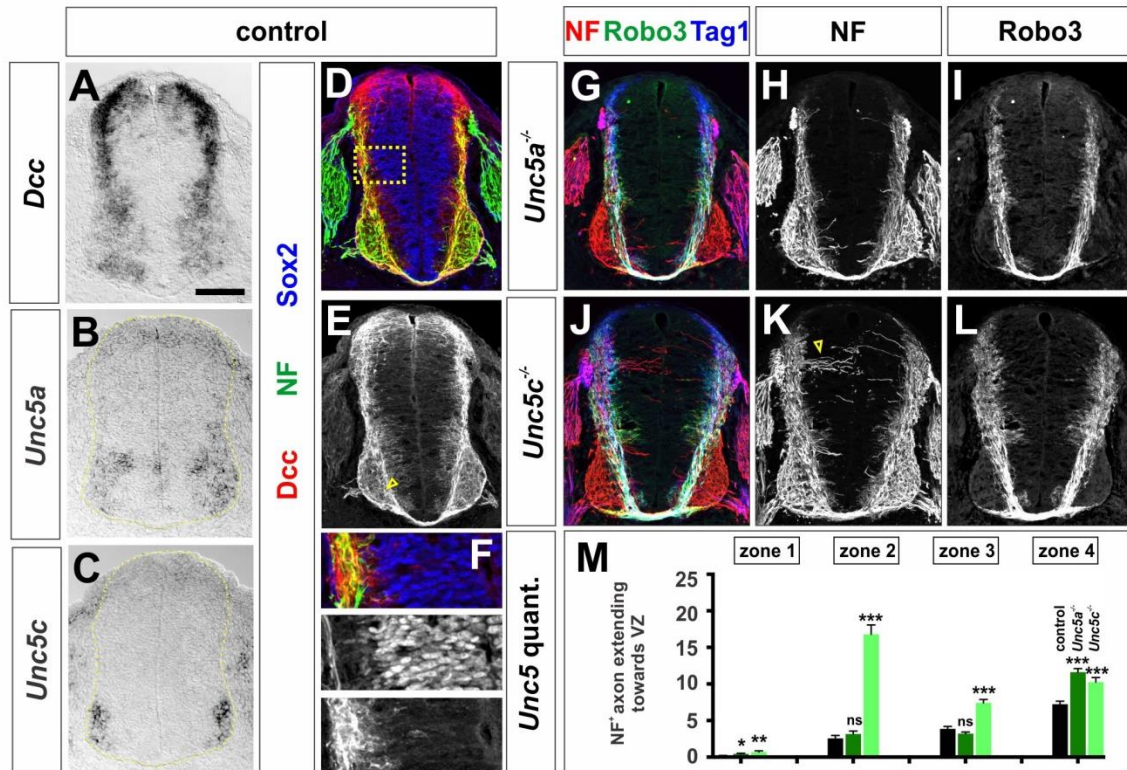
(A-C) *in situ hybridization* showing the mRNA expression patterns of netrin1 receptors. *Dcc* is expressed at high levels in many post-mitotic neurons in the dorsal spinal cord and at lower levels in the ventral spinal cord, including the motor columns (A). Of the Unc5 family, only *Unc5a* and *Unc5c* have detectable expression in postmitotic neurons in the spinal cord. *Unc5a* is expressed transiently in the dorsal VZ (data not shown) and then subsequently in the motor columns (B). *Unc5c* is present both in the motor columns and in the DRGs at later stages (C).

(D-F) Dcc protein is present in at high levels in a broad swathe of commissural axons extending to the FP, and at low levels in the motor columns (E). It is not present in the $Sox2^{+}$ VZ (F).

(G-I) In the absence of *Unc5a*, modest numbers of NF^{+} axons project aberrantly into zone 4 (H). $NF^{+}Robo3^{+}$ commissural axon trajectory appears comparable to controls (I).

(J-L) A few NF$^+$ axons extend into zone 3 and 4 in *Unc5c* mutants (K), while the NF$^+$Robo3$^+$ commissural axon trajectory is comparable to controls (L). There is more robust *Unc5c$^{-/-}$* axon growth into zone 2; however, these latter projections are NF$^+$ Tag1$^+$ Robo3$^-$ (arrows, K). This profile suggests that they are DRG axons precociously innervating the spinal cord as previously described [37].

(M) The trajectory of spinal axons in *Unc5* mutants is considerably less perturbed compared to *Dcc* mutants (Figure 4P). Control: n=36 sections from 5 embryos, *Unc5a$^{-/-}$*: n=67 sections from 7 embryos and *Unc5c$^{-/-}$*: n=57 sections from 4 embryos.

Supplementary Movie 2-S1 (related to **Figure 2-3**): **Netrin1 protein is present on nestin$^+$ filaments**

Transverse sections of E11.5 thoracic mouse spinal cord processed for netrin1 (red), nestin (green) and laminin (blue) staining. A series of Imaris renderings permits the visualization of all netrin1 labeling, following by the netrin1 specifically associated with nestin and then laminin.

Supplementary Movie 2-S2 and 2-S3 (related to **Figure 2-4**): **Netrin1 accumulates in axons in a *Dcc* dependent manner**

Transverse sections of E11.5 thoracic control (movie 2) and *Dcc* mutant (movie 3) mouse spinal cord processed for netrin1 (red) and NF (green). Imaris rendering permits the visualization of netrin1 labeling specifically associated with NF+ axons.

BIBLIOGRAPHY

1. Phan KD, Hazen VM, Frendo M, Jia Z, Butler SJ. The bone morphogenetic protein roof plate chemorepellent regulates the rate of commissural axonal growth. J Neurosci 2010;30(46):15430-40.

2. Butler SJ, Tear G. Getting axons onto the right path: the role of transcription factors in axon guidance. Development 2007;134(3):439-48.

3. Tessier-Lavigne M, Goodman CS. The molecular biology of axon guidance. Science 1996;274(5290):1123-33.

4. Kennedy TE, Serafini T, de la Torre JR, Tessier-Lavigne M. Netrins are diffusible chemotropic factors for commissural axons in the embryonic spinal cord. Cell 1994;78(3):425-35.

5. Serafini T, Kennedy TE, Galko MJ, Mirzayan C, Jessell TM, Tessier-Lavigne M. The netrins define a family of axon outgrowth-promoting proteins homologous to C. elegans UNC-6. Cell 1994;78(3):409-24.

6. de la Torre JR, Hopker VH, Ming GL, Poo MM, Tessier-Lavigne M, Hemmati-Brivanlou A, Holt CE. Turning of retinal growth cones in a netrin-1 gradient mediated by the netrin receptor DCC. Neuron 1997;19(6):1211-24.

7. Ming GL, Song HJ, Berninger B, Holt CE, Tessier-Lavigne M, Poo MM. cAMP-dependent growth cone guidance by netrin-1. Neuron 1997;19(6):1225-35.

8. Sloan TF, Qasaimeh MA, Juncker D, Yam PT, Charron F. Integration of shallow gradients of Shh and Netrin-1 guides commissural axons. PLoS Biol 2015;13(3):e1002119.

9.   Lai Wing Sun K, Correia JP, Kennedy TE. Netrins: versatile extracellular cues with diverse functions. Development 2011;138(11):2153-69.

10.   Brankatschk M, Dickson BJ. Netrins guide Drosophila commissural axons at short range. Nat Neurosci 2006;9(2):188-94.

11.   Timofeev K, Joly W, Hadjieconomou D, Salecker I. Localized netrins act as positional cues to control layer-specific targeting of photoreceptor axons in Drosophila. Neuron 2012;75(1):80-93.

12.   Akin O, Zipursky SL. Frazzled promotes growth cone attachment at the source of a Netrin gradient in the Drosophila visual system. Elife 2016;5.

13.   Serafini T, Colamarino SA, Leonardo ED, Wang H, Beddington R, Skarnes WC, Tessier-Lavigne M. Netrin-1 is required for commissural axon guidance in the developing vertebrate nervous system. Cell 1996;87(6):1001-14.

14.   Kennedy TE, Wang H, Marshall W, Tessier-Lavigne M. Axon guidance by diffusible chemoattractants: a gradient of netrin protein in the developing spinal cord. J Neurosci 2006;26(34):8866-74.

15.   Carter SB. Principles of cell motility: the direction of cell movement and cancer invasion. Nature 1965;208(5016):1183-7.

16.   Fazeli A, Dickinson SL, Hermiston ML, Tighe RV, Steen RG, Small CG, Stoeckli ET, Keino-Masu K, Masu M, Rayburn H and others. Phenotype of mice lacking functional Deleted in colorectal cancer (Dcc) gene. Nature 1997;386(6627):796-804.

17.   Matise MP, Epstein DJ, Park HL, Platt KA, Joyner AL. Gli2 is required for induction of floor plate and adjacent cells, but not most ventral neurons in the mouse central nervous system. Development 1998;125(15):2759-70.

18. Williams ME, Lu X, McKenna WL, Washington R, Boyette A, Strickland P, Dillon A, Kaprielian Z, Tessier-Lavigne M, Hinck L. UNC5A promotes neuronal apoptosis during spinal cord development independent of netrin-1. Nat Neurosci 2006;9(8):996-8.

19. Ackerman SL, Kozak LP, Przyborski SA, Rund LA, Boyer BB, Knowles BB. The mouse rostral cerebellar malformation gene encodes an UNC-5-like protein. Nature 1997;386(6627):838-42.

20. Bielle F, Griveau A, Narboux-Neme N, Vigneau S, Sigrist M, Arber S, Wassef M, Pierani A. Multiple origins of Cajal-Retzius cells at the borders of the developing pallium. Nat Neurosci 2005;8(8):1002-12.

21. Kong JH, Yang L, Dessaud E, Chuang K, Moore DM, Rohatgi R, Briscoe J, Novitch BG. Notch activity modulates the responsiveness of neural progenitors to sonic hedgehog signaling. Dev Cell 2015;33(4):373-87.

22. Mao X, Fujiwara Y, Chapdelaine A, Yang H, Orkin SH. Activation of EGFP expression by Cre-mediated excision in a new ROSA26 reporter mouse strain. Blood 2001;97(1):324-6.

23. Han H, Tanigaki K, Yamamoto N, Kuroda K, Yoshimoto M, Nakahata T, Ikuta K, Honjo T. Inducible gene knockout of transcription factor recombination signal binding protein-J reveals its essential role in T versus B lineage decision. Int Immunol 2002;14(6):637-45.

24. Harfe BD, Scherz PJ, Nissim S, Tian H, McMahon AP, Tabin CJ. Evidence for an expansion-based temporal Shh gradient in specifying vertebrate digit identities. Cell 2004;118(4):517-28.

25. Lang D, Lu MM, Huang L, Engleka KA, Zhang M, Chu EY, Lipner S, Skoultchi A, Millar SE, Epstein JA. Pax3 functions at a nodal point in melanocyte stem cell differentiation. Nature 2005;433(7028):884-7.

26. Poliak S, Morales D, Croteau LP, Krawchuk D, Palmesino E, Morton S, Cloutier JF, Charron F, Dalva MB, Ackerman SL and others. Synergistic integration of Netrin and ephrin axon guidance signals by spinal motor neurons. Elife 2015;4.

27. Ericson J, Morton S, Kawakami A, Roelink H, Jessell TM. Two critical periods of Sonic Hedgehog signaling required for the specification of motor neuron identity. Cell 1996;87(4):661-73.

28. Phan KD, Croteau LP, Kam JW, Kania A, Cloutier JF, Butler SJ. Neogenin may functionally substitute for Dcc in chicken. PLoS One 2011;6(7):e22072.

29. Butler SJ, Bronner ME. From classical to current: analyzing peripheral nervous system and spinal cord lineage and fate. Dev Biol 2015;398(2):135-46.

30. Kadison SR, Murakami F, Matise MP, Kaprielian Z. The role of floor plate contact in the elaboration of contralateral commissural projections within the embryonic mouse spinal cord. Dev Biol 2006;296(2):499-513.

31. Matise MP, Lustig M, Sakurai T, Grumet M, Joyner AL. Ventral midline cells are required for the local control of commissural axon guidance in the mouse spinal cord. Development 1999;126(16):3649-59.

32. Brunet I, Gordon E, Han J, Cristofaro B, Broqueres-You D, Liu C, Bouvree K, Zhang J, del Toro R, Mathivet T and others. Netrin-1 controls sympathetic arterial innervation. J Clin Invest 2014;124(7):3230-40.

33. Laumonnerie C, Tong YG, Alstermark H, Wilson SI. Commissural axonal corridors instruct neuronal migration in the mouse spinal cord. Nat Commun 2015;6:7028.

34. Hockfield S, McKay RD. Identification of major cell classes in the developing mammalian nervous system. J Neurosci 1985;5(12):3310-28.

35. Kolodkin AL, Tessier-Lavigne M. Mechanisms and molecules of neuronal wiring: a primer. Cold Spring Harb Perspect Biol 2011;3(6).

36. Engelkamp D. Cloning of three mouse Unc5 genes and their expression patterns at mid-gestation. Mech Dev 2002;118(1-2):191-7.

37. Masuda T, Watanabe K, Sakuma C, Ikenaka K, Ono K, Yaginuma H. Netrin-1 acts as a repulsive guidance cue for sensory axonal projections toward the spinal cord. J Neurosci 2008;28(41):10380-5.

38. Leonardo ED, Hinck L, Masu M, Keino-Masu K, Ackerman SL, Tessier-Lavigne M. Vertebrate homologues of C. elegans UNC-5 are candidate netrin receptors. Nature 1997;386(6627):833-8.

39. Baker KA, Moore SW, Jarjour AA, Kennedy TE. When a diffusible axon guidance cue stops diffusing: roles for netrins in adhesion and morphogenesis. Curr Opin Neurobiol 2006;16(5):529-34.

40. Deiner MS, Kennedy TE, Fazeli A, Serafini T, Tessier-Lavigne M, Sretavan DW. Netrin-1 and DCC mediate axon guidance locally at the optic disc: loss of function leads to optic nerve hypoplasia. Neuron 1997;19(3):575-89.

41. Hazen VM, Phan K, Yamauchi K, Butler SJ. Assaying the ability of diffusible signaling molecules to reorient embryonic spinal commissural axons. J Vis Exp 2010(37).

42.   Moore SW, Zhang X, Lynch CD, Sheetz MP. Netrin-1 attracts axons through FAK-dependent mechanotransduction. J Neurosci 2012;32(34):11574-85.

43.   Rousso DL, Pearson CA, Gaber ZB, Miquelajauregui A, Li S, Portera-Cailliau C, Morrisey EE, Novitch BG. Foxp-mediated suppression of N-cadherin regulates neuroepithelial character and progenitor maintenance in the CNS. Neuron 2012;74(2):314-30.

44.   Hiramoto M, Hiromi Y, Giniger E, Hotta Y. The Drosophila Netrin receptor Frazzled guides axons by controlling Netrin distribution. Nature 2000;406(6798):886-9.

CHAPTER 3 – Netrin1 establishes multiple growth-boundaries for axons in the developing spinal cord

ABSTRACT

Netrin1 has been defined as a long-range diffusible chemotropic signal for axons in the embryonic spinal cord. These axons extend and fasciculate to navigate laterally, avoiding the ventricular zone (VZ). Surprisingly, we find that these behaviors depend on short-range actions of netrin1 produced by neural progenitors in the VZ, and mediated by its receptor Dcc. The loss of netrin1 from the VZ results in profound axon defasciculation and profuse medial axon growth into the VZ. Here we show that netrin1 first orients ventrally-directed growth of pioneering axons in the spinal cord. Second, netrin1 also sculpts subsequent domains of axonal growth adjacent to the dorsal root entry zone, suggesting a universal role as a locally-acting architect of axon trajectories. Together, our data suggest that netrin1 establishes short-range boundaries that provide a local growth substrate for axon extension, while also preventing local innervation of *netrin1*-expressing domains.

This chapter is modified from:

SGV and SJB (2017). Netrin1 establishes multiple growth-boundaries for axons in the developing spinal cord. *In preparation for publication.*

SGV performed the experiments and wrote the manuscript under the guidance of SJB.

INTRODUCTION

Neural circuits are formed during development when axons navigate precise pathways and reach their synaptic endpoints. To ensure that axons travel these distances correctly, molecules known as guidance cues are present at specific spatial and temporal locations along an axon's trajectory, providing either repulsive or attractive cues. Therefore, axons encounter several intermediate cues that act as guideposts, before reaching their final synaptic partner. These cues can be classified as short-range or long-range cues based on the distance over which these cues can elicit a response[1,2]. Guidance cues can also be classified as attractive or repulsive depending on the nature of the response provoked by a growth cone, at the leading edge of the axon[1,2].

Canonical long-range cues include the netrins[3,4], semaphorins [5,6], slits [7,8] and morphogens, such as the Bone Morphogenetic Proteins[9] and sonic hedgehog (Shh)[10]. In contrast, short-range cues are generally regarded as providing local permissive or non-permissive substrates for axon outgrowth, such as ability of laminin to support the outgrowth of retinal ganglion axons in the optic tract [11], or ephrin/Eph signaling regulating motor axon trajectories in developing vertebrate limb [12]. While netrin1 was initially identified as an attractive cue acting over long-range[3,4,13], many studies since have shown that short-range activity of netrin1 is sufficient to attract commissural axons and repel motor axons in the drosophila nerve cord[14,15]. Subsequent studies have also shown that netrin1 has many other functions in directing tissue morphogenesis, as well as regulating migration of progenitor cells[16].

Our studies provide further evidence that netrin1 is a major axonal architect, shaping the trajectories of many classes of axons within the embryonic spinal cord. However, rather than

acting as a long-range attractant from the FP, our data indicate that netrin1 acts to establish short-range growth-boundaries that likely combine both attractive and repulsive activities[17]. We examined the specific contributions of netrin1 produced by the VZ versus the FP and found that *netrin1*expressed by neural progenitors in the VZ specify a growth boundary that dictates the trajectory of axons, preventing them from entering the VZ[17]. However these studies were limited to a specific developmental time-point at E11.5, when most commissural axons have reached and crossed the FP.

We set out to determine the role of netrin1 expressed by neural progenitors during the earliest stages of development when the pioneering axons are born[18]. We also examined the role of netrin1 two days later at E12.5, when commissural axons have crossed the floor plate[13,19], before the central branches of sensory axons invade the spinal cord to form to dorsal funiculus[20].

We find that the dorsal boundary of netrin1 first orients pioneering axons ventrally. Subsequently netrin1 specifies bilaterally symmetric growth boundaries adjacent to the dorsal root entry zone (DREZ) that shape the trajectory of axons while preventing them from entering *netrin1* expression regions. These data indicate that netrin1 sequentially shapes axonal trajectories by specifying multiple boundaries at various timepoints during development.

MATERIALS AND METHODS

Generation of mutant mice: *Netrin1*[13] and Ngn2::tauGFP[21] mice were bred into 129/Sv backgrounds and maintained as heterozygous mating pairs. Embryos were collected from timed matings. The presence of a vaginal plug was considered embryonic day E0.5. Heads were used to isolate the mRNA and cDNA and were amplified by PCR to identify the genotypes of each

embryo. All analyses were done using littermate controls. All animal procedures were carried out in accordance with University of California Los Angeles IACUC guidelines.

Tissue processing: Spinal cords were fixed using 4% paraformaldehyde for 2 hours at 4°C. After fixation, the tissue was cryoprotected in a 30% sucrose solution overnight, following which the tissue was mounted in optimal cutting temperature (OCT) and cryosectioned at 30µm. Sections were collected on slides and processed for immunohistochemistry or *in situ* hybridization as previously described[17].

Immunohistochemistry: The following primary antibodies were used overnight at 4°C: Rabbit: Neurofilament (Cell Signaling Technology #C28E10, 1:200), Sox2, Shh (H4[22], 1:200); Goat: Sox2 (Santa Cruz Biotechnology #17320, 1:2000), human-Robo3 (R&D #AF3076, 1:200), β-galactosidase (1:2000), Netrin1 (R&D #AF1109, 1:500); Mouse: Neurofilament (DSHB #3A10, 1:100), Sox2 (Santa Cruz Biotechnology E4 #365823, 1:1000), Nkx2.2 (DSHB #74.5 A5-s, 1:100), mAB Tag1 (DSHB #4D7, 1:100); Guinea Pig: Olig2[23] (1;20, 000). Secondary antibodies were incubated for 2 hours at RT. Netrin1 anitbody signal was boosted using antigen retrieval methods as described previously[17].

In situ hybridization: Netrin1 digioxigenin probes[13] were used for labeling and *in situ hybridization* was performed on 12um sections as described previously[17]. NBT/BCIP and anti-DIG antibody conjugated to an alkaline phosphatase (Roche) were used to visualize the mRNA.

RESULTS

Axons navigate circumferentially around the ventricular zone

The spinal cord is organized into layers from its earliest genesis: Sox2^{+} neuroepithelial progenitors within the VZ give rise to postmitotic neurons that migrate laterally to form the mantle layer and extend axons in the lateral marginal zone[24]. Spinal axons, including all neurofilament[+] (NF) axons, and the Tag1^{+} and Robo3^{+} populations of commissural axons respect the boundary of the VZ as they project towards FP at the ventral midline (**Figure 1-1**). From the earliest stages of spinal axogenesis, NF[+], Tag1^{+} and Robo3^{+} axons are located adjacent to, but segregated from, the cell bodies of Sox2^{+} neural progenitors in the VZ [25,26] (**Figure 1-1 A-E**). By E11.5, when most dorsal commissural axons have reached and crossed the ventral midline, there is a clear inverse relationship between the neural-progenitor rich VZ and the axon-rich mantle zone (**Figure 1-1 F-J**). This segregation continues in E12.5 (**Figure 1-1 K-O**). Together, these observations suggest the presence of a guidance cue that establishes the VZ as a boundary from the earliest stages of axogenesis.

Netrin1 is present in the spinal ventricular zone throughout axogenesis

Our previous studies demonstrated that at E11.5, *netrin1* in the VZ and netrin1 in the pial surface mediate growth boundaries that specify regions where axons can grow[17]. We further examined the expression of netrin1 protein in comparison to *netrin1 expression* at earlier and later stages of development. We used a reporter mouse in which *lacZ* is inserted into the *netrin1* genomic locus[13]. The presence of a genetically encoded marker, β-galactosidase (β-gal), recapitulates the distribution of *netrin1* mRNA (**Figures 3-2 A, E, H and Supplementary Figure 3-2 S1A-S1C**)[13], while providing a highly sensitive readout of the location of any cell

expressing the *netrin1* gene. As described previously[13], netrin1::β-gal is present at high levels in the FP. However, netrin1::β-gal is also found in a broad swathe of the VZ, from the ventral midline to a boundary in the dorsal spinal cord (dotted lines, **Figure 3-2 A, E**) at the same level as the dorsal root entry zone (DREZ, dotted region)[17]. At E10.5, when axogenesis commences for many populations of spinal axons, netrin1::β-gal is present at high levels throughout the FP and at lower levels in the intermediate VZ (**Figure 3-2 A**). Strikingly, netrin1::β-gal is absent from early Olig2$^+$ motor neuron progenitors[23] at caudal levels of the ventral spinal cord (**Figure 3-2 C', D**), which may result in the permanent depletion of netrin1 from the motor column (**Figure 3-2 D**).

By E12.5, additional bilaterally symmetric domains of netrin1::β-gal are observed immediately adjacent to DREZ[20] (arrowheads, **Figure 3-2 H and Supplementary Figure 3-2 S1C**). We quantified the extent and intensity of netrin1::β-gal in E10.5-E12.5 embryos within four zones of the spinal cord (**Figure 3-2 G**); quantification showed that the dorsal-most neural progenitors in zone 1 do not express *netrin1* (**Figure 3-2 J**). Netrin1::β-gal has a high–low distribution in the spinal cord, from zone 4, which includes the FP and motor columns to zone 2, at the level of the DREZ (**Figure 3-2 J**). The absolute intensity of netrin1::β-gal in each zone remains constant from E10.5-E12.5, suggesting that netrin1 is stably maintained over time, i.e. this distribution pattern does not result from the perdurance of β-gal. This conclusion is supported by the absence of β-gal tracing into postmitotic spinal neurons.

Similar to *netrin1* RNA, netrin1 protein is present at low levels in the VZ (**Figure 3-2 B, F**, dotted line) and DREZ domains (**Figure 3-2 I**, dotted line) and at high levels in the FP (**Figure 3-2 F, I**)[27]. However, our previous studies have shown that netrin1 protein produced by neural progenitors in the VZ is transported along nestin filaments to be deposited on the pial

surface (**Figure 3-2 F,** arrow), as well as on commissural axons (**Figure 3-2F**, chevrons)[17]. We find that, netrin1 protein is deposited on the pial surface as early as E10.5 and this accumulation continues to E12.5 (**Figure 3-2 B and I**, arrows). Together, these data show that netrin1 is present on the pial surface throughout the stages when axons are navigating their circumferential trajectories in the spinal cord.

Spinal axons avoid netrin1-expressing domains, while accumulating netrin1 protein

We next investigated the spatial relationship between spinal axon extension and the domains of both *netrin1* transcript and netrin1 protein. In E10.5 embryos, NF$^+$ axon growth coincides 70% of the time on the dorsal border of the netrin1::β-gal domain in the VZ (arrows and dotted lines, **Figure 3-3 A, A' and Figure 3-4 I**) as well as the netrin1 domain on the pial surface (arrows, **Figure 3-3 B, B'**). This distribution suggests that NF$^+$ axons initiate oriented growth as they encounter VZ-derived netrin1.

At E11.5, when the later-born commissural axons have reached and crossed the FP (REF), Tag1$^+$ NF$^+$ population of commissural axons extend underneath the netrin1::β-gal$^+$ FP cells (dotted lines, **Figure 3-3 G, G'**). Similarly, commissural axons extend in a tightly fasciculated bundle, below the netrin1$^+$ FP cells (**Figure 3-3 H, H'**). Netrin1::β-gal expression is absent in the commissure, while netrin1$^+$ commissural axons are seen crossing under the FP (**Figure 3-3 G-H**). In contrast, dI4 commissural commissural interneurons labeled using the Neurog2::*taugfp* genetically encoded reporter[21] extend axons into a concentrated field of Shh[10], which specifically decorates the fasciculated axons as they extend through the FP (**Figure 3-3 I, I'**). Together, these protein distributions are consistent with netrin1 being the key substrate that promotes axon fasciculation, while Shh mediates diffusible chemoattraction[10].

The netrin1::β-gal$^+$ VZ boundary is maintained in E12.5 embryos, with NF$^+$ and Tag1$^+$ axons continuing to extend around the VZ (**Figure 3-3 C, C'**) and under the FP (**Figure 3-3 D, D'**). The DREZ-adjacent netrin1::β-gal$^+$ domain also appears to sculpt axon growth: NF$^+$ axon trajectories grow around this domain (dotted lines, **Figure 3-3 E,E'**). As development proceeds, the axon trajectories markedly curve to extend around an increasing netrin1::β-gal$^+$ domain, in between the VZ and the transient DREZ-adjacent domain, in regions with low-β-gal expression (dotted lines, **Figure 3-3 F, F'**).

Taken together, these observations suggest the hypothesis that netrin1 acts as a general architect for all spinal axons. We propose that netrin1 establishes multiple boundaries that orient axon extension and promote fasciculated axon growth, while also acting as a boundary to prevent the innervation of key domains within the spinal cord, namely the VZ and DREZ-adjacent regions.

Axons extend dorsally and medially in the absence of netrin1

Defects are observed from the earliest stages in axogenesis in E10.5 *netrin1* mutant embryos (**Figure 3-4**). NF$^+$ axon growth now initiates only ~40% of the time on the netrin1::β-gal dorsal border in *netrin1$^{lacZ/lacZ}$* embryos compared to control littermates (**Figure 3-4 A-I**). The orientation of axons is highly aberrant, with an increase in the number of NF$^+$ Robo3$^+$ commissural axons growing into the dorsal-most spinal cord towards the RP (compare brackets, **Figure 3-4 D and H**). Quantification showed NF$^+$ axons projecting medially into all four zones of the spinal cord in mutants, with up to a ~3 fold increase in axons invading the VZ compared to controls (**Figure 3-4 T and U**). NF$^+$ Robo3$^+$ commissural axons also robustly extend into the VZ, in all zones of the spinal cord, constituting ~50% of the total misprojecting NF$^+$ axons (**Figure 3-4 O-T**). For example, there is a ~9-fold and ~4-fold increase in the number of NF$^+$

69

Robo3$^+$ axons projecting into zone 1 (arrowheads, **Figure 3-4 F, H and U**) and zone 3 (**Figure 3-4 O, P and U**) respectively. These neurites appear to be actively extending axons, rather than trailing processes, since numerous Robo3$^+$ growth cones can be observed at the tips of the medially projecting NF$^+$ axons (**Figure 3-4 V**). Both Robo3$^+$ (**Figure 3-4 M and R**) and Tag1$^+$ (**Figure 3-4 N and S**) axon extension is reduced, either because growth is stalled[13], or because the initiation of growth is delayed.

A further example of this second phenotype is observed in E12.5 embryos: NF$^+$ axons normally grow around the bilaterally symmetric netrin1$^+$ DREZ domain (**Figure 3-3 E-F, Figure 3-5 A-D**). However many NF$^+$ axons extend through this putative boundary in *netrin1$^{lacZ/lacZ}$* spinal cord (**Figure 3-5 E-I**). Axons continue to extend into the VZ in E12.5 *netrin1* mutant embryos (dotted line, **Figure 3-5 K, P and T**). By this stage in control littermates, the Tag1$^+$ Robo3$^+$ commissural axons resolve into medial and lateral fascicles (arrows, **Figure 3-5 J, L and N**). These Tag1$^+$ Robo3$^+$ fascicles are highly defasciculated in E12.5 *netrin1* mutants, projecting randomly throughout the ventral spinal cord (arrows, **Figure 3-5 O, Q and S**). Quantification showed that NF$^+$ and Robo3$^+$ axons continue to project aberrantly into all four zones of the spinal cord (**Figure 3-5 U**); however the frequency of NF$^+$ Robo3$^+$ axons invading the VZ boundary declines slightly compared to E10.5 and E11.5 embryos (**Figure 3-4 T and Figure 3-5 T**) suggesting that this phenotype might ultimately be transient for commissural axons.

Taken together, this analysis supports the hypothesis that neural progenitor-derived netrin1 is a major architect of spinal axon growth. Axon growth appears to be shaped by both the region that produces *netrin1* transcript and the presence of netrin1 protein at the pial surface and on axons. Thus, the polarized deposition of netrin could both position axon growth at the lateral

margins of the spinal cord and encourage axons to avoid the source of netrin1 production in the

VZ.

DISCUSSION

Netrin1 was identified as a diffusible guidance molecule produced by the FP, that acts over hundreds of microns to attract commissural axon outgrowth and turning[3,4]. Our studies suggest a key role for VZ-derived netrin1 providing guidance boundaries for axons in the developing spinal cord [17]. We show that netrin1 is expressed by ventricular zone (VZ) neural progenitors and transported to the basal pial surface where it positions fasciculated axon outgrowth during early axogenesis (**Figure 3-6 A**). As development progresses, *netrin1-*expressing domains act as boundaries for spinal axons: they promote fasciculated axon outgrowth along the edge of these domains (**Figure 3-6 B**), but prevent growth within the domain itself (**Figure 3-6 B, C**). Although *netrin1* is expressed at lower intensities in the dorsolateral spinal cord and VZ compared to the FP, we find that in the absence of *netrin1* expression, axons profusely extend into these domains without obeying the boundary, even at the earliest stages of axon growth. Thereby suggesting that *netrin1* specifies a boundary regardless of the intensity of *netrin1*expression.

Evidence has accumulated for short-range guidance activities of netrin1 in both vertebrates and invertebrates *in vivo* [14,28,29]. Our data shows that netrin1 associates with the ECM along the pial surface of the spinal cord *in vivo*, consistent with it acting as a short-range cue. Nonetheless, netrin1 appears to move sequentially between surfaces through a series of local interactions, such as Dcc$^+$ axons contacting the pial surface[17]. The ability to transfer between substrates would permit netrin1 to impact axon guidance behaviors at a considerable distance from where it is first produced, the hallmark of a long-range cue. The concordance between our studies and those in different tissues and species, suggests a new mode by which netrin1

functions as an axon guidance factor in the spinal cord: it sculpts axon trajectories by directing short-range adhesive interactions.

The mechanism(s) by which netrin1 specifies a boundary is not yet fully understood. However, preliminary observations indicate that the occasional aberrant axon, projecting medially into the VZ in control spinal cords, does not accumulate netrin1 protein. One possible mechanism by which netrin1 could provide a boundary is by preventing netrin1$^+$ axons from entering *netrin1*-expressing regions. Another possibility is that netrin1 accumulation on Dcc$^+$ commissural axons[17] promotes sufficient adhesive forces that prevent axons from entering the VZ.

In the canonical model, netrin1 is produced by guidepost cells in the FP to attract commissural axons towards the ventral midline. Our studies demonstrate that VZ-derived netrin1 has an important role in defining multiple spatial boundaries that guide spinal axon trajectories. This reiterative role of netrin1 in specifying sequential boundaries would play an important role in orchestrating axonal trajectories. Similar growth-boundaries are likely to apply to axon growth outside of the spinal cord. Motor axons notably grow alongside netrin1::βgal boundaries as they innervate the limb[30]. Netrin1 has also been implicated in the neuronal responses after spinal cord injury[31]; a mechanistic understanding of its capacity to direct axon growth is critical if it to be deployed correctly in therapeutic regenerative contexts.

FIGURES

Figure 3-1: All spinal axons project precisely around the ventricular zone
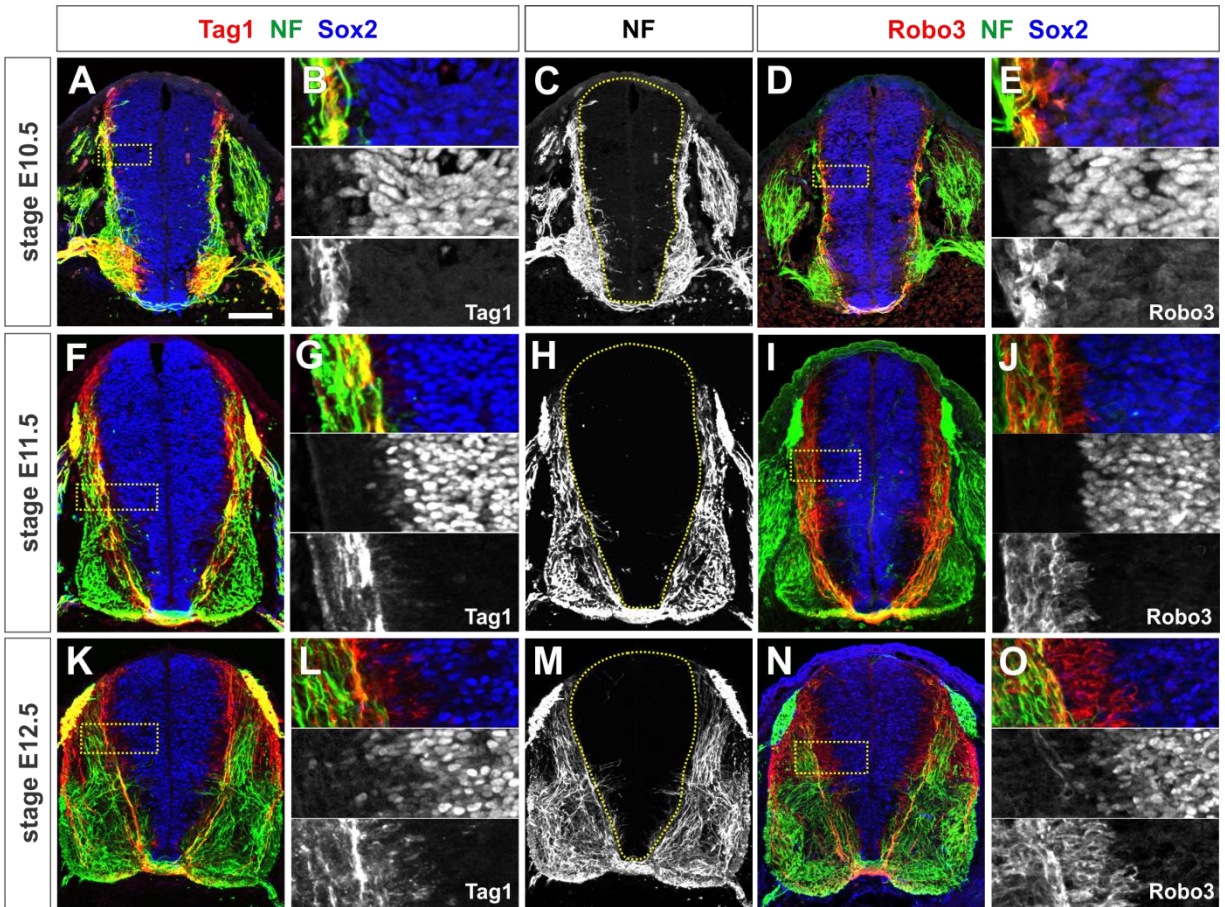
(A-O) Thoracic level sections of embryonic (E) day 10.5 (A-E), E11.5 (F-J) or E12.5 (K-O) mouse spinal cords labeled with antibodies against Tag1 (red, A, B, F, G, K, L), Robo3 (red, D, E, I, J, N, O), neurofilament (NF, green) and Sox2 (blue).

(A-E) In E10.5 mouse embryos, the earliest axon projections of Tag1$^+$ (A, B) and Robo3$^+$ (D, E) commissural axons avoid the Sox2$^+$ (A, B, D, E) ventricular zone (VZ, dotted line, C, H and M). This behavior is generally observed for all NF$^+$ spinal axons (A, C, E). High magnification

images (inset in A and D shown in B and E respectively) show precise inverse relationship between progenitors in the VZ and axons in the mantle zone (B, E).

(F-J) All three classes of spinal axons continue to avoid the Sox2$^+$ VZ in E11.5 spinal cords as the commissural axons complete their trajectory to the floor plate (FP) at the ventral midline.

(K-L) This spinal architecture is maintained in E12.5 mouse embryos.

Scale bar: 100 μm

Figure 3-2: Distribution of netrin1 in the spinal cord
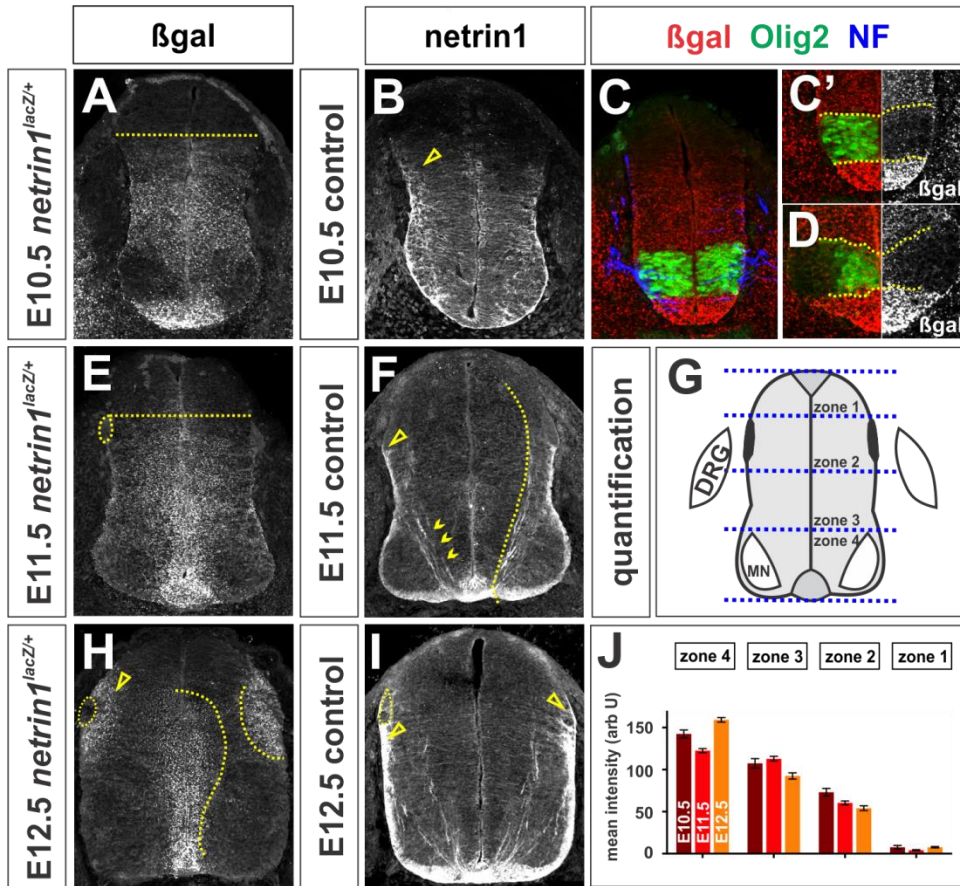
(A-I) Lumbar level transverse sections of E10.5 (C), thoracic E10.5 (A, B, D), E11.5 (E-F) or E12.5 (H-I) control (B, F, I) or *netrin1$^{lacz/+}$* (A, C-D, E, H) mouse spinal cords, labeled with antibodies against β-galactosidase (β-gal, A, C-E, H), netrin1 (B, F, I), Olig2 (green, C, D) and NF (blue, C). The distribution of β-gal in *netrin1$^{lacz/+}$* embryos permits the most sensitive read out of the extent of cells producing netrin1. Panels B, G and J were performed with antigen retrieval.

(A-B) At stage E10.5, *netrin1* is expressed with the highest levels at the floor plate (FP) and progressively lower levels in the VZ. Netrin1 protein is also observed on the pial surface (arrowhead, B).

(C, D) Netrin1::β-gal expression is excluded from Olig2$^+$ motor neuron progenitors and the early post-mitotic motor column. Changes in netrin1::β-gal expression corresponds to changes in the Olig2$^+$ progenitor pool.

(E-F) By E11.5, netrin1::β-gal is present at high levels in FP, lower levels in the VZ extending from the FP into the dorsal spinal cord, with very low levels in mantle zone (immediately right of the dotted line, E). Netrin1 continues to decorate the pial surface (arrowhead, F) as well as commissural axons (chevrons, F).

(G) The spinal cord was divided into four roughly equal regions for quantification. These are referred to as zones 1-4.

(H-I) The graded expression of netrin1::β-gal is maintained in the VZ of E12.5 spinal cords. Netrin1 is now also observed in a lateral region of the spinal cord, immediately ventral to the dorsal root entry zone (DREZ, arrowheads, H, I).

(J) The intensity of netrin1::β-gal levels was measured in zones 1- 4. Netrin1::β-gal extends into zone 2, and remains consistent throughout the E10.5 - E12.5 period (E10.5: n= 45 sections from 2 embryos; E11.5: n= 61 sections from3 embryos; E12.5: n= 36 sections from 2 embryos).

Note that the absolute intensity of netrin1::β-gal in each zone remains constant from E10.5-E12.5, suggesting that netrin1 is stably maintained over time, i.e. this distribution pattern does not result from the perdurance of β-gal. This conclusion is supported by the absence of β-gal tracing into postmitotic spinal neurons.

Scale bar: 120 μm

Figure 3-3: Spinal axons project precisely around domains of *netrin1* expression
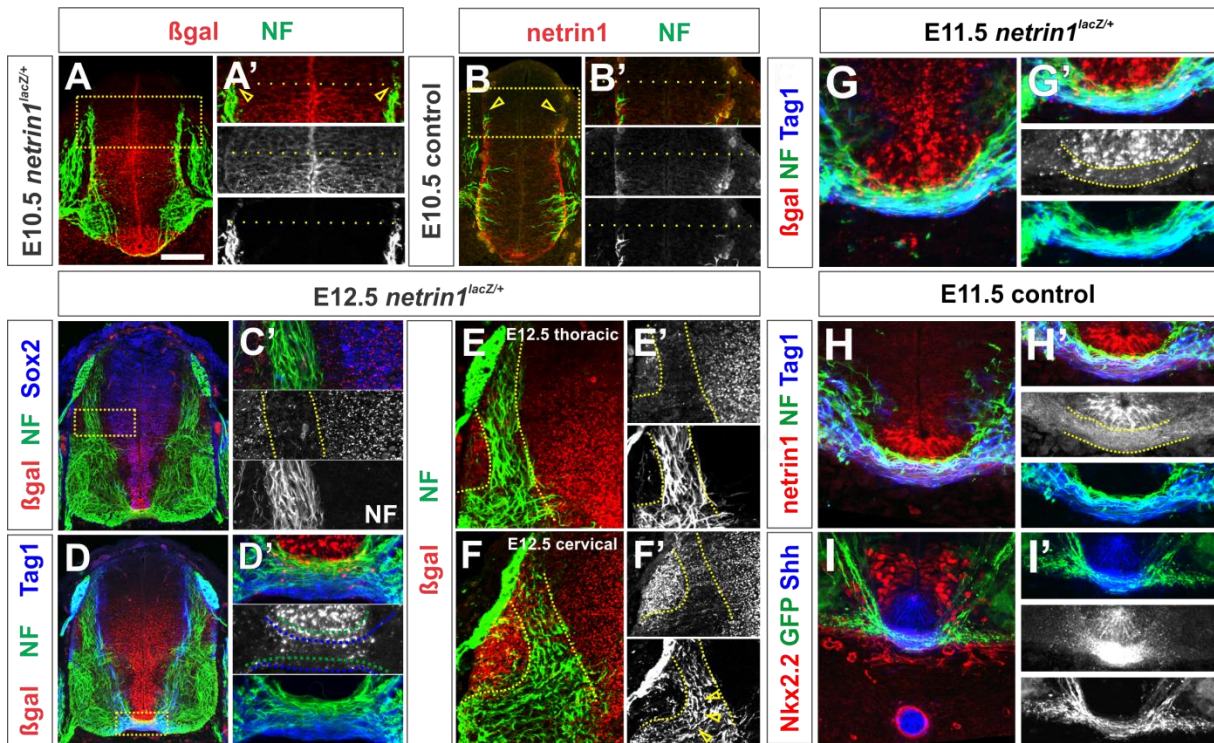
(A-I) Thoracic (A, C-E, G-I), lumbar (B) or cervical (F) level transverse sections of E10.5 (A), E11.5 (G) or E12.5 (C-F) *netrin1^{lacz/+}* and E10.5 (B) and E11.5 (H-I) *netrin1^{+/+}* mouse spinal cords labeled with antibodies against β-gal (red, A, C-G), netrin1 (red, B, H: panel B was processed with antigen retrieval), Nkx2.2 (red, I), NF (green, A-H), GFP (green, I), Sox2 (blue, C), Tag1 (blue, D, G-H) and Shh (blue, I).

(A-B) NF⁺ axon extension is co-incident with the dorsal border of both netrin1::β-gal expression (arrowheads and dotted line, A') and netrin1 protein at the pial surface (arrowheads and dotted line B').

(C-D) By E12.5, NF⁺ and Tag1⁺ (D) axons project within the region where netrin1::β-gal is lowest, resulting in axons growing around a continuous border of netrin1::β-gal⁺ cells, that spans

78

from the dorsal VZ (dotted lines, C') to the apical FP (dotted lines, D'). Commissural axons are most fasciculated as they project beneath the domain of netrin1::β-gal at the FP (D').

(E-F) At E12.5, NF$^+$ spinal axons are also excluded from the DREZ domain of netrin1::β-gal, with NF$^+$ axons curving more markedly as development proceeds to circumvent this region (dotted lines, E' F' and arrowheads, F')

(G-H) NF$^+$ and Tag1$^+$ axons project precisely underneath the lumenal-domain of either βgal (G) netrin1 expressed by FP cells (H).

(I) In contrast to βgal or netrin1, commissural axons labelled with Ngn2::GFP project directly through the domain of Shh. Nkx2.2$^+$ V3 interneurons mark the region directly above the Shh$^+$ FP.

Scale bar: 105μm.

Figure 3-4: Netrin1 initiates oriented growth around the circumference of the spinal cord
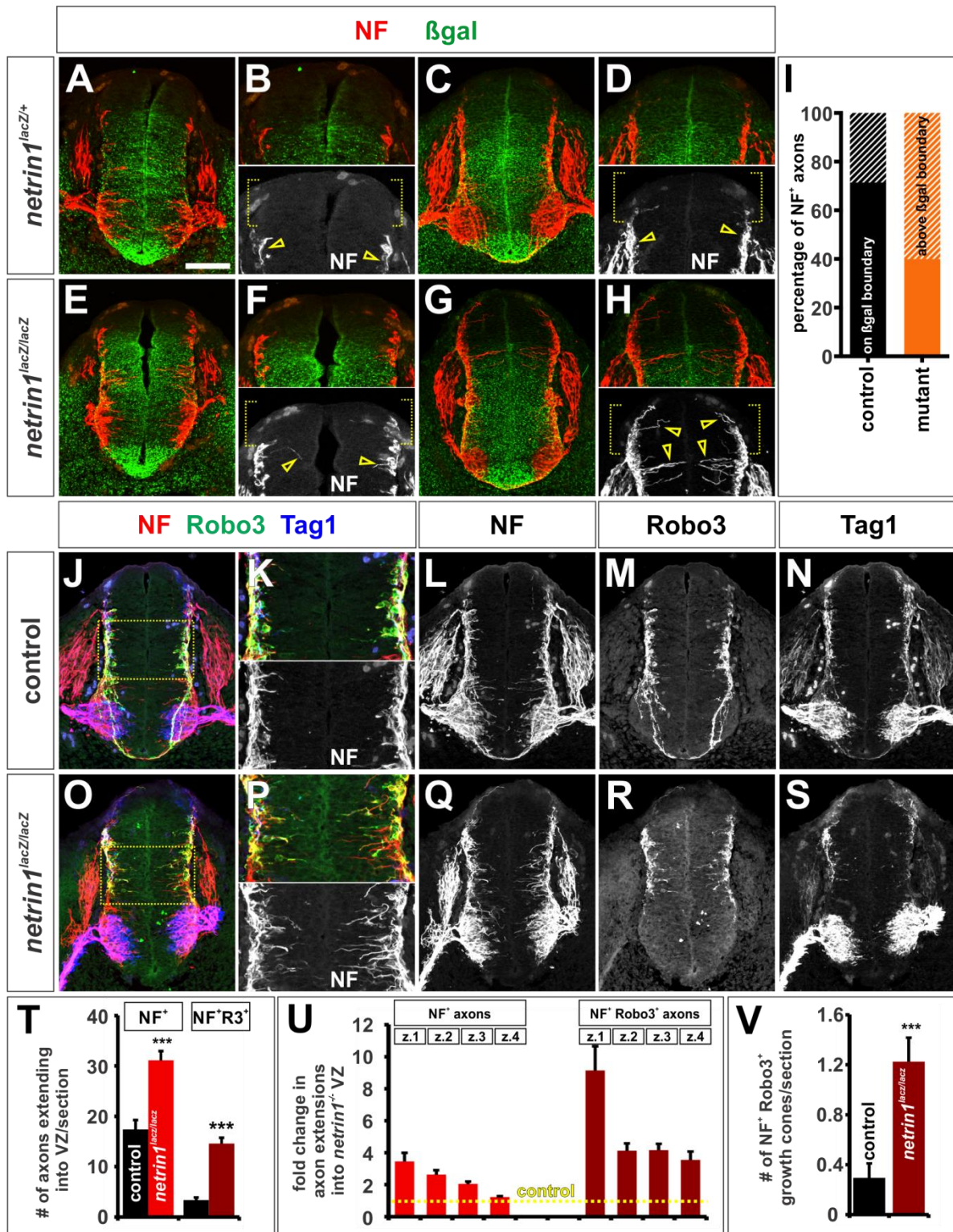
(A-S) Thoracic (C, D, G, H, J-S) and lumbar (A, B, E, F) level transverse sections of E10.5 *netrin1*$^{+/+}$ (J-N), *netrin1*$^{lacZ/+}$ (A-D) or *netrin1*$^{lacz/lacZ}$ (E-H, O-S) mouse spinal cords labeled with antibodies against NF (red), β-gal (green, A-H), Robo3 (green, J-K, O-P), and Tag1 (blue).

(A-D) Ventrally-directed NF$^+$ axon growth starts at a position within the spinal cord co-incident with both the DREZ and the dorsal-most border of the netrin1::β-gal VZ domain (arrowheads B, D).

(E-H) In contrast, in *netrin1* mutant spinal cords, NF$^+$ axons grow more randomly (arrowheads, F, H), robustly extending both above the netrin1::β-gal dorsal boundary into zone 1 and laterally in the VZ into zone 2.

(I) Quantification showed that NF$^+$ axon growth commenced at the netrin1::β-gal dorsal border in >70% of control sections (n= 35 sections, 2 mice) , whereas there was growth above this border in > 60% of sections taken from netrin1 mutant sections (n= 55 sections from 4 mice).

(J-N) Control NF$^+$, Robo3$^+$ and Tag1$^+$ commissural axons are in the process of pioneering their path to the FP at the ventral midline.

(O-S) In *netrin1* mutants, NF$^+$ and Robo3$^+$ axons project randomly into the VZ along the dorsal-ventral axis of the spinal cord (shown magnified in P). Tag1$^+$ (S) and Robo3$^+$ (R) commissural axons additionally show an axon growth defect, either stalled growth[13] or a delay in the initiation of axon growth.

(T) Quantification of the NF$^+$ and NF$^+$ Robo3$^+$ axons projecting into the VZ in control = 17.4±1.9 NF$^+$ axons/section; n=34 sections from 3 embryos and mutant embryos = 31.1±1.8 NF$^+$ axons/section; n=62 sections from 4 embryos.

(U) The NF$^+$ and NF$^+$ Robo3$^+$ mis-projecting axons in (T) were also assigned to four zones within the spinal cord (See Figure 2G) to show the fold change in axon extension into the *netrin1*$^{lacZ/lacZ}$ VZ across the dorsal-ventral axis. n as for (T).

(V) Many Robo3$^+$ *netrin1* mutant growth cones are observed extending towards the lumen. Quantification showed that these NF$^+$ Robo3$^+$ axons extend growth cones into the VZ starting at E10.5: control = 0, 0, 3, 7 growth cones in zones 1, 2, 3, 4 respectively, mutant = 12, 15, 38, 11 growth cones in zones 1, 2, 3, 4 respectively. n as for (T).

Data represented as mean±SEM.

Probability of similarity between control and mutant, *** p< 0.0005, Student's *t*-test.

Scale bar: 130 μm

Figure 3-5: Netrin1 maintains axonal fasciculation and establishes additional boundaries as development proceeds
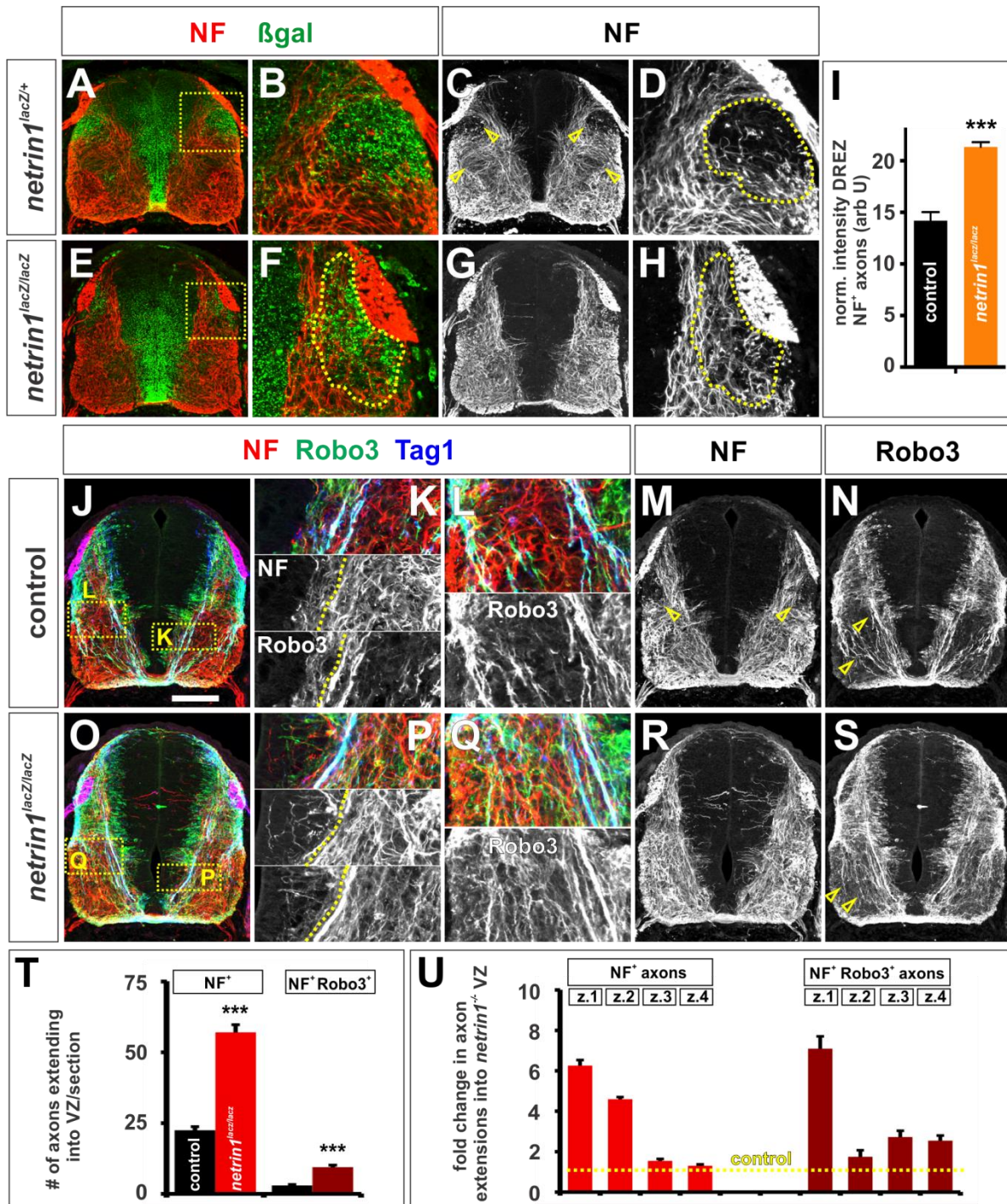
(A-R) Brachial (A-H) or thoracic (J-S) level transverse sections of E12.5 *netrin1*$^{+/+}$ (J-N), *netrin1*$^{lacZ/+}$ (A-D) or *netrin1*$^{lacZ/lacZ}$ (E-H, O-S) mouse spinal cords labeled with antibodies against NF (red), β-gal (green, A-B, E-F), Robo3 (green, J-L, N, O-Q, S) and Tag1 (blue).

(A-D) In brachial sections, NF^{+} axons project around the lateral netrin1::β-gal domain below the DREZ (dotted lines, D). This sculpting of the NF^{+} trajectories can be observed in multiple places in the mantle zone (arrowheads, C).

(E-H) The sculpting is lost in *netrin1* mutants, with many NF^{+} axons extending through the putative boundary below the DREZ (dotted lines, H)

(I) Quantification of NF^{+} intensity levels, normalized for area, in the E12.5 DREZ β-gal zone suggest that there is ~33% increase in axons in the mutant (*netrin1*$^{lacz/lacZ}$, n=131 hemisections from 4 embryos) compared to control (*netrin1*$^{lacZ/+}$, n=72 hemisections from 2 embryos) embryos.

(J-N) Control E12.5 NF^{+} Robo3^{+} Tag1^{+} axons continue to observe the VZ boundary (dotted line, K). Additional architecture is observed within the NF^{+} axon population (arrowheads, C and M), while the Robo3^{+} (J, L and N) and Tag1^{+} (J) axons form two major fascicles, one adjacent to the VZ and the other lateral to it (magnified, L; arrowheads, N).

(O-S) *Netrin1* mutant E12.5 NF^{+}, Tag1^{+} and Robo3^{+} axons continue to extend robustly into the VZ. The Robo3^{+} (O, Q and S) and Tag1^{+} (Q) fascicles are almost completely defasiculated (magnified, Q; arrowheads, S).

(T) Quantification of the NF^{+} and NF^{+} Robo3^{+} axons projecting into the VZ in E12.5: control = 22.5±1.2 NF^{+} axons/section; n= 29 sections from 3 embryos and mutant embryos = 57.0±2.7 NF^{+} axons/section; n=54 sections from 4 embryos.

(U) The NF$^+$ and NF$^+$Robo3$^+$ mis-projecting axons show the fold change in axon extension into the *netrin1$^{lacZ/lacZ}$* VZ across the dorsal-ventral axis. n as for (T).

Data represented as mean±SEM.

Probability of similarity between control and mutant, *** p< 0.0005 Student's *t*-test.

Scale bar: A-H: 165 µm; J-S: 145 µm

Figure 3-6: Netrin1 provides a growth substrate and specifies multiple boundaries
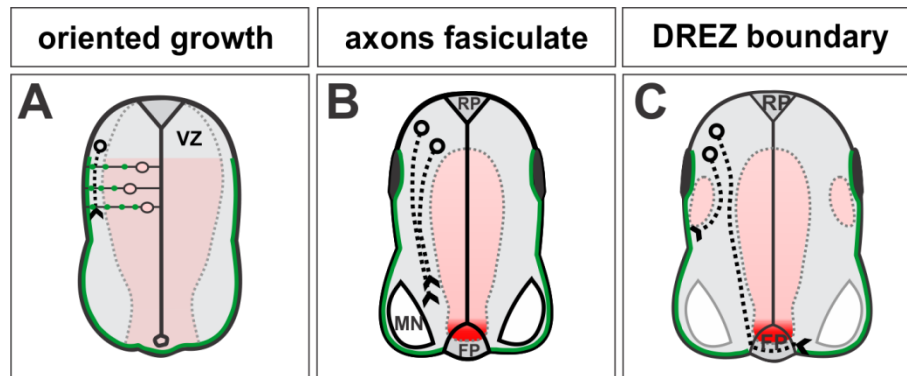
(A) Netrin1 first orients ventrally-directed growth of axons in E10.5 embryos. Netrin1 deposited on the pial surface[17] promotes axon extension (green) while cells expressing *netrin1* in the VZ are refractory to axon growth (red).

(B, C) As development progresses in E11.5 and E12.5 embryos, guidance boundaries emerge in the VZ and adjacent to the DREZ. These boundaries promote axon fasciculation (green line) while preventing innervation (red), such that axons grow along the edges of *netrin1* expression. Together, these activities sculpt axonal trajectories within the spinal cord.

Supplemental Figure 3-S1: Netrin1 expression in the *lacZ* insertion *netrin1* mutation.
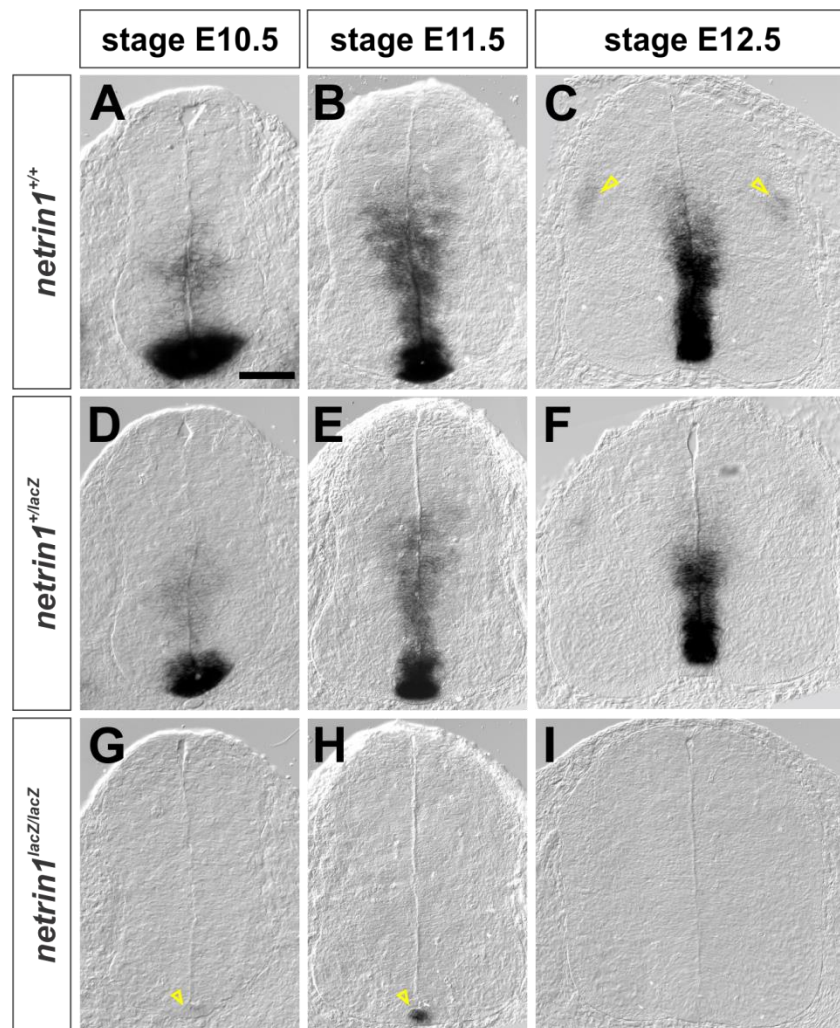
(A-I) Thoracic level transverse sections of E10.5 (A, D, G), E11.5 (B, E, H) or E12.5 (C, F. I) *netrin1*$^{+/+}$ (A-C), *netrin1*$^{+/lacZ}$ (D-F) and *netrin1*$^{lacZ/lacZ}$ (G-I) mouse spinal cords processed for netrin1 *in situ* hybridization. Trace levels of *netrin1* expression remains in the FP in *netrin1*$^{lacZ/lacZ}$ spinal cords (arrowhead, G, H).

Scale bar: 65 μm

BIBLIOGRAPHY

1. Dickson BJ. Molecular mechanisms of axon guidance. Science 2002;298(5600):1959-64.

2. Tessier-Lavigne M, Goodman CS. The molecular biology of axon guidance. Science 1996;274(5290):1123-33.

3. Kennedy TE, Serafini T, de la Torre JR, Tessier-Lavigne M. Netrins are diffusible chemotropic factors for commissural axons in the embryonic spinal cord. Cell 1994;78(3):425-35.

4. Serafini T, Kennedy TE, Galko MJ, Mirzayan C, Jessell TM, Tessier-Lavigne M. The netrins define a family of axon outgrowth-promoting proteins homologous to C. elegans UNC-6. Cell 1994;78(3):409-24.

5. Luo Y, Raible D, Raper JA. Collapsin: a protein in brain that induces the collapse and paralysis of neuronal growth cones. Cell 1993;75(2):217-27.

6. Kolodkin AL, Matthes DJ, Goodman CS. The semaphorin genes encode a family of transmembrane and secreted growth cone guidance molecules. Cell 1993;75(7):1389-99.

7. Kidd T, Bland KS, Goodman CS. Slit is the midline repellent for the robo receptor in Drosophila. Cell 1999;96(6):785-94.

8. Brose K, Bland KS, Wang KH, Arnott D, Henzel W, Goodman CS, Tessier-Lavigne M, Kidd T. Slit proteins bind Robo receptors and have an evolutionarily conserved role in repulsive axon guidance. Cell 1999;96(6):795-806.

9. Augsburger A, Schuchardt A, Hoskins S, Dodd J, Butler S. BMPs as mediators of roof plate repulsion of commissural neurons. Neuron 1999;24(1):127-41.

10. Charron F, Stein E, Jeong J, McMahon AP, Tessier-Lavigne M. The morphogen sonic hedgehog is an axonal chemoattractant that collaborates with netrin-1 in midline axon guidance. Cell 2003;113(1):11-23.

11. de Curtis I, Reichardt LF. Function and spatial distribution in developing chick retina of the laminin receptor alpha 6 beta 1 and its isoforms. Development 1993;118(2):377-88.

12. Kania A, Jessell TM. Topographic motor projections in the limb imposed by LIM homeodomain protein regulation of ephrin-A:EphA interactions. Neuron 2003;38(4):581-96.

13. Serafini T, Colamarino SA, Leonardo ED, Wang H, Beddington R, Skarnes WC, Tessier-Lavigne M. Netrin-1 is required for commissural axon guidance in the developing vertebrate nervous system. Cell 1996;87(6):1001-14.

14. Brankatschk M, Dickson BJ. Netrins guide Drosophila commissural axons at short range. Nat Neurosci 2006;9(2):188-94.

15. Keleman K, Dickson BJ. Short- and long-range repulsion by the Drosophila Unc5 netrin receptor. Neuron 2001;32(4):605-17.

16. Lai Wing Sun K, Correia JP, Kennedy TE. Netrins: versatile extracellular cues with diverse functions. Development 2011;138(11):2153-69.

17. Varadarajan S, Kong J, Kao T, Phan K, Panaitof S, Cardin J, Eltzchig H, Kania A, Novitch B, Butler S. Netrin1 produced by neural progenitors, not floor plate cells, is required for axon guidance in the spinal cord. Neuron2017.

18. Bovolenta P, Dodd J. Guidance of commissural growth cones at the floor plate in embryonic rat spinal cord. Development 1990;109(2):435-47.

19. Colamarino SA, Tessier-Lavigne M. The role of the floor plate in axon guidance. Annu Rev Neurosci 1995;18:497-529.

20. Watanabe K, Tamamaki N, Furuta T, Ackerman SL, Ikenaka K, Ono K. Dorsally derived netrin 1 provides an inhibitory cue and elaborates the 'waiting period' for primary sensory axons in the developing spinal cord. Development 2006;133(7):1379-87.

21. Tran TS, Carlin E, Lin R, Martinez E, Johnson JE, Kaprielian Z. Neuropilin2 regulates the guidance of post-crossing spinal commissural axons in a subtype-specific manner. Neural Dev 2013;8:15.

22. Ericson J, Morton S, Kawakami A, Roelink H, Jessell TM. Two critical periods of Sonic Hedgehog signaling required for the specification of motor neuron identity. Cell 1996;87(4):661-73.

23. Novitch BG, Chen AI, Jessell TM. Coordinate regulation of motor neuron subtype identity and pan-neuronal properties by the bHLH repressor Olig2. Neuron 2001;31(5):773-89.

24. Butler SJ, Bronner ME. From classical to current: analyzing peripheral nervous system and spinal cord lineage and fate. Dev Biol 2015;398(2):135-46.

25. Bylund M, Andersson E, Novitch BG, Muhr J. Vertebrate neurogenesis is counteracted by Sox1-3 activity. Nat Neurosci 2003;6(11):1162-8.

26. Graham V, Khudyakov J, Ellis P, Pevny L. SOX2 functions to maintain neural progenitor identity. Neuron 2003;39(5):749-65.

27. Kennedy TE, Wang H, Marshall W, Tessier-Lavigne M. Axon guidance by diffusible chemoattractants: a gradient of netrin protein in the developing spinal cord. J Neurosci 2006;26(34):8866-74.

28. Baker KA, Moore SW, Jarjour AA, Kennedy TE. When a diffusible axon guidance cue stops diffusing: roles for netrins in adhesion and morphogenesis. Curr Opin Neurobiol 2006;16(5):529-34.

29. Deiner MS, Kennedy TE, Fazeli A, Serafini T, Tessier-Lavigne M, Sretavan DW. Netrin-1 and DCC mediate axon guidance locally at the optic disc: loss of function leads to optic nerve hypoplasia. Neuron 1997;19(3):575-89.

30. Poliak S, Morales D, Croteau LP, Krawchuk D, Palmesino E, Morton S, Cloutier JF, Charron F, Dalva MB, Ackerman SL and others. Synergistic integration of Netrin and ephrin axon guidance signals by spinal motor neurons. Elife 2015;4.

31. Manitt C, Wang D, Kennedy TE, Howland DR. Positioned to inhibit: netrin-1 and netrin receptor expression after spinal cord injury. J Neurosci Res 2006;84(8):1808-20.

CHAPTER 4 – Type Ib BMP receptors mediate the rate of commissural axon extension through inhibition of cofilin activity

ABSTRACT

Bone morphogenetic proteins (BMPs) have unexpectedly diverse activities establishing different aspects of dorsal neural circuitry in the developing spinal cord. Our recent studies have shown that, in addition to spatially orienting dorsal commissural (dI1) axons, BMPs supply 'temporal' information to commissural axons to specify their rate of growth. This information ensures that commissural axons reach subsequent signals at particular times during development. However, it remains unresolved how commissural neurons specifically decode this activity of BMPs to result in their extending axons at a specific speed through the dorsal spinal cord. We have addressed this question by examining whether either of the type I BMP receptors (Bmpr), BmprIa and BmprIb, have a role controlling the rate of commissural axon growth. BmprIa and BmprIb exhibit a common function specifying the identity of dorsal cell fate in the spinal cord, whereas BmprIb alone mediates the ability of BMPs to orient axons. Here, we show that BmprIb, and not BmprIa, is additionally required to control the rate of commissural axon extension. We have also determined the intracellular effector by which BmprIb regulates commissural axon growth. We show that BmprIb has a novel role modulating the activity of the actin-severing protein cofilin. These studies reveal the mechanistic differences used by distinct components of the canonical Bmpr complex to mediate the diverse activities of the BMPs.

This chapter is modified from:

Yamauchi K, Varadarajan SG, Li JE and Butler SJ. (2013). Type Ib BMP receptors mediate the rate of commissural axon extension through inhibition of cofilin activity. *Development* 140(2): 333-342. DOI: 10.1242/dev.089524

INTRODUCTION

As axons grow, they encounter multiple directional cues in the constantly changing environment of the developing embryo[1]. To interpret this guidance information correctly, axons must modulate their speed to reach these cues at the right time in development. What mechanism controls this process? Our studies have suggested that, in addition to directing axon orientation, guidance signals also provide 'temporal' information by regulating actin polymerization in the growth cone to control the rate of axon growth[2]. We have been examining this mechanism using the trajectory of commissural axons within the developing spinal cord as a model system. Commissural (dI1) neurons arise in response to a putative gradient of bone morphogenetic proteins (BMPs) secreted from the roof plate (RP) at the dorsal midline[3]. They subsequently extend axons away from the RP to project towards the floor plate (FP) at the ventral midline. Our studies have identified that BMPs can both orient commissural axon growth away from the RP[4] and regulate their rate of extension through the dorsal spinal cord[2]. Thus, BMPs direct remarkably diverse cellular processes for commissural neurons depending on their stage of development.

How are these disparate activities translated by commissural neurons to result in the correct outcome at the correct time? In the canonical signaling pathway, BMPs activate a heterodimeric complex of type I and type II BMP receptors (Bmprs) to result in the phosphorylation of the receptor-activated Smads, a complex of transcriptional activators[5]. However, the regulation of cytoskeletal changes downstream of BMP signaling has been linked to the Lim domain kinase 1 (Limk1)-cofilin pathway. In this pathway, Limk1 is 'primed' by binding to the tail of BmprII and then activated after BMP binding[6,7]. Limk1 then phosphorylates, and thereby inactivates, cofilin[8]. Active cofilin depolymerizes actin and tends to

94

stimulate neurite outgrowth[9]. The balance between the activation states of Limk1-cofilin is crucial for many axon behaviors, including turning away from chemorepellents[10] and regulating their speed of growth[2,11].

However, the mechanism by which a commissural neuron discriminates between the canonical Smad and non-canonical Limk1-cofilin signaling pathway remains unclear. Our studies have suggested that this choice depends on which type I Bmprs are present in the cell during development[12]. The specification of commissural cell fate is a redundant function of both type I Bmprs, BmprIa and BmprIb[13,14]. By contrast, only BmprIb is required in commissural neurons to reorient their axons away from the RP[12]. Here, we show that BmprIb, but not BmprIa, is also required for the ability of BMPs to control the rate of commissural axon outgrowth, lending further support to a model in which BmprIb uniquely functions to mediate the ability of BMPs to act as axon guidance signals.

What is the mechanistic basis for the distinct activities of BmprIb? Our previous studies have implicated BmprII in the regulation of commissural axon growth rate, by acting as a scaffold for Limk1[2]. Does this interaction further require a particular complement of the Bmpr complex, to ensure the specific regulation of axon outgrowth rate by BMPs? Or is the activation of Limk1 non-specific, such that Limk1 is constitutively activated in the cytosol after dissociating from BmprII? Here, we provide evidence for the former model by showing that BmprIb, but not BmprIa, is required to regulate cofilin activity. The activity of BmprIb inversely affects cofilin activity and can be blocked by an isoform of cofilin that cannot be regulated by Limk1. Taken together, these studies demonstrate for the first time that the activities of Bmpr1a and BmprIb can diverge through the use of distinct second messengers. The presence of BmprIb

confers commissural neurons with the ability to regulate Limk1-cofilin activity and thereby control the speed at which they extend axons.

MATERIALS AND METHODS

Immunohistochemistry: Antibody staining was performed on 30 μm-thick cryosectioned tissues, dissociated neurons or whole-mount tissues as described previously[4]. Fluorescence images were collected on Carl Zeiss LSM510 confocal and Axiovert 200M microscopes. Images were processed using Adobe Photoshop CS4. The intensity of phospho (p)-cofilin staining was quantified using identical settings on the confocal microscope to image sections and dissociated neurons from control and mutant Bmpr littermates that underwent immunohistochemistry on the same slide.

Antibodies against the following proteins were used: mouse: neuronal class III β-tubulin at 1:2000 (Tuj1; Covance), Tag1 at 1:6 (4D7)[15], green fluorescent protein (GFP) at 1:2000 (3E6, Invitrogen), Cre at 1:1000 (Covance), HA at 1:1000 (Covance), His at 1:1000 (Covance), Myc at 1:10 (9E10)[16]; rabbit: yellow fluorescent protein (YFP) recognized by αGFP at 1:2000 (Invitrogen), phosphorylated (p)-cofilin at 1:100 (Santa Cruz Biotechnology), panLh2 (Lhx2/9) at 1:1000 (L1)[17]; sheep: GFP at 1:2000 (Biogenesis); guinea pig: Olig2 at 1:20,000[18]. Cyanine3-, cyanine5- or FITC-coupled secondary antibodies were obtained from Jackson ImmunoResearch.

In ovo **electroporation and expression constructs:** Hamilton and Hamburger (HH) stage 13-15[19] White Leghorn chick embryos (AA Laboratory Eggs) were electroporated and processed as previously described[12]. Math1 (Atoh1) enhancer expression constructs were generated as previously described[2]. Plasmid constructs were electroporated in the following amounts:

Math1::f*Gfp*, 0.1 μg/μl; Math1::*caBmprIb*-HA-IRES-f*Gfp*, 1.5 μg/μl; Math1::*wtcofilin*-myc, 1.0 μg/μl; and Math1::*cofilinS3A*-his, 1.0 μg/μl.

For HH stage 18, the number of commissural neurites was calculated as a percentage of the GFP⁺ Lhx2/9⁺ cells per cryosection. The length of GFP⁺ axons, from cell body to growth cone, was quantified using NIH Image J. For HH stages 22/23 and 27/28, axon outgrowth was quantified as previously described (Fig. 1L)[12]. At HH stage 27/28, the Lhx2/9⁺ cell bodies have started their migration into deeper layers of the dorsal spinal cord, thus there are more axons at the intermediate (INT) level compared with the mid-dorsal (MD) boundary. All statistical analyses used a one-tailed Student's *t*-test.

Generation and analysis of mutant mice: *BmprIb* mice were inbred in a mixed genetic background (129/Sv/C57/B6), whereas all other mice were inbred in an identical background (129/Sv). Mice were genotyped by PCR as previously described: *BmprIa^{flox 20}*, *BmprIb^{21}*, Math1::tau*Gfp^{22}*, Math1::*Cre^{23}*, Rosa26R::*Yfp^{24}*. In all cases, only relevant littermates were used as controls: BmprIa experiments: *BmprIa^{+/+}*±Math1::*Cre*; BmprIb experiments: *BmprIb^{+/+}*.

To assess dI1 cell fate, the number of Olig2⁺ and Cre recombinase⁺ (*BmprIa*) or Lhx2/9⁺ (*BmprIb*) cells were counted in sections from embryonic day (E) 10.5 control and mutant embryos. Data were plotted as the number of Olig2⁺ cells versus either Cre⁺ or Lhx2/9⁺ cells per section and a logarithm trend line was fitted to each data set using Microsoft Excel 2008 for Mac.

Whole-mount fillet preparations were dissected from the upper brachial to lower thoracic region of E10.5 spinal cords from the surrounding mesoderm in dispase-free medium. Spinal

cords were cut along the FP at the ventral midline, embedded in collagen (BD Biosciences), fixed and immunostained. GFP[+] axons were measured from cell body to growth cone and binned according to number of dI1 cells, as assessed by Cre[+] or Lhx2/9^{+} cells, per 100 μm hemi-segment to normalize for developmental age. Math1::*Cre* and Lhx2/9 are present in the same population of neurons[12], but Math1::*Cre* is expressed earlier than Lhx2/9, thus more Cre^{+} cells are present per 100 μm hemi-segment at the earliest stages of commissural axiogenesis compared with Lhx2/9[+].

Time-lapse imaging of fillet preparations: Time-lapse imaging of chicken embryos was performed as described previously[2]. For time-lapse imaging of mouse embryos, fillet preparations of E11.5 lumbar spinal cords were dissected as described above and embedded in collagen in glass-bottom dishes (MatTek). Explants were incubated in OptiMEM (Gibco) and 1×penicillin/streptomycin/glutamine (PSG) (Gibco) for 1 hour prior to imaging in a 37°C, 5% CO_2 cell culture incubator. The remaining embryos were kept in Hibernate E media (Gibco) at 4°C in the dark until ready for dissection. Time-lapse live imaging was performed at 37°C using an enclosed Zeiss Axiovert 200M inverted microscope fitted with an XL S1 incubator, P Lab-Tek S1 heating insert, S temperature module and a XL S heating unit (Pecon). Images were collected every 5 minutes for 4-8 hours in 7 μm z-slice intervals producing 49-84 μm-thick z-stack images. Images were captured with a Zeiss HRm camera and Apotome without optical sectioning.

Axon growth rates were quantified in a region 100-250 μm from the RP, the closest region to the RP where there was no interfering fluorescence from the GFP[+] cell bodies. Retracting axons were not included in the quantification; however, there is no significant

difference in the frequency or rate of retracting axons between control and mutant spinal cords. The growth of axons in the z-plane was compensated for by measuring the depth to which axons grew within the fillet using projected z-stack side views. Movies were exported as AVI files at a rate of 30 minutes per second, converted to Mov files and processed in Final Cut Pro 7.

Dissociated cell culture: The dorsal third of brachial and thoracic E11.5 mouse spinal cords were dissected and dissociated as previously described[25]. Dissociated neurons from each embryo were cultured in parallel on poly-D-lysine-coated german glass coverslips (Bellco Glass) in Neurobasal medium containing 10% fetal bovine serum and 1×PSG. For the experiments measuring axon length, neurons were grown for 24 hours in serum and then for 24 hours without serum. Similar differences in length were observed with or without BMP7, suggesting that there is an endogenous source of BMPs in the cultures. For experiments measuring pcofilin levels, neurons were grown for 20 hours in serum, then in serum-free OptiMEM medium containing 1×PSG for 4 hours. Neurons were stimulated with 25 ng/ml recombinant human BMP7 (R&D Systems) or an equal volume of 0.05% bovine serum albumin (BSA) for 5 minutes, fixed in 4% paraformaldehyde (J.T.Baker) and 0.5% glutaraldehyde (Sigma-Aldrich), and then processed for immunostaining.

RESULTS

Constitutive activation of BmprIb persistently slows commissural axon outgrowth

The RP-resident BMPs control the rate at which commissural axons extend through the dorsal spinal cord[2]. What is the nature of the signaling complex that transduces this activity? Our studies have shown that BmprIb regulates the orientation of commissural axons[12]: these studies

also revealed that expressing a constitutively active (ca) form of BmprIb in chicken commissural neurons resulted in these neurons extending their axons apparently more slowly through the developing spinal cord. By Hamilton and Hamburger (HH) stage 22/23, chicken commissural axons expressing caBmprIb and farnesylated green fluorescent protein (fGFP) under the control of the Math1 enhancer[26] were significantly shorter in length than control GFP[+] axons (**Figures 4-1 E-H and 4-6 I**)[12]. However, it remained unresolved whether this difference in axon length resulted from a delay in commissural axon initiation or if axon outgrowth was rather stalled or slowed.

To determine whether the constitutive activation of BmprIb results in a specific delay in commissural axon initiation, chicken embryos were *in ovo* electroporated with Math1::f*Gfp* or Math1::*caBmprIb*-IRES-f*Gfp* expression constructs at HH stage 13/14. The embryos were permitted to develop to HH stage 18 (**Figures 4-1 A-D**), the stage at which commissural axon extension begins[2]. The introduction of caBmprIb does not result in any alterations in the specification of dorsal commissural neuron fate: Lhx2/9[+] dI1 commissural neurons[17] are present in similar numbers on the electroporated and non-electroporated sides of spinal cords (**Supplementary Figure 4-S1**). Moreover, there was no significant difference in the number of control and experimental Lhx2/9^{+} neurons initiating axiogenesis (**Figure 4-1 K**). However, the experimental GFP[+] commissural axons were found to be ∼40% shorter on average than the control GFP[+] axons (**Figure 4-1 M**). Thus, the presence of caBmprIb does not delay axon initiation, but rather results in the immediate slowing of axon outgrowth.

To examine whether the defect observed at HH stage 22/23 resulted from stalled or slowed axon growth, embryos were allowed to develop to HH stage 27/28 to determine the extent of axon outgrowth from caBmprIb^{+} commissural neurons ∼1 day later in development.

100

Axon outgrowth was quantified by counting the number of Lhx2/9^{+} neurons that extended GFP[+] axons past four arbitrary boundaries in the spinal cord: mid-dorsal (MD), intermediate (INT), mid-ventral (MV) and floor plate (FP) (**Figures 4-1 L**)[12]. By HH stage 27/28, the control commissural axons have largely completed their trajectories through the transverse plane of the spinal cord: of the Lhx2/9[+] GFP^{+} neurons that extended axons to the MD level, 90% of these axons subsequently reached the FP (**Figures 4-1 I, K**). Although a similar number of Lhx2/9[+] caBmprIb-IRES-GFP^{+} neurons extend axons beyond the MD boundary (**Figures 4-1 J**), progressively fewer axons reached the subsequent levels compared with controls (**Figures 4-1 K**). However, the observed decrease in commissural axon outgrowth was far less than that seen in HH stage 22/23 spinal cords (**Figures 4-1 H and; Figure 4-6 I**)[12], suggesting that elevating BMP signaling slowed, rather than stalled, axon outgrowth. Strongly supporting this model, imaging live axons growing in elecroporated tissue explants *in vitro* demonstrated that the caBmprIb-IRES-GFP[+] axons had a ~30% slower average velocity than control GFP[+] axons as they grew through the dorsal spinal cord (**Figure 4-1 N and Supplementary Movie 4-S1**). This decreased rate of growth is consistent with the shorter length of axons extending from caBmprIb-IRES-GFP[+] axons (**Figures 4-1 M and 4-6 I**).

Taken together, these studies demonstrate that the constitutive activation of BmprIb in dI1 neurons results in persistent reduction in the speed of commissural axons growing through the dorsal spinal cord.

Commissural neurons deficient in BmprIb, but not BmprIa, extend longer axons *in vitro*

If elevating BMP signaling in commissural neurons slows axon growth, then, conversely, lowering BMP signaling should accelerate the rate of axon outgrowth. Moreover, our previous

studies have also suggested that BmprIb specifically transduces the ability of BMPs to regulate commissural axon orientation. The other type I Bmpr, BmprIa, did not have a significant effect on commissural axon outgrowth when misexpressed in chicken spinal cords[12]. Thus, if BmprIb is the critical receptor that mediates the ability of BMPs to control the rate of axon outgrowth, then commissural axon growth should be accelerated in the absence of BmprIb, but not in the absence of BmprIa.

To address this question, we examined mice mutant for either *BmprIa* or *BmprIb* in combination with a genetically encoded Math1::tau*Gfp* reporter, which expresses GFP in the dI1 population of dorsal commissural axons[22,27]. Although *BmprIb* loss-of-function mutants are viable[21], the loss of *BmprIa* is lethal[28]. Therefore, we took a conditional approach to inactivate *BmprIa*, crossing a floxed allele of *BmprIa*[20] to transgenic mice expressing Cre recombinase under control of the Math1 enhancer[23]. To check that Cre recombination was active in commissural neurons, we crossed mice from the Math1::*Cre* line to a Rosa26R(lox-stop-lox)::*Yfp* reporter strain[24]. At E10.5 and E11.5, Cre protein was observed in Lhx2/9$^+$ commissural neurons (**Supplementary Figures 4-S2 B,F**)[12] and YFP was present both in the cell bodies and Tag1 (Cntn2)$^+$ axons of commissural neurons (**Supplementary Figure 4-S2 C, D, G, H,** arrows).

As a first approach to examining whether the loss of *BmprIa* or *BmprIb* alters commissural axon outgrowth, we assessed the length of GFP$^+$ axons extending from dissociated control (Math1::*Cre*; Math1::tau*Gfp*; *BmprIa*$^{+/+}$ or Math1::tau*Gfp*; *BmprIb*$^{+/+}$) and mutant (Math1::*Cre*; Math1::tau*Gfp*; *BmprIa*$^{flox/flox}$ or Math1::tau*Gfp*; *BmprIb*$^{-/-}$) commissural neurons (**Figure 4-2 A**). *BmprIa* mutant commissural axons were similar in length to those from littermate control commissural neurons (**Figure 4-2 B, C, F**). By contrast, *BmprIb*$^{-/-}$ neurons

extended axons that were almost 20% longer on average than the controls (**Figure 4-2 D-F**). Thus, the absence of BmprIb, but not BmprIa, results in increased commissural axon growth *in vitro* supporting the hypothesis that a specific activity of BmprIb is to slow the rate of commissural axon extension.

Commissural axons deficient in BmprIb, but not BmprIa, show accelerated growth *in vivo*

In a second approach to examine the effect of functionally inactivating the type I Bmprs on the growth rate of commissural axons, we compared the length of commissural axons growing *in vivo* in E10.5 type I Bmpr control and mutant spinal cords. To avoid complications that could arise from even minor developmental heterogeneities between embryos, we sought to use the number of either Lhx2/9$^+$ or Cre$^+$ commissural neurons as an indicator of developmental age, rather than the axial level of the spinal cord. This strategy requires that the removal of either type I Bmpr has no effect on the number of commissural neurons. To assess this possibility, we correlated a BMP-independent indicator of spinal cord development[29], the number of Olig2$^+$ motor neuron progenitors (pMNs)[30], with the extent of either Lhx2/9$^+$ or Cre$^+$ commissural neuron development in E10.5 control (**Supplementary Figure 4-S3 A, B**) or mutant (**Supplementary Figure 4-S3 C, D**) spinal cords. The number of Olig2$^+$ pMNs declined in a similar manner with respect to Cre$^+$ neurons in *BmprIa* control and mutant spinal cords (**Supplementary Figure 4-S3 E**), and Lhx2/9$^+$ neurons in *BmprIb* control and mutant spinal cords (**Supplementary Figure 4-S3 F**). This observation strongly suggests that the specification of commissural cell fate is normal in the type I Bmpr mutant mice and that the numbers of commissural neurons can be used as an accurate indicator of the stage of spinal cord development.

To assess the extent of commissural axon outgrowth, longitudinal 'fillet' preparations of the spinal cord were dissected from E10.5 type I Bmpr control and mutant spinal cords (**Figure 4-3 A**). At E10.5, commissural neurons are in the process of extending axons away from the RP[4] and towards the FP[31,32], such that the length of the commissural trajectories markedly increases along the caudal-to-rostral axis of the spinal cord. Similar to our observations using *in vitro* cultures, the length of the GFP[+] commissural axons growing *in vivo* were indistinguishable in *BmprIa* mutant and control fillets (**Figure 4-3 B-G, N,** brackets). By contrast, the GFP[+] commissural axons extending in the caudal regions of *BmprIb*^{−/−} fillets were on average 10-20% longer than those in control fillets (**Figure 4-3 H-M, O,** brackets). However, although this trend persisted, the difference in commissural axon length was not statistically significant at more rostral levels of the spinal cord, most likely because of the challenge of scoring GFP[+] commissural axon length against the background staining of Math1::tau*Gfp* in the motor column[27].

To examine whether the difference in axon length observed in *BmprIb* mutants results from commissural axons growing at an accelerated rate, we directly measured the velocity of commissural axon growth in the dorsal spinal cord using time-lapse imaging. Supporting our previous results that BmprIa does not transduce the ability of the BMPs to regulate the rate of commissural axon outgrowth, *BmprIa* mutant commissural axons grew at 13±0.5 μm/hour on average, a statistically identical velocity to that of littermate control commissural axons (**Figure 4-4 C**). By contrast, commissural axons in *BmprIb*^{−/−} fillets grew at 17±0.8 μm/hour, an average velocity 3 μm/hour faster than the littermate controls (**Figure 4-4 A-C; Supplementary Movie 4-S2**). This 20% average increase in velocity is in good agreement with the 18.5% increase in commissural axon length seen at caudal levels in *BmprIb* mutants (**Figure 4-3 O**).

We further examined how the rate of commissural axon outgrowth changed as the axons extended through specific 50 μm regions of the dorsal spinal cord, starting at a region 100-250 μm from the RP. Control and *BmprIa* mutant commissural axons grew at a rate of 11-15 μm/hour throughout the interval examined, showing no statistical differences in the speed within each 50 μm region (**Figure 4-4 C**; data not shown). However, the *BmprIb*$^{-/-}$ commissural axons showed striking variations in their velocities. They grew ∼45% faster than control axons within the 50 μm interval closest to the RP, at an average rate of 21±1.6 μm/hour (**Figure 4-4 C**). The commissural axons slowed in the next 50 μm interval, dropping to an average velocity similar to control (**Figure 4-4 C**), and then grew ∼25% faster than control in the next 50 μm interval, at a rate of 18±1.5 μm/hour (**Figure 4-4 C**). Thus, the *BmprIb* mutant axons showed a much wider range in the rate at which they grew, compared with either control or *BmprIa* mutant axons.

Taken together, these studies show that the loss of BmprIb, and not BmprIa, results in accelerated axon outgrowth *in vivo*, suggesting that the BMPs slow commissural axon outgrowth by specifically activating BmprIb.

BmprIb is required to downregulate cofilin activity

What is the mechanism by which BmprIb controls the rate of commissural axon outgrowth? Our recent studies have suggested that BMPs alter the balance between the activation states of Limk1 and cofilin to regulate the speed of commissural axon extension[2]. In particular, BMP7 stimulation of commissural neurons resulted in the activation of Limk1, which in turn phosphorylated, and thereby inactivated, cofilin[2]. In light of these previous results, we examined whether the altered rates of axon outgrowth, observed after modulating BmprIb activity, were a consequence of BmprIb regulating the activity of Limk1-cofilin in commissural neurons. This

hypothesis predicts that decreased BmprIb activity will result in a decrease in the level of phosphorylated inactive cofilin.

To assess whether BmprIa or BmprIb is required for the BMP-mediated inactivation of cofilin, we examined the distribution of phosphorylated (p)-cofilin in transverse sections taken from E10.5 *BmprIa* and *BmprIb* control and mutant embryos. Whereas the loss of BmprIa had no effect on the intensity of pcofilin staining in the dorsal spinal cord (**Figure 4-5 A, B, E**), there was a 20% decrease in the level of pcofilin in the BmprIb mutants (**Figure 4-5 C-E**), suggesting that only BmprIb regulates cofilin activity. To determine whether *BmprI*-deficient neurons responded appropriately to BMP stimulation, we briefly treated cultures of dissociated commissural neurons taken from E11.5 control or mutant mouse spinal cords with either BMP7 recombinant protein or a vehicle control. The loss of BmprIa had no effect on the response of commissural neurons to BMP7 (**Figure 4-5 N**; data not shown). By contrast, there was no increase in the level of pcofilin after BMP7 stimulation of $BmprIb^{-/-}$ commissural neurons (**Figure 4-5 J-N**) whereas pcofilin was significantly increased in the $BmprIb^{+/+}$ commissural neuron cultures treated with BMP7 (**Figure 4-5 H, I, N**). Thus, BmprIb is required to transduce the ability of BMP7 to phosphorylate cofilin.

A non-phosphorylatable form of cofilin rescues the growth defects observed after constitutively activating BmprIb

To examine further whether BmprIb regulates cofilin activity, we assessed whether increasing the amount of cofilin was sufficient to rescue the delay in axon outgrowth observed after constitutively activating BmprIb. Moreover, we wanted to determine whether BmprIb works through Limk1 to alter the activation state of cofilin. Towards these goals, we assessed the

effect on commissural axon outgrowth of two forms of cofilin: wild-type (wt) cofilin, which can be regulated by Limk1, and cofilinS3A, an analog that cannot be phosphorylated by Limk1[8]. Our previous studies have shown that overexpressing wt-cofilin in chicken commissural neurons results in their extending significantly faster growing axons than neurons electroporated with the Math1::f*Gfp* control construct alone[2]. We confirmed these studies (**Figure 4-6 A, B, I**), and also observed that cofilinS3A[+] commissural axons grow at rates comparable to wt-cofilin[+] commissural axons (**Figure 4-6 E, F, I**). Thus, increasing the amount of free cofilin can, by itself, enhance axon outgrowth.

However, these two forms of cofilin do not have equivalent abilities to rescue the BmprIb-mediated axon outgrowth defect. By HH stage 22/23, ~20% of control GFP^{+} commissural neurons have extended axons to the FP (**Figure 4-6 I**). By contrast, only 10% of the caBmprIb[+] commissural axons have reached the FP (**Figure 4-6 I**). Co-expression of Math1::*cofilinS3A* with Math1::*caBmprIb*-IRES-f*Gfp* in commissural neurons rescues this defect: 20% of co-electroporated neurons now project axons to the FP (**Figure 4-6 G-I**). Thus, cofilinS3A can bypass the upstream regulatory events mediated by caBmprIb, thereby restoring normal axon growth at the FP. However, concomitantly increasing the level of wt-cofilin and caBmprIb further exacerbates the commissural axon growth defect. The rate of axon extension declined even further, such that <5% of the commissural axons reached the FP (**Figure 4-6 C, D, I**). This result strongly suggests a direct regulatory link between BmprIb, Limk1 and cofilin (**Figure 4-6 J**): caBmprIb acting through Limk1 can further slow the rate of commissural axon growth by inactivating both the wt-cofilin and the endogenous cofilin, thereby stabilizing actin in its filamentous form.

107

DISCUSSION

Modulating the activity of BmprIb alters the rate of commissural axon growth

In addition to the guidance cues that provide directional information to orient axons[33], axons also appear to be directed by extrinsic guidance cues to grow at a particular speed. Such 'temporal' information can control the rate and/or time at which directional cues are interpreted and is thus an important mechanism to ensure that axonal circuits develop in synchrony with the rest of the developing embryo. We had previously shown that the BMP RP chemorepellent provides temporal cues to commissural neurons[2], controlling the rate at which they extend axons through the dorsal spinal cord. These studies had implicated the type II BMP receptor (BmprII) as an essential factor that mediates the ability of BMPs to control the speed at which commissural axons grow. Here, we show that the other component of the canonical Bmpr complex, BmprIb, is also required to establish the correct rate of commissural axon growth. BmprIa is not required for temporal control, further demonstrating the specificity of the action of type I Bmprs.

Our previous time-lapse imaging studies had found that commissural axons in chicken embryos normally extend at ~13 μm/hour[2]. However, when BMP signaling was decreased in commissural neurons using a truncated form of BmprII, their axons now grew at ~18 μm/hour. We see remarkably similar changes in the velocity of commissural axons deficient for *BmprIb*. Control mouse axons grow at ~14 μm/hour whereas *BmprIb*$^{-/-}$ neurons extend axons at ~17 μm/hour. Moreover, control axons grew at a relatively constant speed through the dorsal spinal cord. *BmprIb*$^{-/-}$ axons show far more variability: accelerating and decelerating from 15 to 21 μm/hour depending on their distance from the RP. It remains unresolved whether the *BmprIb*$^{-/-}$ axons change their speed consistently as they grow, or if this variability rather reflects a role for

BMP signaling in stabilizing growth rates through the dorsal spinal cord. Supporting this latter possibility, we had predicted that commissural axons might accelerate while growing down the presumptive gradient of BMPs in the dorsal spinal cord. However, this model is not the case in rodents. Rather, commissural axons normally grow at the same average rate through the dorsal spinal cord, suggesting that the BMP chemorepellent establishes the speed of growth from the outset of axiogenesis. That the rate of axon outgrowth becomes more variable in the absence of BmprIb signaling further suggests that BMPs might also function in a long-range manner to keep the rate of growth constant.

BmprIb regulates the balance between the activities of Limk1-cofilin

The regulation of Limk1-cofilin activity is important for balancing commissural axon growth and guidance decisions[2]. However, it remains unclear how the Limk1-cofilin pathway is regulated by BMPs. Other groups have implicated a regulatory interaction between BmprII and Limk1, in which binding to the intracellular tail of BmprII 'primes' Limk1 for activation[6,7]. However, the molecular events that lead to Limk1 being phosphorylated and thereby activated in this context have remained unresolved. Many studies have implicated ROCK and Rho GTPases in the activation of Limk1[34]; however, these are broadly acting factors making it unclear where the specificity of their action resides. Could BmprIb, which is putatively recruited into a complex with BmprII upon BMP binding, have a role in this process? We concentrated on examining how BmprIb regulates cofilin, because cofilin is a direct effector of actin dynamics[35].

Our results show that there is an inverse correlation between the activity of BmprIb and both the activity of cofilin and the rate of axon outgrowth. When signaling through BmprIb was increased, the activity of cofilin decreased and the growth rate of commissural axons slowed.

109

Our studies have also implied that the ratio of active to inactive cofilin is a crucial part of the mechanism that controls the speed of axon growth. When BmprIb signaling was increased and the level of wt-cofilin concomitantly increased, this combination slowed the rate of commissural axon growth even further (**Figure 4-6 I**). This observation suggests that caBmprIb can inactivate both endogenous and ectopically expressed cofilin, thereby further antagonizing actin polymerization and decreasing the rate of axon growth. Finally, our studies have implicated Limk1 as the key intermediate by which BmprIb regulates cofilin. Only cofilinS3A, which functions independently of Limk1 regulation, can rescue the axon outgrowth defect caused by caBmprIb. Thus, if Limk1 activity is bypassed in the presence of caBmprIb, cofilin remains active, strongly implying that BmprIb acts through Limk1 to control the speed of commissural axon outgrowth (**Figure 4-6 J**).

**BmprIb regulates the Limk1-cofilin pathway to regulate the rate of commissural axon outgrowth**

How are the distinct activities of the BMPs translated by commissural neurons into different cellular processes? Our studies[2,27,36] have lent support to a model in which these activities are differentially translated at both the receptor and second messenger levels. In this model, a shared activity of type I Bmprs is to mediate the specification of the dorsal-most cell fates by activating the BMP receptor-regulated Smads[27], the canonical second messenger intermediates[5]. BmprIb alone mediates the guidance activities of BMPs. BmprIb modulates the activity of the Limk1-cofilin pathway to control the rate at which the actin cytoskeleton polymerizes or treadmills (**Figure 4-6 J**)[37]. The ability of BMPs to re-orient commissural axons appears to be controlled through activation of the phosphoinositide-3-kinase pathway[38].

These results imply that there is a mechanistic difference in the ability of BMPs to signal through type I Bmprs to specify cellular identity versus axon growth rate. The basis of this mechanistic difference is unresolved; the different BMP ligands present in the RP might differentially activate the type I Bmprs[17,39]. Alternatively, the intrinsic context in which the type I Bmprs are activated might change as commissural neural development proceeds. The correct 'context' for a specific activity could simply be determined by the composition of the Bmpr complex or the complement of second messengers present in commissural neurons. Thus, the presence of both type I Bmprs might activate the Smad transcription factors, whereas the presence of only BmprIb results in signaling through Limk1. The presence or absence of Limk1 may also be crucial in determining 'context'. Limk1 is only present in post-mitotic spinal neurons[2]. The direct interaction of Limk1 with BmprII followed by BMP dimerization of the Bmpr complex might result in a downstream response that either bypasses or works in conjunction with the canonical Smad signaling pathway[27,36].

In summary, BmprIb is required with BmprII to regulate commissural axon outgrowth through the Limk1-cofilin pathway. These studies have shed light on the specific identity of the receptor complex that permits the diverse activities of the BMPs to be translated within commissural neurons and have also further described the intrinsic signaling pathway by which axon outgrowth can be accelerated *in vivo*. This mechanism is likely to have clinical relevance; the intrinsic mechanisms by which axon growth is inhibited *in vivo* must be overcome for the regeneration of neural circuitry to be successful. Moreover, the modulation of these mechanisms may provide a means of accelerating the regeneration of neural circuits, thereby speeding up the lengthy process of re-growing neural circuits in a human patient.

Figure 4-1: Constitutive activation of BmprIb persistently delays commissural axon outgrowth
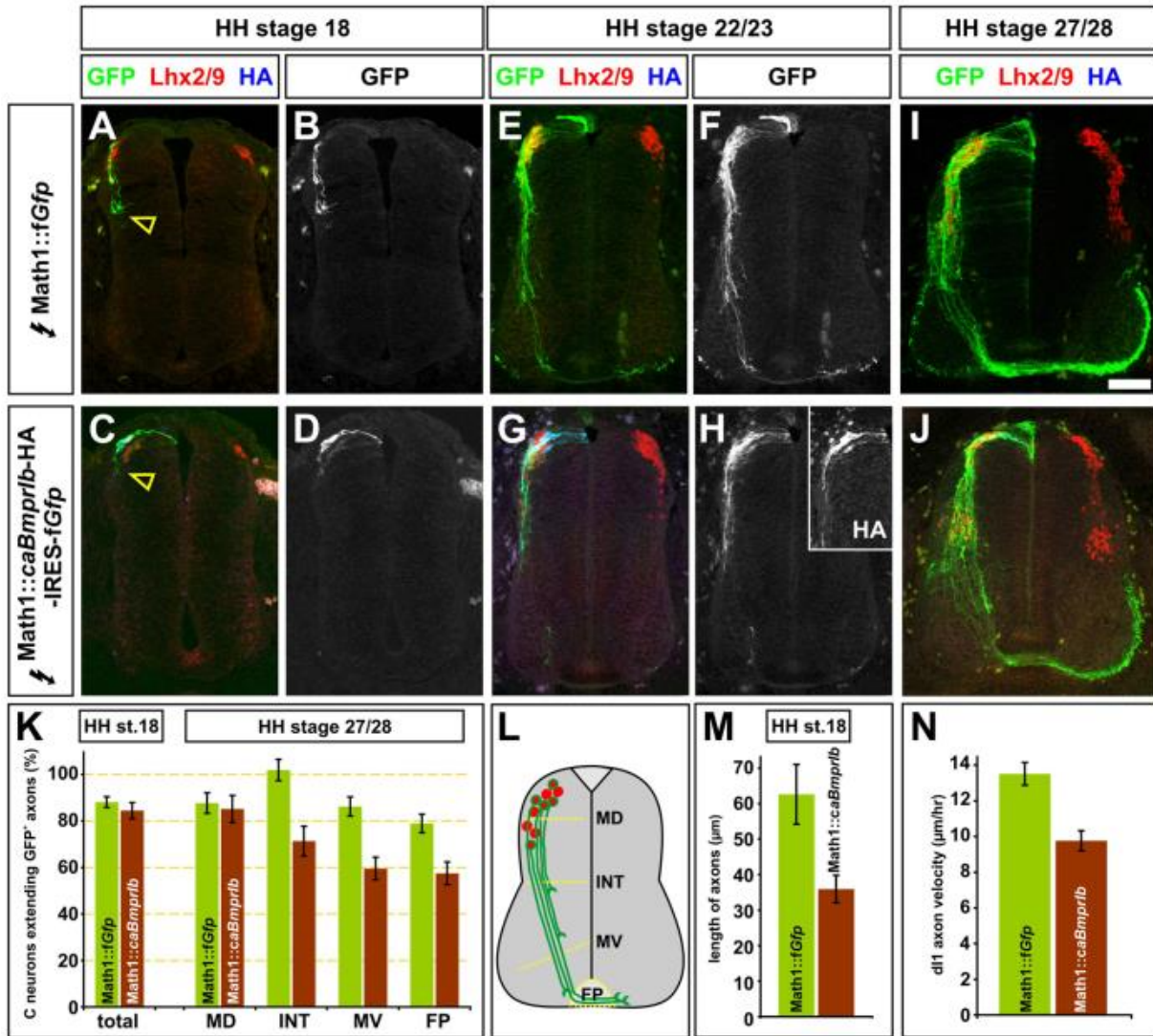
(**A-K, M**) Constructs encoding farnesylated (f) GFP (control, A,B,E,F,I) or constitutively active

(ca) BmprIb-HA-IRES-fGFP (experimental, C,D,G,H,J) were ectopically expressed under the

control of the Math enhancer by *in ovo* electroporation at either Hamburger-Hamilton (HH)

112

stages 13/14 (A-D) or 14/15 (E-J). Chicken embryos were harvested at HH stages 18 (A-D), 22/23 (E-H) or 27/28 (I, J). Transverse sections of the spinal cord were examined for the extent of fGFP$^+$ (green) and HA$^+$ (blue) axon outgrowth and number of Lhx2/9$^+$ commissural neurons (red). The distribution of HA-tagged BmprIb was indistinguishable from fGFP expressed from the IRES cassette (inset panel, H).

(A-D, K, M) Control and experimental Lhx2/9$^+$ neurons are born in similar numbers and initiate axon growth at the same time. Over 80% of Lhx2/9$^+$ neurons electroporated with fGFP (n=69 sections, three embryos) or caBmprIb (n=68 sections, four embryos) have initiated axon growth (probability of similarity between the control and experimental conditions, P>0.18, Student's t-test). However, the caBmprIb-IRES-fGFP$^+$ axons (n=43 sections, five embryos) have extended significantly less (P<0.0036) than the GFP$^+$ axons (n=49 sections, three embryos).

(E-J, K) caBmprIb$^+$ commissural axons continue to grow more slowly than fGFP$^+$ axons. By HH stage 27/28, 87% of commissural neurons had extended GFP$^+$ axons, 90% of these axons subsequently reached the FP (n=132 sections, six embryos). Similarly, 85% of caBmprIb-IRES-fGFP$^+$ neurons (n=56 sections, four embryos) extended axons (P>0.38). However, progressively fewer of these axons reach the different boundaries in the spinal cord, such that only 70% of these axons have reached the FP (P<1.9×10^{-3}).

(**L**) The extent of commissural axon outgrowth was quantified by determining whether axons had crossed one of four arbitrary boundaries: mid-dorsal (MD), intermediate (INT), mid-ventral (MV) or the FP.

(**N**) Control axons extending through HH stage 20/21 dorsal spinal cords have a velocity of 13.5±0.6 μm/hour (n=11 neurons, two embryos) whereas the caBmprIb$^+$ axons grow

significantly slower (*P<0.002*) with a velocity of 9.8±0.8 μm/hour (*n=13* neurons, three embryos). Error bars represent s.e.m. Scale bar: in A-D, 40 μm; in E-H, 50 μm; in I,J, 70 μm.

Figure 4-2: Dissociated *BmprIb$^{-/-}$* neurons extend longer axons than controls *in vitro*
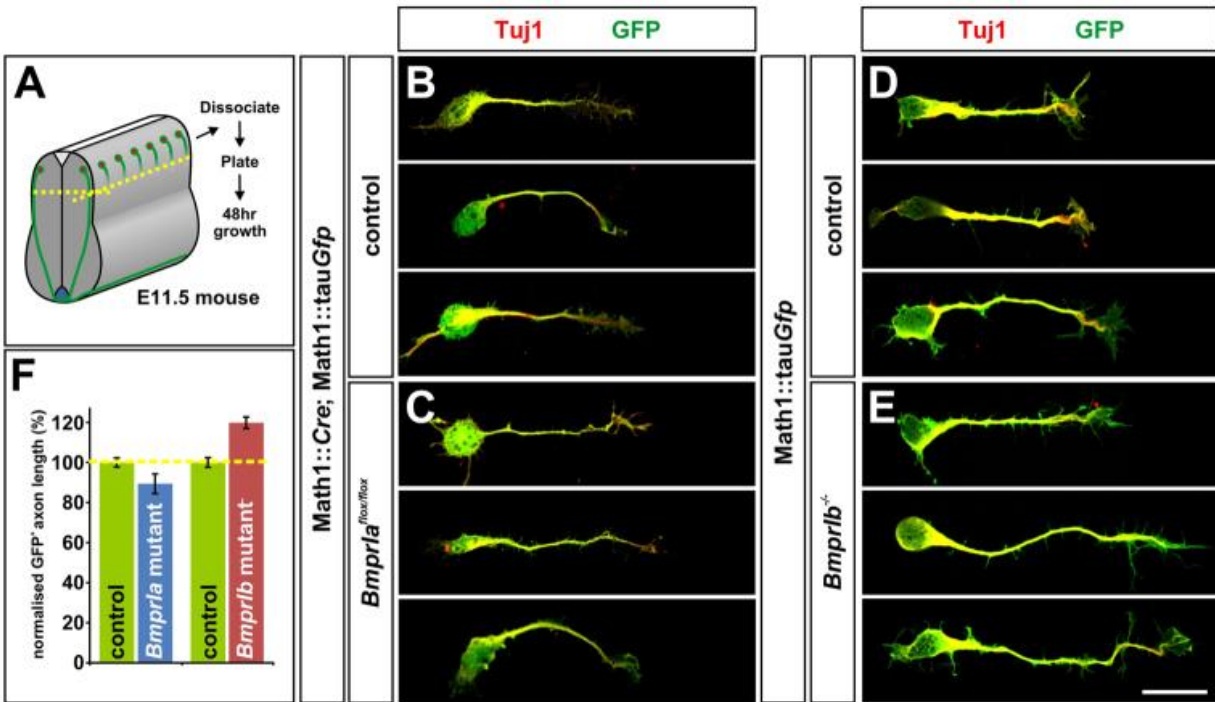

(A) Schematic of the experimental procedure for dissociated neuron cultures. Dissociated neurons from the dorsal third of brachial and thoracic E11.5 mouse spinal cords (dissected as indicated by yellow dotted lines) were analyzed after 48 hours growth (see Materials and methods for details).

(**B-F**) Commissural axons were detected using antibodies against type III β-tubulin (Tuj1, red in B-E) which label all neuronal processes[40] and a genetically encoded reporter, Math1::tau*Gfp*[22] (green in B-E). Tuj1$^+$ GFP$^+$ axon outgrowth was comparable (*P*>0.048, Student's *t*-test) in *BmprIa* control (Math1::*Cre***;***BmprIa$^{+/+}$*; *n*=354 neurons, eight embryos) and mutant (Math1::*Cre***;***BmprIa$^{flox/flox}$, n*=80 neurons, four embryos) littermates. By contrast, the *BmprIb$^{/-}$* Tuj1$^+$ GFP$^+$ axons extended almost 20% further (*P*<1.2×10^{-6}; *n*=287 neurons,

three embryos) than those from control littermates (*n=327* neurons, three embryos). Error bars represent s.e.m. Scale bar: 20 μm.

**Figure 4-3: Commissural axons extend more rapidly *in vivo* in the absence of *BmprIb***
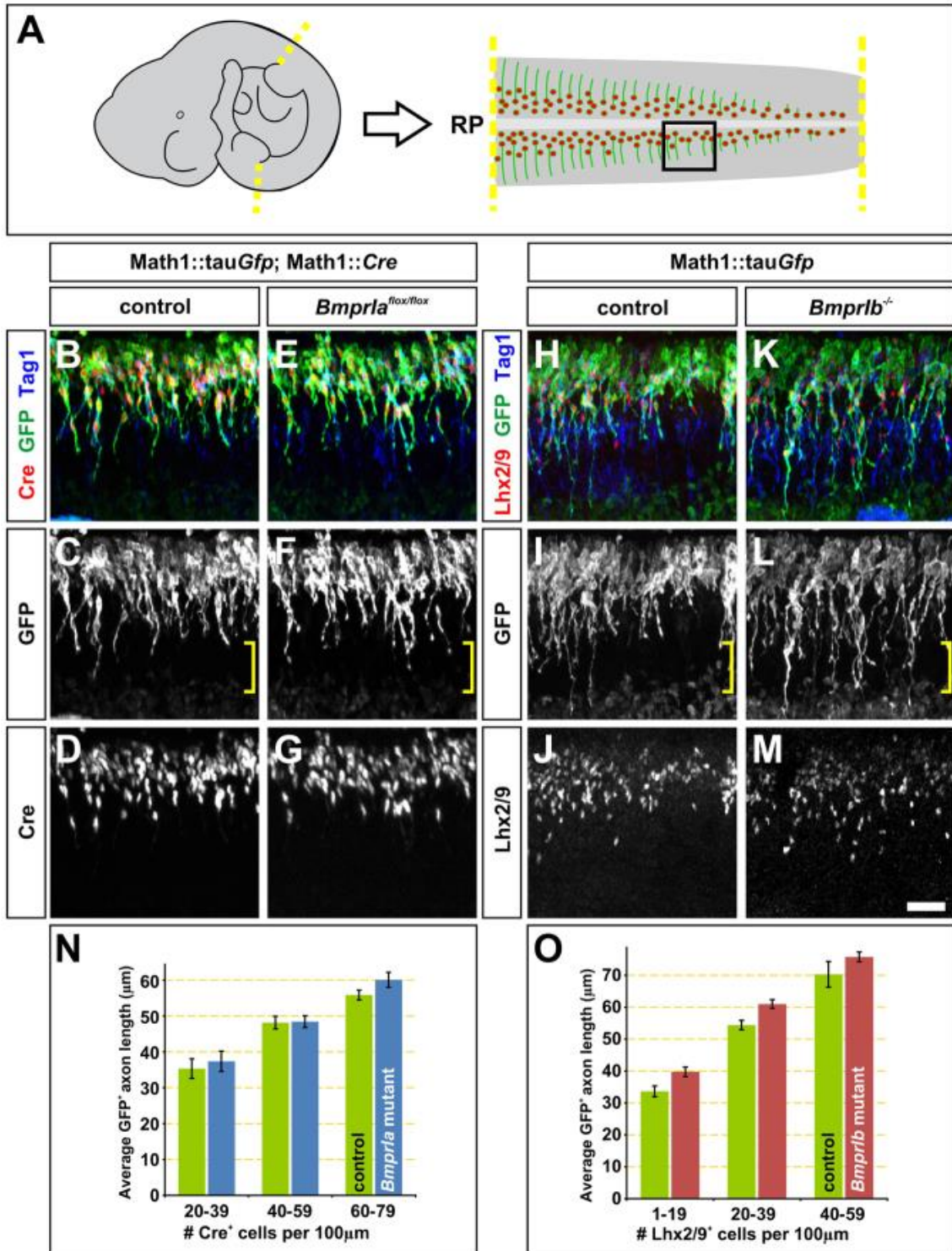
(**A**) Explants were taken from the brachial and thoracic levels of E10.5 mouse spinal cord. The boxed region represents the orientation of the images in panels B-M.

(**B-M**) Commissural axons were detected using antibodies against Tag1 (blue in B,E,H,K) and a genetically encoded reporter, Math1::tauGfp (green in A,B,E,H,K). Antibodies against Cre (red in B,E) or Lhx2/9 (red in H,K) were used to normalize the stage of commissural neuron development. The extent of commissural axon outgrowth was equivalent in the $BmprIa$ control (Math1::Cre; Math1::tauGfp; $Bmpr1a^{+/+}$; bracket in C) and mutant (Math1::Cre; Math1::tauGfp; $Bmpr1a^{flox/flox}$; bracket in F) fillets. By contrast, commissural axons extended further in the $BmprIb^{-/-}$ fillets (bracket in I) compared with control fillets (bracket in L).

(**N**) There was no significant difference between axon growth within the $BmprIa$ mutant and control fillets at three stages of Cre^+ commissural neuron development: 20-39 Cre^+ neurons ($P>0.30$, Student's t-test; control: $n=61$ axons, eight embryos, mutant: $n=63$ axons, three embryos); 40-59 Cre^+ neurons ($P>0.45$; control: $n=196$ axons, mutant: $n=210$ axons); and 60-79 Cre^+ neurons ($P>0.04$, control: $n=440$ axons, mutant: $n=240$ axons).

(**O**) By contrast, the $BmprIb$-deficient axons extended up to 18.5% further than the control axons: 1-19 Lhx2/9$^+$ neurons ($P<0.0091$, control: $n=159$ axons, four embryos, mutant: $n=262$ axons, six embryos); 20-39 Lhx2/9$^+$ neurons ($P<0.0014$, control: $n=387$ axons, mutant: $n=520$ axons); and 40-59 Lhx2/9$^+$ neurons ($P>0.20$, control: $n=85$ axons, mutant: $n=566$ axons). Error bars represent s.e.m. Scale bar: 50 μm.

Figure 4-4: *BmprIb*$^{-/-}$ axons have accelerated growth rates in the mouse dorsal spinal cord
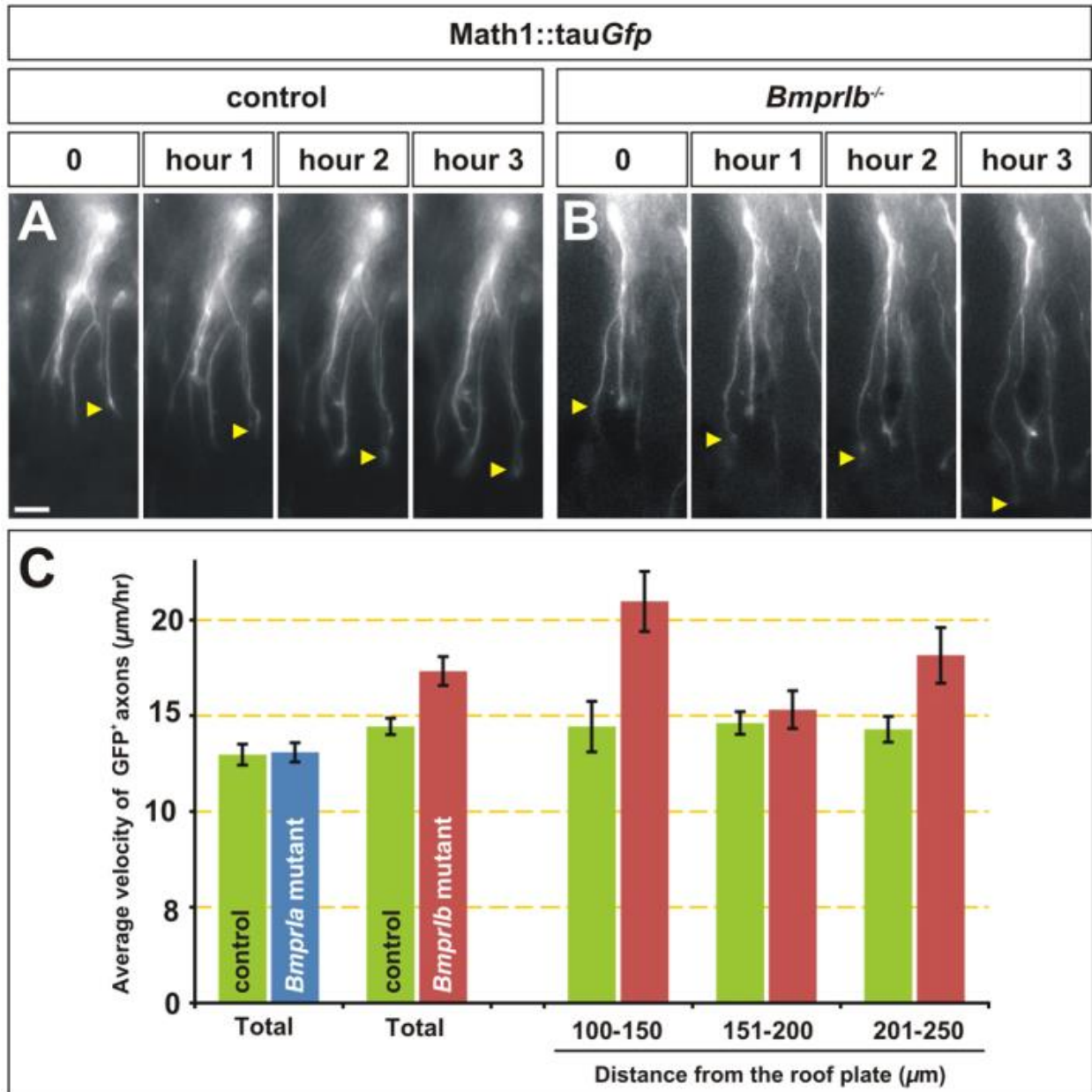

(**A-C**) The growth rate of GFP$^+$ commissural axons was monitored using time-lapse imaging in longitudinal preparations of lumbar spinal cord taken from E11.5 *BmprIa* control (Math1::*Cre*; Math1::tau*Gfp*; *Bmpr1a*$^{+/+}$) mutant (Math1::*Cre*; Math1::tau*Gfp*; *Bmpr1a*$^{flox/flox}$)

or *BmprIb* control (Math1::tau*Gfp*; *Bmpr1b*$^{+/+}$) and mutant (Math1::tau*Gfp*; *Bmpr1b*$^{-/-}$) littermates.

(A, B) Stills taken from a *BmprIb* control (A) and mutant (B) spinal cord (see also supplementary material Movie 2). The arrows indicate the progress of an advancing growth cone. Scale bar: 20 μm.

(C) There was no statistical difference in the rate of growth of GFP$^+$ axons in *BmprIa* mutants and controls (*P*>0.43, Student's *t*-test; control, *n*=53 neurons, five embryos; mutant, *n*=48 neurons, four embryos). By contrast, *BmprIb* mutant commissural axons grew on average 20% faster than their respective littermate controls (*P*<0.00017; control, *n*=107 neurons, seven embryos; mutant, *n*=67 neurons, five embryos). Moreover, the control GFP$^+$ axons grew consistently at about 15 μm/hour, whereas the speed of the *BmprIb*$^{-/-}$ GFP$^+$ axons varied significantly as follows: 100-150 μm from the RP, 45% faster than control axons (*P*<0.0018; control, *n*=37 measurements; mutant, *n*=52 measurements); 150-200 μm from the RP, no difference (*P*>0.25; control, *n*=154; mutant, *n*=108); 200-250 μm from the RP, 25% faster than control axons (*P*<0.012; control, *n*=171; mutant, *n*=34). Error bars represent s.e.m.

Figure 4-5: BmprIb is required to regulate cofilin activity in response to BMP stimulation
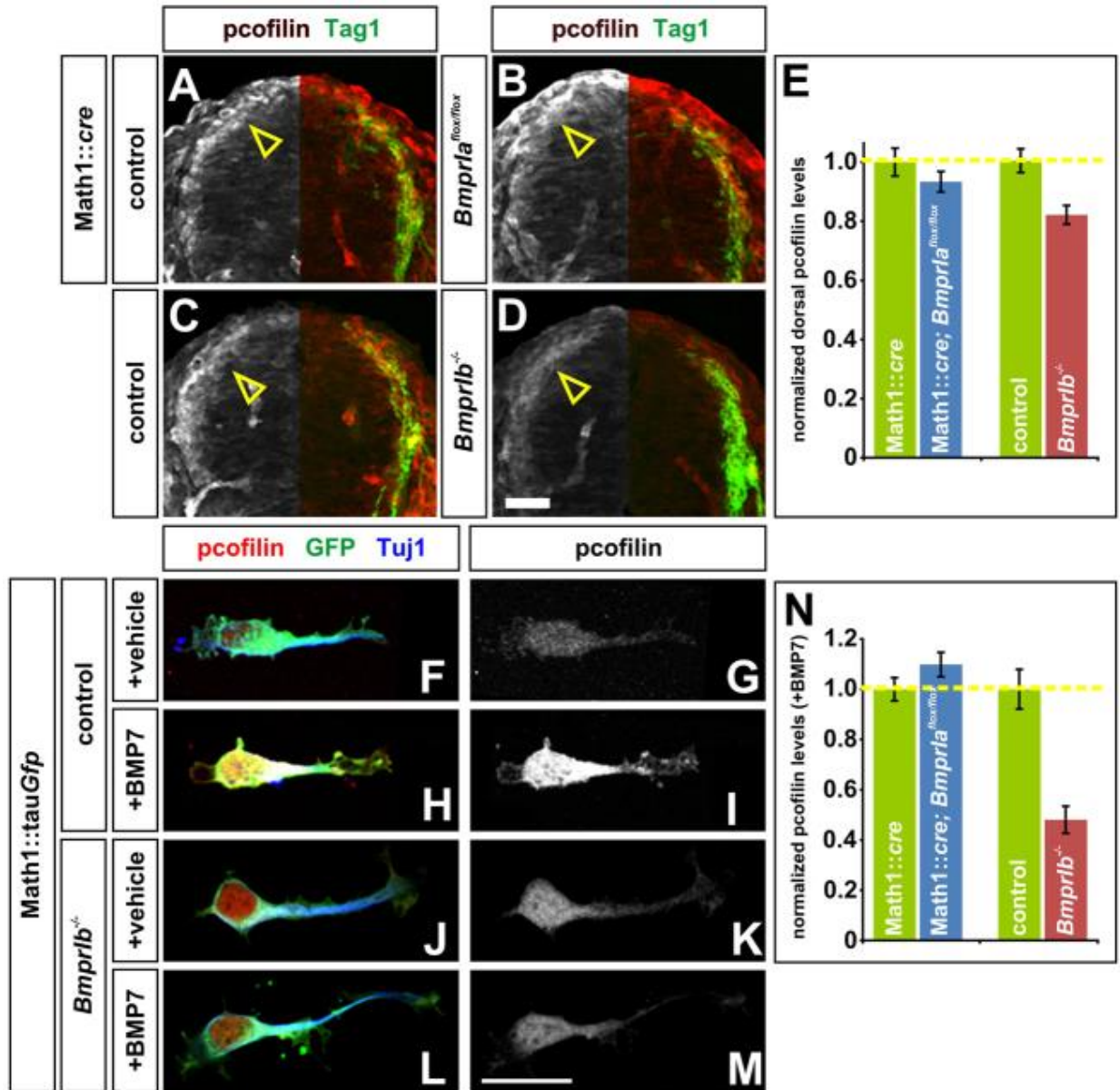
(**A-E**) E10.5 control [Math1::*cre* (A) or ***BmprIb***$^{+/+}$ (C)], or mutant [Math1::***Cre***; ***BmprIa***$^{flox/flox}$ (B) or ***BmprIb***$^{-/-}$ (D)], mouse brachial spinal cords labeled with antibodies against phospho (p)-cofilin (red and gray) and Tag1, which labels commissural

121

neurons (green). The intensity of dorsal pcofilin staining was similar (P>0.12, Student's t-test) in **BmprIa** mutant (**n**=200 sections, three embryos) and control littermates (**n**=144 sections, four embryos). By contrast, pcofilin staining was 20% lower (P<2.4×10^{-4}) in **BmprIb**$^{-/-}$ embryos (**n**=195 sections, five embryos) compared with control littermates (**n**=212 sections, five embryos).

(**F-N**) Dissociated E11.5 mouse commissural neurons from *BmprIa* and *BmprIb* control or mutant littermates were stimulated in parallel with either vehicle (mock stimulation) or BMP7 recombinant protein and then labeled with antibodies against pcofilin (red or gray, F-M), GFP to distinguish the Math1^{+}commissural neurons (green, F,H,J,L) and type III β-tubulin (blue, Tuj1, F,H,J,L). Control (*n*=141 neurons, five embryos) and mutant (*n*=291 neurons, eight embryos) *BmprIa* neurons behave equivalently in response to BMP7 or mock stimulation (N and data not shown, *P*>0.05). By contrast, there was >50% decrease in pcofilin activation in the *BmprIb*$^{-/-}$ neurons (L,M; *n*=50 neurons, three embryos) compared with the controls (H,I; *P*<2.57×10^{-7}; *n*=39 neurons, three embryos), such that the level of pcofilin was similar in BMP7-treated (M) and mock-treated (G,K) cultures. Error bars represent s.e.m. Scale bars: in A-D, 30 μm; in F-M, 20 μm.

Figure 4-6: Cofilin overexpression rescues the axon growth delay seen after constitutive activation of BmprIb
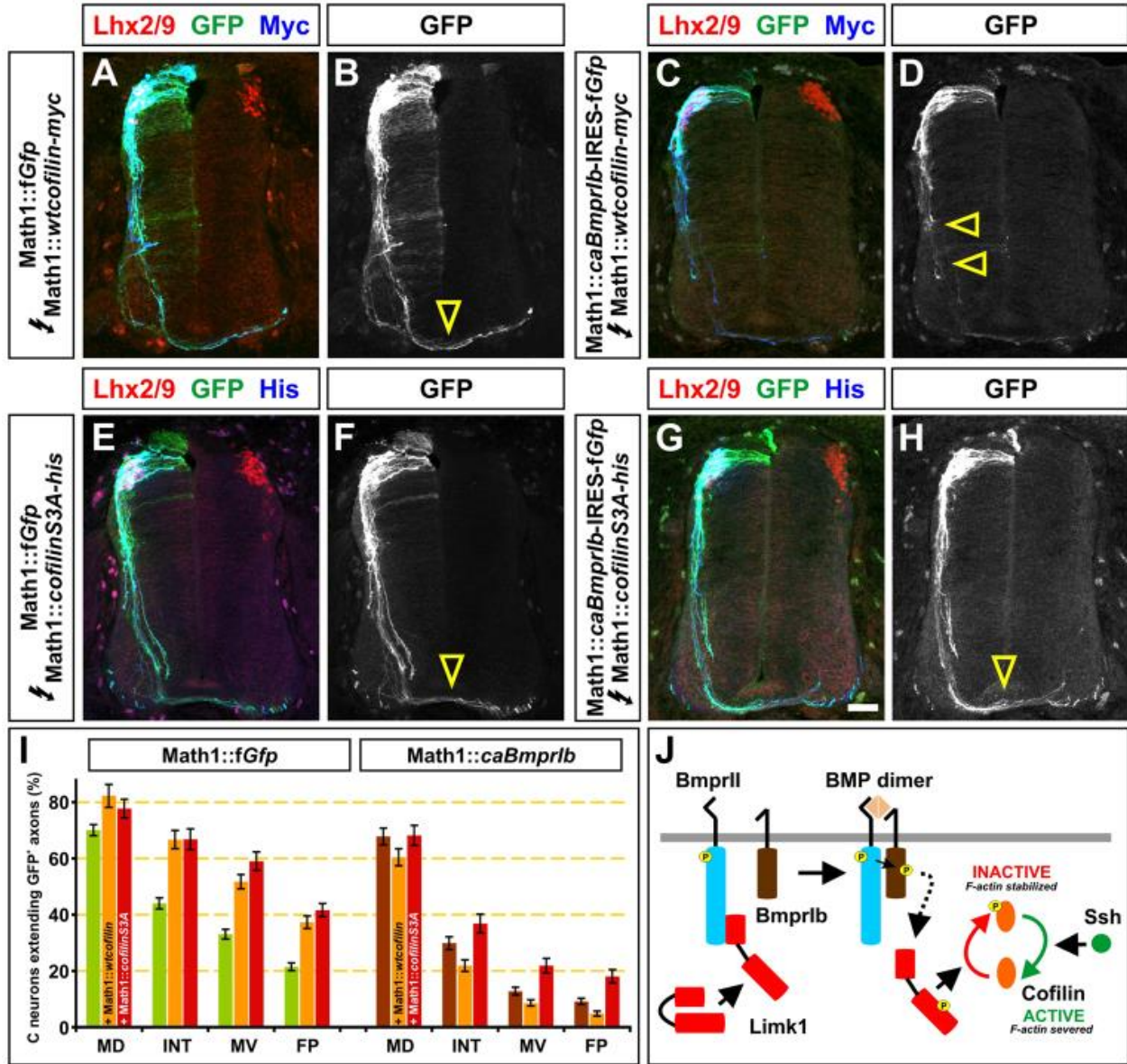

(**A-H**) Constructs encoding wild-type (wt) cofilin-myc (A-D) or cofilinS3A-his (E-H) were overexpressed in the spinal cord under the control of the Math1 enhancer in combination with

either Math1::f*Gfp* (A,B,E,F) or Math1::*caBmprIb-HA*-IRES-*fGfp* (C,D,G,H). Chicken embryos were *in ovo* electroporated at HH stage 14/15 and harvested at HH stage 22/23. Transverse sections of the spinal cord were examined for the extent of GFP$^+$ axon outgrowth (green) and number of Lhx2/9$^+$ commissural neurons (red). (C-H) The presence of wtcofilin-myc in Math1$^+$ neurons does not rescue the delay in axon outgrowth caused by caBmprIb expression. By contrast, the presence of cofilinS3A-his restores the axon growth to a similar extent as observed in the Math1::f*Gfp* control. Yellow arrowheads indicate the extent of axon outgrowth. Scale bar: 30 μm.

(**I**) About 20% of commissural neurons electroporated with Math1::f*Gfp* extended axons to the FP (*n*=200 sections, 11 embryos). Electroporation of Math1::*wtcofilin* (*n*=48 sections, four embryos) or Math1::*cofilinS3A* (*n*=54 sections, four embryos) results in ~40% of GFP$^+$ axons reaching the FP (compared with Math1::f*Gfp* control: wtcofilin, $P<2.4\times10^{-7}$; cofilinS3A $P<2.6\times10^{-12}$, Student's *t*-test). Less than 10% of caBmprIb$^+$ Math1$^+$ neurons (compared with Math1::f*Gfp* control, $P<9.4\times10^{-10}$; *n*=122 sections, six embryos) and <5% of caBmprIb$^+$ wtcofilin$^+$ Math1$^+$ neurons extend axons to the FP (compared with Math1::*caBmprIb, P*<0.0013; *n*=121 sections, five embryos). By contrast, co-electroporation of cofilinS3A and caBmprIb rescued the caBmprIb axon outgrowth phenotype to similar levels to that seen in the Math1::f*Gfp* control (*P*>0.13; *n*=54 sections, four embryos). Error bars represent s.e.m.

(**J**) Model for the regulation of cofilin activity by the BMP signaling pathway. The activity of Limk1 is 'primed' by binding to a site on the tail of BmprII. Upon BMP binding, Limk1 is released into the cytosol in a phosphorylated, activated form, that inactivates cofilin. These studies suggest that BmprIb is required for the activation of Limk1 (dotted arrow).

Supplementary Figure 4-S1: Quantification of the number of Lhx2/9+ cells in control and caBmprIb electroporated spinal cords.
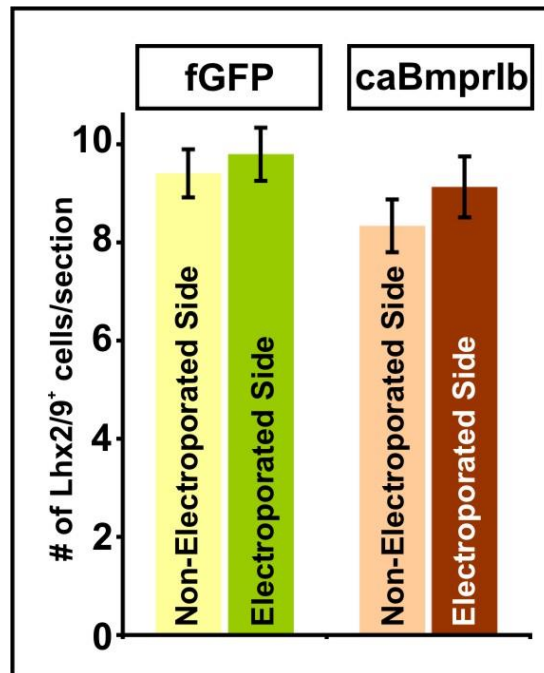
Electroporation of fGFP (*n*=69 sections from three embryos) or caBmprIb-IRES-fGFP+ (*n*=68 sections from four embryos) does not affect the number of Lhx2/9+ neurons generated. Equivalent numbers of Lhx2/9+ neurons are present on the electroporated and non-electroporated sides of HH stage 18 spinal cords (fGFP: probability of similarity, *P*>0.29; caBmprIb: probability of similarity, *P*>0.16). Error bars represent s.e.m.

Supplementary Figure 4-S2: The Math1 enhancer drives YFP expression in commissural neurons
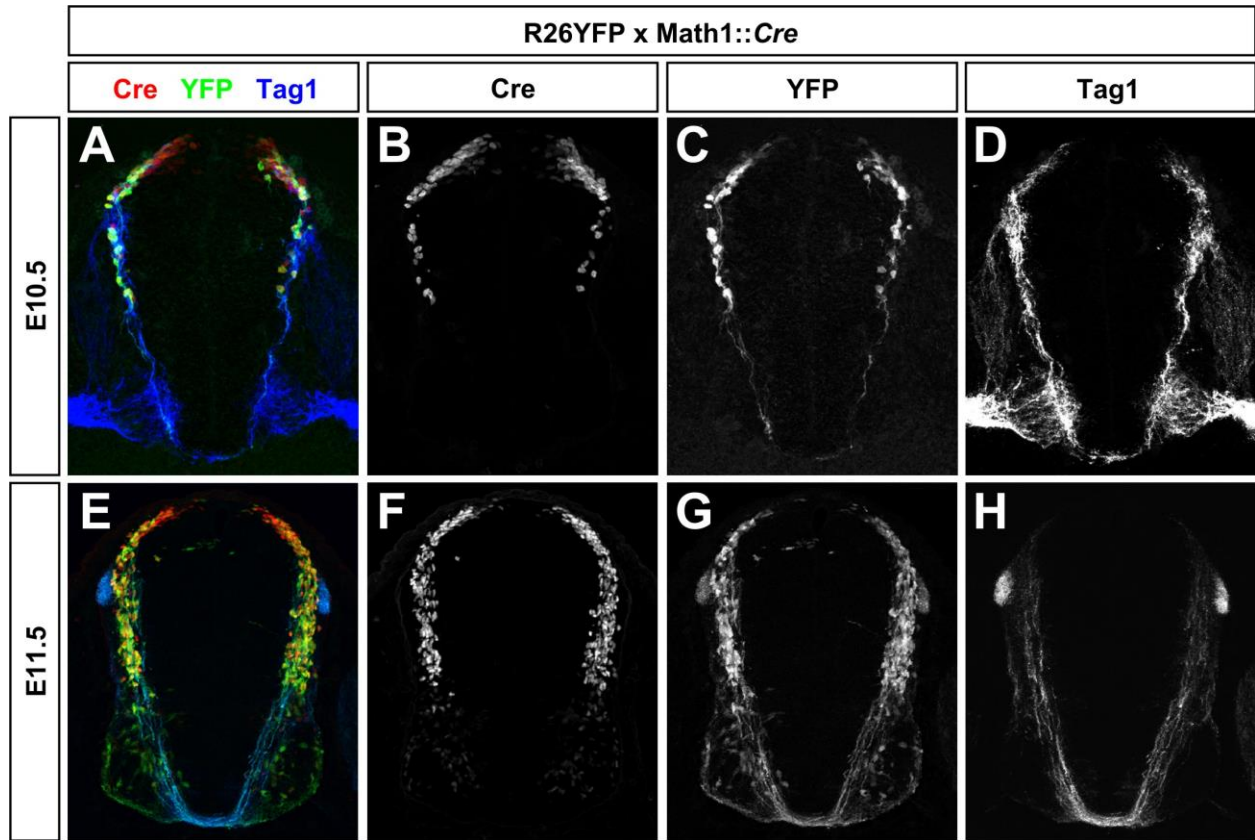
(**A-H**) The Math1::*Cre* line can drive the expression of YFP in Tag1+ commissural axons (arrowheads, C,G) when crossed to the Cre reporter strain, Rosa26R(lox-stoplox)::*Yfp*. Transverse spinal sections, taken from E10.5 (A-D) and E11.5 (E-H) Math1::*Cre*; Rosa26R::*Yfp* embryos, were labeled with antibodies against Cre (red, A,B,E,F), GFP (green, A,E,C,G) and Tag1 (blue, A,E,D,H). Scale bars: 45 mm in A-D; 55 mm in E-H.

Supplementary Figure 4-S3: The loss of BmprIa or BmprIb has no effect on the fate of commissural neurons
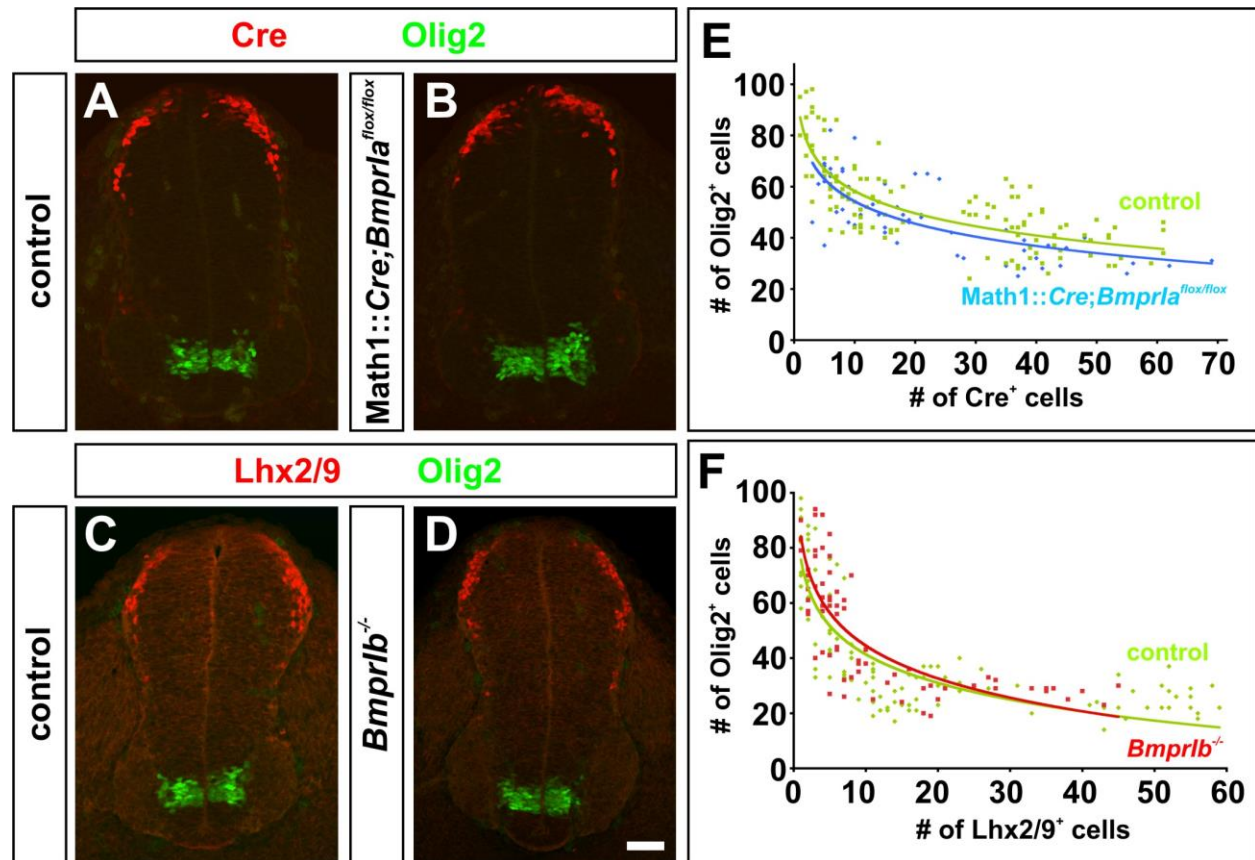
(**A-D**) There was no observable difference in the number of Lhx2/9+ cells in the presence or absence of either BmprIa or BmprIb. Transverse sections were taken from brachial or thoracic levels of the spinal cord from E10.5 Math1::*Cre*; *BmprIa+/+*(control, A), Math1::*Cre*; *BmprIaflox/flox* (B), *BmprIb+/+* (control, C) and *BmprIb–/–* (D) embryos and labeled with antibodies against Cre (red, A,B), Lhx2/9 (red, C,D) and Olig2 (green).

(**E,F**) The numbers of Cre+ (E) or Lhx2/9+ (F) cells were plotted as a function of Olig2+ cell number to normalize the extent of development between embryos. A logarithmic regression

127

analysis reveals no difference between the distribution of Cre+/Olig2+ cells in sections from Math1::*Cre*; *BmprIaflox/flox* (*n*=59 sections from three embryos) and control (*n*=29 sections from two embryos) littermates or Lhx2/9+/Olig2+ cells in sections from *BmprIb–/–* (*n*=59 sections from four embryos) and *BmprIb+/+/BmprIb+/–* (*n*=40 sections from four embryos) littermates. Scale bar: 25 mm.

Supplementary [Movie 4-S1](): Comparison of GFP$^+$ and caBmprIb-IRES-fGFP$^+$ commissural axon outgrowth.

Longitudinal preparations of HH stage 20/21 spinal cords electroporated with either Math1::f*Gfp* or Math1::*caBmprIb-IRES-fGfp*. Time is indicated in minutes. Scale bar: 20 μm.

Supplementary [Movie 4-S2](): Comparison of control and *BmprIb*$^{-/-}$ commissural axon outgrowth.

Longitudinal preparations of lumbar spinal cords taken from E11.5 Math1::tau*Gfp*; *Bmpr1b*$^{+/+}$ (control) or Math1::tau*Gfp*; *Bmpr1b*$^{-/-}$ embryos. Time is indicated in minutes. Scale bar: 50 μm.

BIBLIOGRAPHY

1. Dickson BJ. Molecular mechanisms of axon guidance. Science 2002;298(5600):1959-64.

2. Phan KD, Hazen VM, Frendo M, Jia Z, Butler SJ. The bone morphogenetic protein roof plate chemorepellent regulates the rate of commissural axonal growth. J Neurosci 2010;30(46):15430-40.

3. Lee KJ, Jessell TM. The specification of dorsal cell fates in the vertebrate central nervous system. Annu Rev Neurosci 1999;22:261-94.

4. Augsburger A, Schuchardt A, Hoskins S, Dodd J, Butler S. BMPs as mediators of roof plate repulsion of commissural neurons. Neuron 1999;24(1):127-41.

5. Heldin CH, Miyazono K, ten Dijke P. TGF-beta signalling from cell membrane to nucleus through SMAD proteins. Nature 1997;390(6659):465-71.

6. Foletta VC, Lim MA, Soosairajah J, Kelly AP, Stanley EG, Shannon M, He W, Das S, Massague J, Bernard O and others. Direct signaling by the BMP type II receptor via the cytoskeletal regulator LIMK1. J Cell Biol 2003;162(6):1089-98.

7. Lee-Hoeflich ST, Causing CG, Podkowa M, Zhao X, Wrana JL, Attisano L. Activation of LIMK1 by binding to the BMP receptor, BMPRII, regulates BMP-dependent dendritogenesis. EMBO J 2004;23(24):4792-801.

8. Arber S, Barbayannis FA, Hanser H, Schneider C, Stanyon CA, Bernard O, Caroni P. Regulation of actin dynamics through phosphorylation of cofilin by LIM-kinase. Nature 1998;393(6687):805-9.

9. Meberg PJ, Bamburg JR. Increase in neurite outgrowth mediated by overexpression of actin depolymerizing factor. J Neurosci 2000;20(7):2459-69.

10.   Wen Z, Han L, Bamburg JR, Shim S, Ming GL, Zheng JQ. BMP gradients steer nerve growth cones by a balancing act of LIM kinase and Slingshot phosphatase on ADF/cofilin. J Cell Biol 2007;178(1):107-19.

11.   Endo M, Ohashi K, Mizuno K. LIM kinase and slingshot are critical for neurite extension. J Biol Chem 2007;282(18):13692-702.

12.   Yamauchi K, Phan KD, Butler SJ. BMP type I receptor complexes have distinct activities mediating cell fate and axon guidance decisions. Development 2008;135(6):1119-28.

13.   Timmer JR, Wang C, Niswander L. BMP signaling patterns the dorsal and intermediate neural tube via regulation of homeobox and helix-loop-helix transcription factors. Development 2002;129(10):2459-72.

14.   Wine-Lee L, Ahn KJ, Richardson RD, Mishina Y, Lyons KM, Crenshaw EB. Signaling through BMP type 1 receptors is required for development of interneuron cell types in the dorsal spinal cord. Development 2004;131(21):5393-403.

15.   Dodd J, Morton SB, Karagogeos D, Yamamoto M, Jessell TM. Spatial regulation of axonal glycoprotein expression on subsets of embryonic spinal neurons. Neuron 1988;1(2):105-16.

16.   Evan GI, Lewis GK, Ramsay G, Bishop JM. Isolation of monoclonal antibodies specific for human c-myc proto-oncogene product. Mol Cell Biol 1985;5(12):3610-6.

17.   Liem KF, Tremml G, Jessell TM. A role for the roof plate and its resident TGFbeta-related proteins in neuronal patterning in the dorsal spinal cord. Cell 1997;91(1):127-38.

18.   Skaggs K, Martin DM, Novitch BG. Regulation of spinal interneuron development by the Olig-related protein Bhlhb5 and Notch signaling. Development 2011;138(15):3199-211.

19.   Hamburger V. Ontogeny of neuroembryology. J Neurosci 1988;8(10):3535-40.

20. Mishina Y, Hanks MC, Miura S, Tallquist MD, Behringer RR. Generation of Bmpr/Alk3 conditional knockout mice. Genesis 2002;32(2):69-72.

21. Yi SE, Daluiski A, Pederson R, Rosen V, Lyons KM. The type I BMP receptor BMPRIB is required for chondrogenesis in the mouse limb. Development 2000;127(3):621-30.

22. Imondi R, Jevince AR, Helms AW, Johnson JE, Kaprielian Z. Mis-expression of L1 on pre-crossing spinal commissural axons disrupts pathfinding at the ventral midline. Mol Cell Neurosci 2007;36(4):462-71.

23. Matei V, Pauley S, Kaing S, Rowitch D, Beisel KW, Morris K, Feng F, Jones K, Lee J, Fritzsch B. Smaller inner ear sensory epithelia in Neurog 1 null mice are related to earlier hair cell cycle exit. Dev Dyn 2005;234(3):633-50.

24. Srinivas S, Watanabe T, Lin CS, William CM, Tanabe Y, Jessell TM, Costantini F. Cre reporter strains produced by targeted insertion of EYFP and ECFP into the ROSA26 locus. BMC Dev Biol 2001;1:4.

25. Moore SW, Kennedy TE. Dissection and culture of embryonic spinal commissural neurons. Curr Protoc Neurosci 2008;Chapter 3:Unit 3 20.

26. Helms AW, Abney AL, Ben-Arie N, Zoghbi HY, Johnson JE. Autoregulation and multiple enhancers control Math1 expression in the developing nervous system. Development 2000;127(6):1185-96.

27. Hazen VM, Andrews MG, Umans L, Crenshaw EB, Zwijsen A, Butler SJ. BMP receptor-activated Smads confer diverse functions during the development of the dorsal spinal cord. Dev Biol 2012;367(2):216-27.

28.   Mishina Y, Suzuki A, Ueno N, Behringer RR. Bmpr encodes a type I bone morphogenetic protein receptor that is essential for gastrulation during mouse embryogenesis. Genes Dev 1995;9(24):3027-37.

29.   Liem KF, Jessell TM, Briscoe J. Regulation of the neural patterning activity of sonic hedgehog by secreted BMP inhibitors expressed by notochord and somites. Development 2000;127(22):4855-66.

30.   Novitch BG, Chen AI, Jessell TM. Coordinate regulation of motor neuron subtype identity and pan-neuronal properties by the bHLH repressor Olig2. Neuron 2001;31(5):773-89.

31.   Tessier-Lavigne M, Placzek M, Lumsden AG, Dodd J, Jessell TM. Chemotropic guidance of developing axons in the mammalian central nervous system. Nature 1988;336(6201):775-8.

32.   Placzek M, Tessier-Lavigne M, Jessell T, Dodd J. Orientation of commissural axons in vitro in response to a floor plate-derived chemoattractant. Development 1990;110(1):19-30.

33.   Butler SJ, Tear G. Getting axons onto the right path: the role of transcription factors in axon guidance. Development 2007;134(3):439-48.

34.   Scott RW, Olson MF. LIM kinases: function, regulation and association with human disease. J Mol Med (Berl) 2007;85(6):555-68.

35.   Bamburg JR, Bernstein BW. ADF/cofilin. Curr Biol 2008;18(7):R273-5.

36.   Hazen VM, Phan KD, Hudiburgh S, Butler SJ. Inhibitory Smads differentially regulate cell fate specification and axon dynamics in the dorsal spinal cord. Dev Biol 2011.

37.   Bernard O. Lim kinases, regulators of actin dynamics. Int J Biochem Cell Biol 2007;39(6):1071-6.

38.   Perron JC, Dodd J. Inductive specification and axonal orientation of spinal neurons mediated by divergent bone morphogenetic protein signaling pathways. Neural Dev 2011;6:36.

39.   Butler SJ, Dodd J. A role for BMP heterodimers in roof plate-mediated repulsion of commissural axons. Neuron 2003;38(3):389-401.

40.   Geisert EE, Frankfurter A. The neuronal response to injury as visualized by immunostaining of class III beta-tubulin in the rat. Neurosci Lett 1989;102(2-3):137-41.

CONCLUSIONS

The identification of axon guidance cues, since the early 90s has really changed our understanding of how neural circuits are formed during development. Axons grow great lengths during development, interacting with several guidance cues and intermediate targets *en route*, before they reach their synaptic endpoints. Although many guidance cues, their corresponding receptors and the mode of guidance have been identified in the last two decades, majority of these studies have either dissected out the identifying mechanisms *in vitro* or looked specifically at a single cue. Netrin1 is one such cue that was identified as a chemoattractant using biochemical assays and then tested *in vivo* using chicken and mouse embryos, primarily looking at mRNA distributions. However, these studies have not taken into account the distribution of netrin1 protein and any contributions the protein may have in the guidance of axons. Very few studies have examined the role of netrin1 protein in the spinal cord: MacLennan et al., showed that netrin1 protein is present through most of the dorsal neuroepithelium in stage 15 chicken spinal cords, when the commissural axons have just started to differentiate and migrate and also along the lateral borders of the spinal cord in later stages with the very low intensities in the FP[1]. Kennedy at al., showed that netrin1 protein is present as a graded distribution in the neuroepithelium, as well as in the trajectory of commissural axons as they cross the ventral midline[2]. However, these studies did not address the distribution of netrin1 protein in the pial surface and in the axons. Further, these studies suggest that netrin1 protein is present all along the trajectory of growing commissural axons, calling in to question the necessity of a long-range guidance mechanism.

In Chapter 2, I have examined the contributions of *netrin1* in the VZ and the FP using E11.5 mouse embryonic spinal cords, when commissural axons have reached and crossed the ventral midline. I find that *netrin1* is expressed by neural progenitors in the VZ independent of the FP, and that netrin1 protein produced in the VZ is transported to the pial surface along nestin filaments and their endfeet that contact the laminin+ basement membrane. Further, I have shown that VZ-derived netrin1 specifies a growth-boundary that acts locally to prevent many classes of axons from entering the VZ, again independent of FP-derived netrin1. This activity of netrin1 enables axons to maintain their trajectories and facilitate commissural axons to cross the ventral midline by providing short-range guidance.

In Chapter 3, I have assessed this new role of netrin1 in earlier stages when the pioneering axons have just started to traverse the spinal cord. I find that in the absence of *netrin1* axons lose their orientation and project dorsally towards the FP, suggesting that netrin1 on the pial surface and *netrin1* in the VZ provide an adhesive substrate that specifies ventrally-directed growth. I also examined the role of netrin1 at a later stage when majority of commissural axons have crossed the ventral midline, and found that in addition to directing sensory axon growth[3,4], dorsally derived *netrin1* also shapes central spinal axon growth by specifying growth-boundaries. Overall, I have shown that in the absence of VZ-derived netrin1: 1) axons lose their orientation and project dorsally, 2) axons project medially and grow aberrantly into the VZ and 3) axons are highly defasciculated.

In Chapter 4, we have shown the importance of regulating axon extension, indicating the importance of both positive and negative effectors of axon extension. Previous studies showed that BMPs regulate cell fate and provide guidance cues. Later studies showed that BmprIa and BmprIb can both specify cell fate[5,6], while only BmprIb is required to provide guidance cues[7].

While cell fate determination is suspected to act through receptor-activated Smads, the mechanistic basis for how the BMPs regulate guidance is not known. BmprIb is responsible for regulating the rate of commissural axon growth by inversely affecting cofilin. Increasing levels of BmprIb decreased levels of active cofilin, i.e. thus slowing axon extension. These experiments indicate the importance of regulating the balance between cofilin and Limk1 and their effect on axon extension.

The complexity of our nervous system is afforded in part, by the ability of several guidance cues to interact with each other and modulate the response of a growth cone. Together, this work demonstrates the importance of understanding the many ways in which a guidance cue can mediate responses from axons. These experiments also highlight the importance of teasing out the finer details between a molecule's ability to act *in vitro* and its actual role *in vivo*. While *in vitro* studies provide an excellent means to understand the mechanistic details of a response, one caveat to bear in mind is the complex nature of molecular interactions taking place *in vivo* that can significantly alter the activity of guidance cues. The mechanistic details of how netrin1 specifies growth-boundaries are not fully understood, however it is important to consider the following aspects:

Factors affecting responses towards netrin1

A string of *in vitro* experiments using *Xenopus* spinal neurons have shown that the response to netrin1 can be modulated by affecting the status of second messengers: changes in the levels of cyclic AMP (cAMP) using a competitive analog or protein kinase A (PKA) inhibitor switched the response from attraction to repulsion[8,9]. Additionally blocking Dcc abolished the attractive response towards netrin1 in these assays[8], indicating that netrin1 required

136

Dcc to mediate attraction. Similar studies using rat hippocampal neurons have shown that protein kinase C (PKC) regulates the endocytosis and thereby surface availability of Unc5A in cells, thus modulating repulsion[10], while increasing levels of PKA recruits Dcc intracellularly thus modulating attraction[11]. However, subsequent studies demonstrated that the intracellular concentrations of cAMP/PKA or the nature of the response was not altered by netrin1 in rat embryonic neurons; rather inhibiting or activating PKA altered the sensitivity of growth cones to netrin1, and hence the distance over which growth cones responded to netrin1[12]. cAMP levels have also been shown to play an important role in improved regeneration after injury by overcoming myelin associated inhibition[13,14]. Consequently, extracellular interactions that affect PKA and PKC could be an important step in mediating attraction or repulsion towards netrin1.

Interaction with ECM molecules

ECM molecules also have binding partners such as integrins, heparins and proteoglycans[15]. These serve as binding partners to present a molecule rather than as a receptor to a ligand. An important aspect yet to be fully understood is whether netrin1 is secreted and whether there is a need for netrin1 to diffuse *in vivo* at all. While my studies show a requirement for short-range activity of netrin1, I find that many netrin1 molecules are present specifically within a 1um distance of nestin$^+$ radial glial fibers, outside the VZ where the mRNA is not expressed: netrin1 could freely move in close association to nestin fibers suggesting a need for both secretion and diffusion *in vivo*. However, the dorsal most spinal cord, above netrin1 mRNA expression, does not show any protein accumulation in the VZ or the pial surface indicating limited diffusivity, if any. Alternatively, netrin1 could bind to an ECM molecule such as an

integrin via its C-terminal domain and thereby move around the neuroepithelium, which would indicate that netrin1 is still acting in bound form.

Another factor modulating the response of axons to netrin1 are interactions with ECM molecules such as laminin and fibronectin: *in vitro* studies have shown that interactions with high concentrations of a laminin substrate or soluble laminin can mediate the response of growth cones to be repelled by netrin1[16]. One possibility, in my studies, is that the interaction between netrin1 and laminin on the pial surface marks the outer boundary within which axons need to grow, while also providing an adhesive surface to grow on.

Hederal boundaries

In this work, I have shown that the canonical model of netrin1 as a chemoattractant is not required, and that netrin1 in fact provides short-range cues to specify axon growth. However, the mode by which netrin1 mediates guidance is not fully understood. The dorsal boundary of netrin1, both at the pial surface as well as the VZ, seems to exert a force that pulls axons and orients them ventrally, indicating a contact attractive behavior. Nonetheless, it remains unclear why axons project so precisely around *netrin1*[+] domains without innervating them, particularly when commissural axons express the receptor that mediates attraction towards netrin1, i.e. how do Dcc[+] axons avoid entering the *netrin1* expressing VZ and maintain their circumferential trajectory?

Alternatively, netrin1 might be providing a repulsive signal, both in the VZ and on the pial surface, demarcating the edges of a corridor for axon growth in combination with laminin[16]. In support of this, I find that axons invade the *netrin1*-expressing VZ in the absence of either *netrin1* or *Dcc*, suggesting the presence of a repulsive boundary. However, a purely repulsive

138

signal could not support the orienting ability of pial-netrin1 seen during early axogenesis or explain the presence of netrin1 on axons.

Finally, in my preferred model, I propose that netrin1 establishes a growth boundary, which combines both attractive and repulsive activities to orient and shape axon trajectories. In the intermediate spinal cord, commissural axons separate away from the pial surface to follow the edge of the VZ until they reach the ventral midline. This suggests that axons are adhering onto the *netrin1*-expressing VZ as a substrate while perhaps the pial netrin1 marks the outer edge of growth in order to confine axon growth inside the spinal cord. In favor of this model, Dcc[+] commissural axons that accumulate the highest amounts of netrin1 are the most tightly fasciculated as well as the closest to the netrin1-expressing VZ boundary. In the absence of such a defined corridor provided by both push and pull forces[17,18], some axons lose their ventral orientation and project dorsally, while others invade the VZ.

The presence of axonal-netrin1 in highly fasciculated axons appears to depend on the presence or absence of Dcc. In *Dcc* mutants, axonal accumulation of netrin1 seems greatly diminished and axons are highly defasciculated suggesting that the presence of netrin1 on axons promotes fasciculation. There are at least two possibilities: first, Dcc captures netrin1[19] thereby encouraging axons to grow on the *netrin1*-expressing VZ by homophilic adhesion similar to cell adhesion molecules[17]. Second, preliminary observations have shown that the rare axon that strays into the VZ in control embryos is netrin1[-], suggesting that axons accumulating netrin1 protein are kept out of the *netrin1*-expressing VZ by homophobic repulsion. Supporting this, repulsive signals have previously been shown to promote fasciculation: expression of an inhibitory molecule, AL-1, on astrocytes repelled cortical neurons causing the axons to fasciculate[17,20].

Similarly, *netrin1* expressed by neural progenitors in the VZ, could also play an important role in supporting fasciculation by specifying a repulsive boundary.

I am proposing that this collection of guidance activities be called a "hederal" boundary from the analogy of a wall supporting a growing hedera (ivy plant). The wall promotes growth of the plant along the substrate while preventing penetration of itself.

Significance

Netrin1 has been shown to play an important role during development in regulating many diverse functions. Various factors have also been implicated in mediating the response towards netrin1. Therefore, it is imperative to understand the context in which netrin1 is presented and also to understand how interactions with other molecules influence the response of cells or axons. Further, netrin1 has also been known to play a role in adult rodents: surprisingly, majority of netrin1 protein was found to be associated with ECM and not freely soluble[21]. Many classes of spinal interneurons in the superficial laminae of the dorsal horn, motoneurons in the ventral horn and oligodendrocytes were found to express *netrin1*, while netrin1 protein was found in these cell bodies as well as in a fibrous manner suggesting presence in neurites[21]. Netrin1 is also known to have functional roles in adults: spinal commissural interneurons have also been shown to play a role in determining left-right alternation during locomotion and is found to be disrupted in *netrin1* mutants[22]. In injury models, an increase in cAMP levels has been shown to improve axon growth in the central branches of DRG axons[13,14]. In more recent studies using spinal cord injury models, rat corticospinal axons were shown to regenerate robustly when placed in close contact with a graft of neural progenitors obtained from E14 rat spinal cords, but not when the grafts were placed even 50μm away[23]. The age and source of the neural progenitor grafts and the

behavior of the regenerating axons in conjunction with my work, suggest that netrin1 may be involved in guiding these regenerating axons at short-range. Such translational studies have significant importance in improving regeneration after injury and restoring functional neural circuits. Thus, if netrin1 can play a role in adult systems, it is very important to understand the context in which netrin1 needs to be presented *in vivo* in order to promote axon growth and improve regeneration.

In conclusion, this thesis provides important insights into the mechanisms by which netrin1 mediates guidance in axons in the developing spinal cord. Now that netrin1 has been shown to act as a short-range cue in the vertebrate spinal cord, it would be very exciting to reassess the role of netrin1 in many systems, especially in therapeutic strategies.

BIBLIOGRAPHY

1.   MacLennan AJ, McLaurin DL, Marks L, Vinson EN, Pfeifer M, Szulc SV, Heaton MB, Lee N. Immunohistochemical localization of netrin-1 in the embryonic chick nervous system. J Neurosci 1997;17(14):5466-79.

2.   Kennedy TE, Wang H, Marshall W, Tessier-Lavigne M. Axon guidance by diffusible chemoattractants: a gradient of netrin protein in the developing spinal cord. J Neurosci 2006;26(34):8866-74.

3.   Watanabe K, Tamamaki N, Furuta T, Ackerman SL, Ikenaka K, Ono K. Dorsally derived netrin 1 provides an inhibitory cue and elaborates the 'waiting period' for primary sensory axons in the developing spinal cord. Development 2006;133(7):1379-87.

4.   Masuda T, Watanabe K, Sakuma C, Ikenaka K, Ono K, Yaginuma H. Netrin-1 acts as a repulsive guidance cue for sensory axonal projections toward the spinal cord. J Neurosci 2008;28(41):10380-5.

5.   Timmer JR, Wang C, Niswander L. BMP signaling patterns the dorsal and intermediate neural tube via regulation of homeobox and helix-loop-helix transcription factors. Development 2002;129(10):2459-72.

6.   Wine-Lee L, Ahn KJ, Richardson RD, Mishina Y, Lyons KM, Crenshaw EB. Signaling through BMP type 1 receptors is required for development of interneuron cell types in the dorsal spinal cord. Development 2004;131(21):5393-403.

7.   Yamauchi K, Phan KD, Butler SJ. BMP type I receptor complexes have distinct activities mediating cell fate and axon guidance decisions. Development 2008;135(6):1119-28.

8. Ming GL, Song HJ, Berninger B, Holt CE, Tessier-Lavigne M, Poo MM. cAMP-dependent growth cone guidance by netrin-1. Neuron 1997;19(6):1225-35.

9. Song HJ, Ming GL, Poo MM. cAMP-induced switching in turning direction of nerve growth cones. Nature 1997;388(6639):275-9.

10. Williams ME, Wu SC, McKenna WL, Hinck L. Surface expression of the netrin receptor UNC5H1 is regulated through a protein kinase C-interacting protein/protein kinase-dependent mechanism. J Neurosci 2003;23(36):11279-88.

11. Bouchard JF, Moore SW, Tritsch NX, Roux PP, Shekarabi M, Barker PA, Kennedy TE. Protein kinase A activation promotes plasma membrane insertion of DCC from an intracellular pool: A novel mechanism regulating commissural axon extension. J Neurosci 2004;24(12):3040-50.

12. Moore SW, Kennedy TE. Protein kinase A regulates the sensitivity of spinal commissural axon turning to netrin-1 but does not switch between chemoattraction and chemorepulsion. J Neurosci 2006;26(9):2419-23.

13. Qiu J, Cai D, Dai H, McAtee M, Hoffman PN, Bregman BS, Filbin MT. Spinal axon regeneration induced by elevation of cyclic AMP. Neuron 2002;34(6):895-903.

14. Neumann S, Bradke F, Tessier-Lavigne M, Basbaum AI. Regeneration of sensory axons within the injured spinal cord induced by intraganglionic cAMP elevation. Neuron 2002;34(6):885-93.

15. Yebra M, Montgomery AM, Diaferia GR, Kaido T, Silletti S, Perez B, Just ML, Hildbrand S, Hurford R, Florkiewicz E and others. Recognition of the neural chemoattractant Netrin-1 by integrins alpha6beta4 and alpha3beta1 regulates epithelial cell adhesion and migration. Dev Cell 2003;5(5):695-707.

16. Höpker VH, Shewan D, Tessier-Lavigne M, Poo M, Holt C. Growth-cone attraction to netrin-1 is converted to repulsion by laminin-1. Nature 1999;401(6748):69-73.

17. Tessier-Lavigne M, Goodman CS. The molecular biology of axon guidance. Science 1996;274(5290):1123-33.

18. Oakley RA, Tosney KW. Contact-mediated mechanisms of motor axon segmentation. J Neurosci 1993;13(9):3773-92.

19. Hiramoto M, Hiromi Y, Giniger E, Hotta Y. The Drosophila Netrin receptor Frazzled guides axons by controlling Netrin distribution. Nature 2000;406(6798):886-9.

20. Meima L, Kljavin IJ, Moran P, Shih A, Winslow JW, Caras IW. AL-1-induced growth cone collapse of rat cortical neurons is correlated with REK7 expression and rearrangement of the actin cytoskeleton. Eur J Neurosci 1997;9(1):177-88.

21. Manitt C, Colicos MA, Thompson KM, Rousselle E, Peterson AC, Kennedy TE. Widespread expression of netrin-1 by neurons and oligodendrocytes in the adult mammalian spinal cord. J Neurosci 2001;21(11):3911-22.

22. Rabe N, Gezelius H, Vallstedt A, Memic F, Kullander K. Netrin-1-dependent spinal interneuron subtypes are required for the formation of left-right alternating locomotor circuitry. J Neurosci 2009;29(50):15642-9.

23. Kadoya K, Lu P, Nguyen K, Lee-Kubli C, Kumamaru H, Yao L, Knackert J, Poplawski G, Dulin JN, Strobl H and others. Spinal cord reconstitution with homologous neural grafts enables robust corticospinal regeneration. Nat Med 2016;22(5):479-87.